BIOCHEMICAL CHARACTERIZATION AND ACTION OF CONNECTIVE TISSUE GROWTH FACTOR AND ITS RECEPTOR IN CORNEAL SCARRING

by

TIMOTHY DANIEL BLALOCK

A DISSERTATION PRESENTED TO THE GRADUATE SCHOOL
OF THE UNIVERSITY OF FLORIDA IN PARTIAL FULFILLMENT
OF THE REQUIREMENTS FOR THE DEGREE OF
DOCTOR OF PHILOSOPHY

UNIVERSITY OF FLORIDA

2003

The work presented in this dissertation is dedicated to LeeAnn Blalock, for her love and encouragement in the pursuit of my higher education in biomedical science. I would also like to dedicate this dissertation to my parents, James and Ida Blalock, along with the rest of my family, for their support in this endeavor.

ACKNOWLEDGMENTS

I would like to express my deepest gratitude to my mentor and friend Dr. Gregory Schultz, for his encouragement, support, and understanding throughout the course of my work for this dissertation. His expertise and advice in this endeavor have been indispensable to my success. I would also like to sincerely thank the members of my doctoral thesis committee: Dr. Henry Baker, Dr. Nancy Denslow, Dr. Susan Frost, and Dr. Alfred Lewin. Their advice was crucial to my success in this research.

I would also like to extend my thanks to Dr. Nasser Chegini, Dr. David Muir, Dr. Michael Goldstein, Dr. Gary Grotendorst, Dr. Matthew Duncan, Dr. Heather MacArthur, Dr. Rong Yuan, Dr. Santosh Gowda, Dr. Franck Ollivier, Cecilia Lopez, Helene Klapper, Kavita Gandhi, Alpesh Mehta, Brian Morrison, Kelly Brinsko, Samer Jaber, Julia Burrows, Siva Radhakrishnan and Juan Varela for all of the experimental advice, friendship, and support they have shown me throughout my time at the University of Florida. The help extended to me by these individuals as well as others too numerous to mention has been essential to my success.

Finally, I would like to thank my wife, LeeAnn Talarico Blalock; my parents, James and Ida Blalock; as well as Jim, Connie, Jaime, Alicia, Bob, Lisa, and Chris Blalock for all of the support they have offered to me over the years.

TABLE OF CONTENTS

page

LIST OF TABLES

LIST OF FIGURES

KEY TO ABBREVIATIONS

bp	base pair
BSA	bovine serum albumin
CTGF	connective tissue growth factor
DEPC	diethyl pyrocarbonate
DMEM	Dulbecco's Modified Eagle medium
ECM	extracellular matrix
EDTA	ethylenediaminetetraacetic acid
EGF	epidermal growth factor
FGF	fibroblast growth factor
HEPES	N-2-Hydroxyethylpiperazine-N'-2-ethanesulfonic acid
IGF	insulin-like growth factor
IGF-IIR	type II insulin-like growth factor receptor
kDa	kilodalton
LB	Luria Bertani medium
LRP	low-density lipoprotein (LDL) receptor-related protein
M6P	mannose-6-phosphate
MPR	mannose-6-phosphate receptor
PCR	polymerase chain reaction
PDGF	platelet-derived growth factor

PEG	polyethylene glycol
PMSF	phenylmethylsulfonyl fluoride
PRK	photorefractive keratectomy
RAP	receptor-associated protein
RT	reverse transcription
RT-PCR	reverse transcription polymerase chain reaction
PDGF	platelet-derived growth factor
SDS-PAGE	sodium dodecyl sulfate-polyacrylamide gel electrophoresis
TGF-α	transforming growth factor alpha
TGF-β	transforming growth factor beta
TGF-β-IIR	type II transforming growth factor beta receptor
VEGF	vascular endothelial growth factor

Abstract of Dissertation Presented to the Graduate School of the University of Florida in Partial Fulfillment of the Requirements for the Degree of Doctor of Philosophy

BIOCHEMICAL CHARACTERIZATION AND ACTION OF CONNECTIVE TISSUE GROWTH FACTOR AND ITS RECEPTOR IN CORNEAL SCARRING

by

Timothy Daniel Blalock

August 2003

Chair: Gregory S. Schultz
Department: Biochemistry and Molecular Biology

Connective tissue growth factor (CTGF) is a 38 kilodalton, cysteine-rich, secreted peptide with mitotic and chemotactic functions. CTGF expression is upregulated by transforming growth factor beta (TGF-β), leading to the synthesis of connective tissue and extracellular matrix components such as collagen, laminin, integrin, and fibronectin which are predominant components of scar tissue. CTGF mRNA and protein levels are elevated in human fibrotic disorders including renal fibrosis, scleroderma, and keloids. Experimental data suggest that CTGF mediates the effects of TGF-β on contributing to corneal scarring by binding to the type II insulin-like growth factor receptor.

Gene expression profiling experiments, using GeneGhip technology, were performed showing the classes of genes in corneal fibroblasts that are induced upon CTGF stimulation. These results show that CTGF regulates key genes involved in corneal apoptosis, scarring, and angiogenesis. CTGF mRNA and protein expression was stimulated in corneal fibroblasts in response to TGF-β. CTGF also mediated the effects

of TGF-β on cell-associated collagen formation. Photorefractive keratectomy (PRK) was performed on rats to show that CTGF mRNA and protein expression increased dramatically in the corneal fibroblasts and epithelial cells after surgery up to Day 21. To reduce corneal fibrosis, a gene-specific hammerhead ribozyme was developed to target and cleave CTGF mRNA to reduce its expression. Cells transfected with a plasmid encoding the CTGF ribozyme showed a marked decrease in CTGF mRNA and protein expression as well as TGF-β-induced cell proliferation. To characterize the receptor for CTGF, radioligand binding, cross-linking, *in vitro* binding, and immunoprecipitation experiments were performed. These results indicate that CTGF binds to the type II insulin-like growth factor (IGF) receptor in corneal fibroblasts. Binding to this receptor confers biological activity in these cells.

Thus, these experiments show for the first time the induction of CTGF expression in corneal scarring, the application of gene therapy to reduce CTGF expression, and the identity of the CTGF receptor in corneal fibroblasts. Knowledge of the biochemistry and action of CTGF and its receptor will elucidate their roles in the process of wound healing and the development of anti-scarring agents.

CHAPTER 1
LITERATURE REVIEW

The Cornea

The cornea is a transparent, avascular tissue that is exposed to the external environment. The principal physiologic requirement of the cornea is to maintain clarity for proper vision. The maintenance of corneal shape and clarity is critical to refraction since the cornea accounts for more than two-thirds of the total refractive power of the eye (Chaudhuri et al., 1983). A very slight change in the contour of the cornea may result in a serious change of refractive error. Additionally, small changes in surface smoothness or total thickness may result in visual distortion. Many structural components work together to maintain the optical function of the cornea. Most medical and surgical treatments of the cornea are performed to restore corneal transparency (Choi et al., 2002a).

Normal Corneal Anatomy and Physiology

The structure and physiology of the cornea is deceptively complex. The anterior corneal surface is covered by tear film, a physiologically dynamic structure; while the posterior surface is directly bathed by the aqueous humor (Doane et al., 1978). The cornea is a transparent tissue and is continuous with the opaque sclera and the semitransparent conjunctiva. The zone of transition between the cornea and sclera is the richly vascularized limbus, which contains a reservoir of pluripotent stem cells (Moore et al., 2002). Histological examination reveals a complex structure of six layers: epithelium, epithelial basement membrane, Bowman's membrane, stroma, Descemet's

membrane, and the endothelium. The factor that determines the property of corneal transparency is the arrangement of collagen fibers in the stromal layer (Birk and Lande, 1981a). The mean diameter of each collagen fiber and the mean distance between these fibers are homogenous and measure less than half the wavelength of visible light. This anatomic relationship is thought to be responsible for the fact that the incident ray scattered by each collagen fiber is cancelled by interference of the other scattered ray, allowing light to pass through the cornea (Maurice D.M., 1984). When these distances vary because of fibrosis or edema, the cornea loses its transparency and there is random scattering of incident rays (Andreo and Farrell, 1982). The cell types of cells present in the cornea include epithelial cells, keratocytes (corneal fibroblasts) and endothelial cells. Even though the cornea is avascular, it contains almost all of the components of the blood, such as albumin and globulins; whereas the cellular elements are absent (Gullino, 1986). This is important for understanding the regulatory mechanisms for maintaining normal corneal integrity; and for appreciating the pathobiology of various diseases of the cornea.

Over 90% of the cornea is composed of stroma. The epithelial and endothelial layers help to maintain the transparency of the cornea. However it is the anatomical and biochemical characteristics of the corneal stroma that are principally involved in its physical strength, constancy of shape, and transparency (Daxer et al., 1998). The corneal stroma consists of extracellular matrix components, corneal fibroblasts, and nerve fibers; with cellular components comprising only 2% of the total stromal volume (Otori, 1967). Collagen (mainly types I, III, and IV) occupies over 70% of the dry weight of the cornea (Komai and Ushiki, 1991). The pro-α collagen chains and glycosaminoglycans (GAGs)

are synthesized by keratocytes, the predominant cellular component of the corneal stroma (Kenney et al., 1986). These long, spindle-shaped keratocytes are found scattered between the lamellae in the corneal stroma. The chains are then assembled into a procollagen triple helix bundle and are assembled and processed ultimately into mature collagen fibers. Gap junctions are the only junctional complex allowing for communication and exchange between corneal fibroblasts (Nishida et al., 1988). It is through injury or surgery that the keratocytes lose their network connections and behave independently (Birk and Lande, 1981b).

Corneal Scarring

The healing of the corneal stromal wound is slower than in other connective tissues presumably because of the lack of blood vessels. When a corneal wound or incision occurs, fibroblasts around the wound edge die, creating a hypocellular zone (Wachtlin et al., 1999). Beyond this zone, the quiescent keratocytes become activated into fibroblasts and migrate to the site of injury (Snyder et al., 1998). Other cells, such as monocytes can migrate to the wound and transform into fibroblast-like cells (Sunderkotter et al., 1991). Formation of the stromal scar in humans is a dynamic process. Clinical changes have been noted up to 5 years after radial keratotomy (Eiferman, 1992). Dermatan sulfate and keratin sulfate proteoglycans from the adjacent matrix as well as newly synthesized proeoglycans accumulate with the scar (McDermott, 1993). Collagen types I, III, V, and VI are also quite predominant within the scar (Ljubimov et al., 1998). At 1 week after injury, single collagen bundles are seen along the surface of the fibroblasts; but by 3 weeks, a dense network of fibrils is present, in

both parallel and random orientations (Melles et al., 1995). The strength of corneal scars and the surrounding tissue never reaches that of the uninjured cornea.

Growth Factors in Corneal Wound Healing

Histologic changes in wound healing (such as excessive accumulation of extracellular matrix proteins) have been known for many years; but the molecular factors that regulate these processes *in vivo* are newly recognized. A delicate balance exists between growth factors and the matrix in steps of corneal wound healing.

Growth factors were initially discovered because of their ability to stimulate mitosis of quiescent cells in culture in a nutritionally complete medium that lacked serum (Tuft et al., 1989). Growth factors were then found to promote cellular proliferation in an autocrine or paracrine fashion (Steenfos, 1994a). Growth factors also possess chemoattractive and penetrating properties (Clark and Henson, 1996); and play a major role in the wound repair process. Growth factors attract inflammatory cells and fibroblasts into the wound, promote proliferation of fibroblasts and endothelial cells, and stimulate angiogenesis and wound epithelialization. They have a significant effect on the production and degeneration of extrcellular matrix. Growth factors are synthesized and secreted by many types of cells involved in wound healing (including platelets, inflammatory cells, fibroblasts, epithelial cells, and vascular endothelial cells). All peptide growth factors initiate their effects by binding to and activating specific, high-affinity receptor proteins located in the plasma membrane of target cells. Activation of the receptors eventually results in stimulating a number of processes, including those involved in wound healing. Growth factors are usually grouped into families based on structural and functional similarities. Some of the well-characterized growth factors are

included in Table 1-1 and include epidermal growth factor (EGF), transforming growth factor-α (TGF-α), transforming growth factor-β (TGF-β) and platelet-derived growth factor (PDGF). Other growth factors that have been shown to be important in wound healing are the insulin-like growth factors (IGFs), fibroblast growth factor (FGF), tumor necrosis factor-α (TNF-α), the interleukins and growth hormone (Steenfos, 1994b;Greenhalgh, 1996;Mutsaers et al., 1997).

Table 1-1: Growth factors involved in corneal wound healing

Growth factor	Abbreviation	Description
Epidermal growth factor	EGF	Synthesized by corneal epithelial cells, and lachrymal gland; mitogenic and chemotactic factor for all 3 corneal cell types
Transforming growth factor alpha	TGF-α	Structurally similar to EGF; synthesized by corneal epithelial cells and lachrymal gland
Transforming growth factor beta	TGF-β	Three isoforms exist; promotes formation of the ECM; TGF-β2 is present in aqueous humor; probably synthesized by the corneal epithelium
Basic fibroblast growth factor	bFGF	Detected in the basement membrane; synthesized by corneal endothelium
Acidic fibroblast growth factor	aFGF	Detected in the basal layer of corneal epithelial cells and in the basement membrane
Keratinocyte growth factor	KGF	mRNA detected in corneal epithelial cells
Hepatocyte growth factor	HGF	Produced in fibroblasts; mRNA detected in corneal epithelial cells

Taking all of this information into consideration, a model of corneal wound healing can be formulated that integrates the contributions of growth factors secreted by lachrymal cells, inflammatory cells, epithelial cells and stromal cells (van Setten et al., 1994;Wilson et al., 1992a;Li and Tseng, 1995a;Schultz, 1995). When an actue injury occurs that extends through the epithelial layer into the corneal stroma, EGF and its

closely related protein TGF-α (secreted from lachrymal cells into tear fluid) penetrate into the stromal matrix and recruit fibroblasts through chemotaxis to the site of injury through an exocrine mechanism (Grant et al., 1992). Normally, EGF and TGF-α in tears do not significantly penetrate through the intact keratinized layers of uninjuried epithelium. Inflammatory cells such as macrophages secrete multiple growth factors including TGF-α, TGF-β, and PDGF (Madtes et al., 1988). Factors secreted by corneal epithelial cells including TGF-β, TGF-α, EGF, PDGF, bFGF and interleukin-α (IL-α) act by paracrine pathway to stimulate migration and mitosis of stromal fibroblasts (Wilson et al., 1992b;Li and Tseng, 1995b;Wilson et al., 1994c;Murphy et al., 1991). Similarly, fibroblasts secrete keratinocyte growth factor (KGF) which acts on the epithelial cells, but not fibroblasts, to promote epithelial wound healing by a paracrine path (Sotozono et al., 1995).

Refractive Surgery

The practice of refractive surgery comprises many techniques designed to correct errors of refraction and improve uncorrected visual acuity. The field has experienced an explosion in popularity due to advances in laser technology and the refinement of procedures such as radial keratotomy, photorefractive keratectomy (PRK), and laser-assisted in situ keratomileusis (LASIK). Radial keratotomy is a type of refractive surgery performed on 1.5 million patients since its introduction in the United States in 1978 in which radial incisions are made with a diamond knife blade in the peripheral cornea, resulting in a structural weakening (Duffey and Leaming, 2002). This weakening causes peripheral steepening and central flattening, correcting myopia (Applegate and Howland, 1997). In addition, radial keratotomy is often performed with astigmatic

keratotomy to correct astigmatism (Gimbel et al., 2000). In 1993, the excimer laser was introduced to corneal surgeons. The excimer laser emits high-energy ultraviolet light to ablate corneal tissue with submicron precision, without significant injury to non-ablated tissue (Stark et al., 1992). Photorefractive keratectomy (PRK) is a refractive procedure that uses the excimer laser to ablate the corneal epithelium followed by enough layers of corneal stroma to achieve correction of myopia. Over one million PRK procedures have been performed in the United States in the last 10 years (Choi et al., 2002b). Laser-assisted in situ keratomileusis (LASIK) is similar to PRK in that a high-precision excimer laser is used to ablate layers of the corneal stroma. However, LASIK uses an instrument called a microkeratome to remove a flap of corneal epithelium that can be resected after ablation. This procedure has experienced an explosion in popularity in the last few years due as the procedure was refined and the number of qualified surgeons across the country grew (Wu, 2002). In addition patients with high degrees of myopia are better treated by LASIK than radial keratotomy or PRK, because LASIK reduces complications in healing changes.

Although these procedures are relatively noninvasive, complications due to stromal scarring may occur, and these may impair refraction. In the case of radial keratotomy, normal side effects may occur such as pain, glare, short-term vision fluctuation, and anisometropia; but long-term effects due to scar tissue and haze in the stroma may occur (Duffey, 1995). With laser-assisted procedures such as PRK and LASIK, problems in refraction may arise due to corneal haze, a common condition of corneal opacification (Heitzmann et al., 1993). Conditions of corneal haze are associated

with deposition of collagen, fibronectin, and laminin; and an absence of keratin sulfate from the extracellular matrix (Malley et al., 1990;Lee et al., 2001).

Antiscarring Treatments and Complications

Although corneal haze may occur with refractive procedures, the usual practice is to wait until the opacity fades spontaneously. However, the corneal haze may be dense with the presence of fibrosis, in which case topical corticosteroids may be administered (Bilgihan et al., 2000;Siganos et al., 1999). With severe cases, potent topical steroids such as dexamethasone or prednisolone sodium acetate may be used (Price, Jr. et al., 2001). If corneal haze is not alleviated, the surgeon may opt for retreatment with the excimer laser. In many cases, retreament of the cornea is safer than long-term use of topical steroids, because retreatment prevents the patient from developing complications from the use of steroids (Choi et al. 2002). Occasionally, other treatments may be used to reduce scar formation, such as 5-fluorouracil and mitomycin C. The 5-fluorouracil is a pyrimidine analog that inhibits fibroblast proliferation to help reduce scarring. However, it is associated with complications such as corneal erosion, corneal ulceration, wound and suture track leaks, or even disintegration of absorbable sutures during the early postoperative period (Lee, 1994). Long term complications include hemorrhage, endophthalmitis, maculopathy, malignant and pupillary block (Ticho and Ophir, 1993;Parrish and Minckler, 1996). Mitomycin C is an antineoplastic-antibiotic agent, that inhibits fibroblast proliferation and has been shown to decrease corneal haze after PRK (Porges et al., 2003). Mitomycin C shows side effects similar to those of 5-fluorouracil. When administered intra- and post-operatively, mitomycin C prevents post-surgical scarring. However, this is accomplished by causing widespread cell death and

apoptosis; and mitomycin C may cause blindness (Khaw et al., 1993). Therefore, alternative safer agents are needed.

Wound Repair and Regeneration

Tissue regeneration can be impaired by alteration of its cellular architecture, which may occur through physical or genetic-induced tissue damage. Repair of these wounds does not occur simply by release of growth factors resulting in physiological responses such as cell migration and proliferation. Wound repair and regeneration occurs through an integrated series of events involving many mediators, formed blood elements, reorganization of the extracellular matrix, angiogenesis, and proliferation of both fibroblasts and epithelial cells (Singer and Clark, 1999). Tissue regeneration requires the regulation of various genes encoding regulatory and structural molecules participating in both growth and tissue reorganization (Clark and Henson, 1996). The events in wound repair follow a general temporal sequence: inflammation, tissue regeneration, and tissue remodeling (Gharaee-Kermani and Phan, 2001). These general categories usually overlap due to integration of events in each step. During normal wound repair, cells are recruited from connective tissue to the site of injury by directed migration, followed by cell proliferation, and finally deposition of extracellular matrix components (Gillitzer and Goebeler, 2001). These events occur sequentially until normal tissue architecture is restored.

Wound Healing and Repair

The wound healing response begins at the moment an injury occurs. These injuries usually produce damage to vessels, resulting in blood leakage. This leakage leads to vasoconstriction followed by formation of a clot (Mast BA and Schultz GS,

1996;Bennett and Schultz, 1993;Rendell et al., 2002). These events occur early in the inflammatory phase and result in the termination of blood leakage. The clot comprises platelets, cross-linked fibrin molecules, fibronectin, and thrombospondin. The clot acts as a provisional matrix through which cells migrate during wound repair (Guo et al., 1997b). Activated platelets release alpha granules containing adhesion proteins such as fibrinogen, fibronectin, thrombospondin, and von Willebrand factor VIII (Guo et al., 1997a). Adhesion of platelets to these proteins is mediated through the αIIb/β3 integrin surface receptor (Ginsberg et al., 1992). In addition to these crucial events, platelets release leukocyte chemotactic factors such as platelet-derived growth factor (PDGF), insulin-like growth factor I (IGF-I), and transforming growth factors alpha and beta (TGF-α and TGF-β) (Weksler, 2000;Ross et al., 1990;Gutierrez et al., 1987;Sporn and Roberts, 1992). These chemotactic growth factors attract inflammatory cells, resulting in initiation of re-epithelialization, contraction of connective tissue and stimulation of angiogenesis (Clark and Henson, 1996; Mast and Schultz, 1996). The first leukocytes recruited to the site of the injury are neutrophils which attack bacteria that may have been introduced into the tissue at the time of injury (Simpson and Ross, 1972). Levels of neutrophils begin to decline and macrophages begin to take over as the dominant cell type in the wound. Macrophages degrade and remove tissue debris, in preparation for the reparative phases of wound healing (Leibovich and Ross, 1976). Activated platelets release several growth factors such as TGF-β, which recruit neutrophils and monocytes from the bloodstream (Wiseman et al., 1988).

Molecular Biology of Wound Healing

Experiments using purified components of connective tissue showed chemotactic activity for neutrophils, monocytes, and fibroblasts *in vitro*. Examples of these extracellular matrix (ECM) components include collagen, elastin, fibronectin, and laminin as well as their proteolytic cleavage products (Clark RAF and Henson PM, 1996). Many macrophage-derived growth factors and cytokines have been implicated in stimulating synthesis of ECM components in addition to secreting pleiotropic factors that impact cell proliferation and angiogenesis (Hunt et al., 1984). Primary factors of immune regulation are cytokines, such as tumor necrosis factor alpha (TNF-α) and interleukin-1-beta (IL-1β) which are released by both macrophages and neutrophils and have an impact on the inflammatory response (Cohen, 1976). Several pleiotropic factors have been shown to be crucial in wound-repair efficiency (such as TGF-β, PDGF, IGF-1, bFGF, and TGF-α). These growth factors have control over the complex processes in wound healing involving migration, mitosis, and differentiation of epithelial and stromal cells (Schultz et al., 1992). PDGF and vascular endothelial growth factor (VEGF) stimulate vascular endothelial cells to extend new capillaries into the wound site, establishing new blood supply (Mints et al., 2002). These new vessels provide nutrients, oxygen, and other factors necessary for fibroblasts to deposit additional pro-collagen, allowing the further and continued growth of blood vessels (Zhou et al., 2000). This process continues until a network of new vessels bridge the wound as well as continued connective tissue synthesis. Eventually, the fibroblasts synthesize enough ECM to form a scar, replacing the damaged tissue. Components of the ECM in the wound are either glycosaminoglycan polysaccharide chains, structural proteins (such as collagen and elastin) or adhesive

proteins (fibronectin and laminin) (Hay, 1981). All of the events in the process of inflammation must be reversed for the tissue architecture to return to normal. For this to happen, the inflammatory mediators that were generated must be removed, followed by termination of granulocyte emigration from blood vessels, normal vascular permeability, and removal of inflammatory cytokines (Furie and McHugh, 1989). Infiltration of monocytes and neutrophils must decrease for this to occur. Finally, removal of extravasated fluid, protein, cellular debris, granulocytes, and macrophages occurs as the wound regeneration process continues (Daoud et al., 1985).

Wound Regeneration

The sequence of events in the progress of wound regeneration (Pollack 1984) is as follows:

- Activation of coagulation leading to termination of blood leakage and formation of the provisional matrix
- Release of soluble chemotactic factors formed from plasma proteins that attract inflammatory cells to the site of injury
- Influx of neutrophils and monocytes to engulf and neutralize bacteria in the wound site
- Debridement of damaged connective tissue matrix
- Initiation of neovascularization
- Stimulation of cell proliferation and connective tissue matrix remodeling

While in many cases this series of events leads to restoration of normal tissue structure and function, problems often arise. For example, fibrotic disorders occur when scarring results in a loss of function in the particular organ. More specifically, scarring is a result

of abundant cell synthesis by fibroblasts that proliferate and differentiate within the provisional matrix (Lindblad, 1998). Although fibrosis in the skin may sometimes be cosmetic, serious complications may arise when it occurs elsewhere; especially in vital organs, as mentioned earlier in the cornea.

Transforming Growth Factor Beta (TGF-β)

Transforming growth factor beta (TGF-β) has one of the widest ranges of activities in wound healing (of all of the growth factors involved in this process) because of the array of cell types that produce or respond to it and because of its spectrum of activity (Roberts and Sporn, 1990). Its role in the formation of scar tissue is due to its influence on chemotaxis of the mesenchymal cells into the wound, stimulation of growth, and increased synthesis and deposition of ECM components (Roberts and Sporn, 1990). Additionally, TGF-β regulates the expression of proteolytic enzymes such as matrix metalloproteinases (MMPs) and tissue inhibitors of metalloproteinases (TIMPs) (Roberts, 1995). TGF-β is secreted by almost every tissue. Almost all normal cells have functional membrane-bound receptors for this peptide family. The principal sources of TGF-β are macrophages and alpha granules from platelets. After it is released it is chemotactic for monocytes and fibroblasts and inhibitory to keratinocytes and endothelial cells (Ksander et al., 1990). TGF-β is strongly regulated at both the transcription and translation level in macrophages (Noble et al., 1993c). There is an association between macrophages, TGF-β, and collagen deposition in human fibrotic disorders. Evidence shows that in granulomas, one type of fibrosis, TGF-β was localized at the interface between macrophages and the surrounding fibrotic capsule (Khalil et al., 1991). In addition, TGF-β was found in abundance in the macrophages and epithelial cells in

biopsies of patients with lung fibrosis compared to normal patients (Noble et al., 1993b). These results suggest that TGF-β is predominantly provided by macrophages during wound repair and fibrosis.

Roles of TGF-β

TGF-β is released from platelets as two distinct complexes. A larger, latent complex is released into the serum and comprises TGF-β, latency-associated protein (LAP) and the latent TGF-β binding protein. A smaller complex is composed of TGF-β and the associated LAP and is relased from blood clots after dissociation (Roberts, 1995).

Five isoforms of TGF-β exist known as TGF-β1, TGF-β2, TGF-β3, TGF-β4, and TGF-β5. TGF-β1 is the most abundant isoform found in all tissues, and in platelets it is the only one present (Weibrich et al., 2002). TGF-β2 is most abundant in body fluids including aqueous and vitreous humor; while TGF-β3 is usually the least abundant (Noble et al., 1993a). Application of exogenous TGF-β1, 2, and 3 resulted in increased scar formation in incisional wounds (Schmid et al., 1993). In these wounds, expression of TGF-β was auto-induced by the presence of exogenous TGF-β.

TGF-β has a more profound effect on the ECM than any other growth factor. It has a tremendous effect on increasing the strength and maturation of wounds and the ECM in fibrotic disorders. The fibroblasts are targeted by TGF-β in skin wound healing, which are transcriptionally activated by TGF-β (Wikner et al., 1988). TGF-β has been found to regulate matrix proteins by upregulating collagen, fibronectin, glycosaminoglycans, MMPs, and TIMPs while decreasing proteolytic activity and cell adhesion via integrin receptors (Roberts, 1995). Data suggests that a specific cell

population in the early stages of wound healing is optimally targeted by TGF-β since single applications of TGF-β applied topically at the time of wounding are as effective as repeated doses on scar formation (Beck et al., 1990). TGF-β increases collagen synthesis by upregulating procollagen I, II or VI, and parallels the increase in scar strength, even though collagen cross-linking is not a major determinant of TGF-β-dependent improvements in wound repair (Pierce et al., 1991). The increased expression of collagen genes seems to be partly mediated by increased transcription of collagen mRNAs through effects of TGF-β on nuclear factor 1 (NF1) and Sp1 binding sites on the collagen promoter (Inagaki et al., 1994b; Rossi et al., 1988).

A defined interaction exists between the ECM and TGF-β. This interaction can be bidirectional in that a disruption in the basement membrane can contribute to prolonged and increased TGF-β expression (Lankat-Buttgereit et al., 1991). In addition, TGF-β enhances the wound healing response in compromised conditions (like corticosteroid treatment, irradiation, treatment with anti-neoplastic agents, diabetes, and hypoxia) to levels comparable to those of normal tissue (Cromack et al., 1991). Also, fetal wounds contain very little TGF-β and heal without scarring, suggesting a critical role of TGF-β in fibrosis (Piscatelli et al., 1994). The accumulation of ECM in fibrosis may not only be due to a result of increased TGF-β expression but also defects in the signaling pathways that usually suppress ECM formation (Streuli et al., 1993).

In several animal models, it has been shown that post-surgical administration of TGF-β increases the incidence of fibrosis, while neutralizing antibodies to TGF-β effectively reduce the incidence of scarring (Cordeiro et al., 1999a). In rat incision wounds, injections of neutralizing antibodies to TGF-β1 and TGF-β2 at the time of

wound formation reduced inflammation, angiogenesis, and matrix deposition (Shah et al., 1994b). These wounds healed without scarring or the histological appearance of scar tissue. Additionally, subcutaneous injections of TGF-β into mice led to the formation of granulation tissue within two to three days, characterized by induction of neutrophils, macrophages, fibroblasts, and endothelial cells surrounded by newly formed collagen networks (Inagaki et al., 1994a). The effects of TGF-β were reversible, suggesting that availability of TGF-β is important in determining the duration and course of fibrosis. These experimental data suggest that TGF-β is a key mediator of stromal scarring.

TGF-β and Stromal Wound Healing

In corneal cells, the TGF-β isoforms and TGF-β receptors are expressed both in normal tissue and in the wound healing process after injury (Frank et al., 1996). To better understand stromal scarring, the effects of the TGF-β system must be examined fully. The TGF-β isoforms directly stimulate fibroblasts to synthesize ECM proteins including collagen and proteoglycans and suppress the synthesis of matrix metalloproteinases (MMPs) while simultaneously increasing synthesis of the tissue inhibitors of matrix metalloproteinases (TIMPs) (Border and Noble, 1994a;Roberts et al., 1986). In addition, the TGF-β isoforms upregulate their own synthesis by fibroblasts which leads to a prolonged TGF-β response utilizing an autocrine path. These combined actions are hypothesized to occur after excimer laser PRK and lead to the deposition of ECM in the cornea that is clinically visualized as subepithelial haze.

The molecular mechanism and action of the TGF-βs were poorly understood until the recent elucidation of a TGF-β signal transduction network. The three primary isoforms of TGF-β (TGF-β1, 2, and 3), whose biological properties *in vitro* are extremely

similar, exert their effects through TGF-β type I and type II receptors with serine-threonine kinase activity. The type II receptor appears to be required for the signaling by the type I receptor and thus, is the key receptor in the TGF-β response system (Wrana et al., 1994a). TGF-β binds directly to the type II receptor which is a constitutively active kinase. The bound TGF-β is then recognized by type I receptor, which is recruited into the complex and becomes phosphorylated by the type II receptor. Phosphorylation allows the type I receptor to propagate the signal downstream substrate through the *Smad* family (Wrana et al., 1994b;Heldin et al., 1997a). The proteins of the *Smad* family were the first identified substrates of the type I TGF-β receptor kinase and act as the intracellular signal transducer in the TGF-β response pathway. As shown in cell culture studies, *Smad2* and/or *Smad3* are phosphorylated by the type I receptor and form a complex with Smad4 followed by translocation of the complex from cytoplasm to nuclei (Heldin et al., 1997b;Nakao et al., 1997b). The translocated *Smad* complexes recruit transcription factors to form a complex and initiate transcription of genes. Some relevant genes such as collagen type I, fibronectin and type 1 plasminogen activator inhibitor (PAI-1) have been proven to be regulated by TGF-β at the transcriptional level by Smad signal transduction pathway (Nakao et al., 1997a).

Connective Tissue Growth Factor (CTGF)

Connective tissue growth factor (CTGF) is a secreted, cysteine-rich peptide of about 38 kilodaltons. It was discovered in 1991 in the conditioned medium of cultures of human umbilical vein endothelial cells (HUVEC). While a study was being performed on the role of platelet-derived growth factor (PDGF) in HUVEC cells, a new peptide that appeared to be responsible for the PDGF-related mitogen activity in the conditioned

medium was identified and called CTGF (Bradham et al., 1991e). Amino acid analysis revealed that the peptide showed a 45% overall homology to the translational product of the v-src-induced CEF-10 mRNA from chicken embryo fibroblasts. CTGF is a heparin-binding protein and has been shown to be secreted by fibroblasts after activation with TGF-β. CTGF is aptly named, because it has been identified as a major chemotactic and mitogenic factor for cells of the connective tissue, and has PDGF-related biological and immunological properties.

CCN Gene Family

The CTGF gene is located on chromosome 6q23.1, proximal to the *c-myb* gene (Bradham et al., 1991d). It belongs to a family of peptides including serum-induced immediate early gene products such as cyr61, fisp12, a v-src-induced putative gene (CEF-10), and a putative avian transforming gene (nov) (Bradham et al., 1991c;O'Brien and Lau, 1992;Martinerie et al., 1992b). Sequence similarity also exists between CTGF and the twisted gastrulation (*tsg*) gene, one of seven known zygotic genes specifying the fate of dorsal cells in the embryos of *Drosophila* (Mason et al., 1994). This family of peptides (shown in Table 1-2) is characterized by conservation of thirty-eight cysteine residues between species, comprising just over 10% of the total amino acid content. This family also contains a sequence homology of 30-38% to the low-affinity IGF-binding proteins (IGFBPs), and has the conserved IGFBP motif (GCGCCXXC) in the amino terminus with up to seventeen of the cysteines conserved in the IGFBPs (Brigstock, 1999). It has been suggested that CTGF is another member of the low-affinity IGFBP group of genes. This family, along with the high-affinity IGFPB gene make up an

IGFBP superfamily that regulates normal as well as neoplastic growth (Kim et al., 1997a).

The mouse ortholog to CTGF is most likely fisp-12 since it has a 93-94% amino acid sequence homology to human CTGF. Similarly, the *nov* transcript is derived from a distinct gene known as *nov* in humans (Snaith et al., 1996), frog (Ying and King, 1996), mouse (Liu et al., 1999), and chicken (Martinerie et al., 1992a). Additionally, *cyr61* (in humans, frog, and chicken) and *cef10* (in mice) appear to be homologous indicating that at least three distinct genes encode these peptides (CTGF/fisp-12, cef10/cyr61, and nov). Currently, this family has been termed CCN (Bork, 1993d). This suggests that CTGF-related peptides function in a wide array of biological activities ranging from normal embryonic development to tissue regeneration, tumor formation and growth.

Table 1-2: Classification of members of the CCN gene family

Species	CTGF	Nov	Cyr
Homo sapiens (human)	CTGF	h-nov	h-Cyr61
Xenopus laevis (frog)	xCTGF	x-nov	—
Gallus gallus (chicken)	cCTGF	nov	Cyr61
Mus musculus (mouse)	fisp-12	m-nov	CEF10
Drosophila melanogaster (fruit fly)	*Tsg*	—	—

CTGF Protein Structure

The CCN family of proteins reveal four distinct modules, each encoded by a separate exon and possess a signal peptide through normal secretory pathways (Bork, 1993c). Two cysteine-rich domains exist separated by a cysteine-free hinge region in the middle of the peptide (shown in Figure 1-1). An even number of cysteines are present in

each module (22 in the N-terminus and 16 in the C-terminus), possibly contributing to independent disulfide bridges. Mild protease digestions show cleavage in the cysteine-free region yielding separate N- and C-terminal domains without denaturation or reduction of disulfides in the other modules. Overall, this suggests that the protein has two disulfide cross-linked domains separated by a cysteine-free hinge region. Furthermore, extensive proteolytic digestion fails to cleave the cross-linked domains into smaller fragments, suggesting the disulfide bonds are resistant to proteolysis.

The amino-terminus of this protein contains two motifs which may be responsible for its binding to other growth factors (Bork, 1993b). Adjacent to the signal peptide is a sequence encoded in exon 2 which is nearly identical to the IGFBP motif, most likely responsible for its IGF binding property. The second domain is similar to von Willebrand factor type C which is present as a single copy in the CCN peptide family and as multiple copies in *tsg*, all containing multiple cysteine residues (Bork, 1993a). This motif functions to interact with other growth factors to cause complex or dimer formation (Tanaka et al., 2001).

The carboxy-terminus of the CCN family of peptides shares a disulfide linkage pattern with PDGF, TGF-β, and nerve growth factor (NGF), which are involved in heparin binding (Bork, 1993e). The first domain in the C-terminus is the thrombospondin type I repeat which is present in several extracellular matrix proteins. One function of this domain is binding interaction with glycoconjugates such as glycosaminoglycans (Incardona et al., 1996). This domain possesses a high-affinity for heparin, which has similarity to other growth factors such as bFGF and heparin-binding epidermal growth factor (EGF) (Grotendorst, 1997a). The discrete region of the domain

responsible for heparin binding has not yet been identified. The final motif contains six cysteine residues also found in the growth factors PDGF, TGF-β, and NGF. The dimeric nature of TGF-β and PDGF exists due to disulfide bridges not found in CTGF (Murray-Rust et al., 1993). The structural relationship of the heparin-binding domains to known growth factors suggest that CTGF could be involved in signaling and receptor binding.

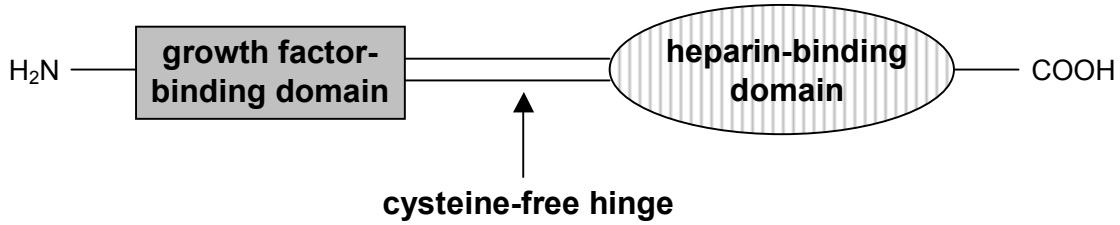

Figure 1-1. Domain structure of the CTGF protein.

CTGF and Fibrosis

The expression of CTGF is believed to be limited to cells derived from the mesenchyme including fibroblasts, vascular endothelial cells, smooth muscle cells, chondrocytes, and renal tubule cells (Dammeier et al., 1998a). Lymphocytes, leukocytes and cells derived from the epithelium of embryos are not known to express CTGF. It is also over-expressed in a variety of fibrotic disorders such as scleroderma (Kikuchi et al., 1995a), systemic sclerosis (Sato et al., 2000), atherosclerosis (Hishikawa et al., 1999b), internal organs in idiopathic pulmonary fibrosis (Igarashi et al., 1998b), liver fibrosis (Ksander et al., 1990), diabetic glomerulosclerosis (Ito et al., 1998a), and renal fibrosis (Goldschmeding et al., 2000). In addition it is over-expressed in tumors such as pancreatic carcinoma (Wenger et al., 1999b), malignant fibrous histocytoma (Igarashi et al., 1998a), and human breast cancer specimens (Hishikawa et al., 1999d). High expression of CTGF mRNA has been detected in myofibroblasts in the fibrotic tissues

surrounding invasive tumors even though TGF-β was not found (Hishikawa et al., 1999c). CTGF may also be important in the formation and stabilization of atherosclerotic plaques since it is expressed abundantly in human aortic smooth muscle cells and induces apoptosis through growth inhibition (Hishikawa et al., 1999a). Together, these results suggest that CTGF plays an important role in stimulating the proliferation of connective tissue and the extracellular matrix.

A wide variety of important biological processes such as normal embryonic development and tissue regeneration seem to be regulated by CTGF-related gene products. Since recombinant CTGF has been produced, it is possible to investigate the biological activity of this growth factor on cells in culture and its possible functions in physiology *in vivo*. Unstimulated mesangial cells in the kidney express and secrete minimal amounts of CTGF protein and minimal amounts of CTGF were secreted from the cells. However, when these cells were treated with sodium heparin, a four-fold increase in media-associated CTGF was observed, suggesting that the major amount of CTGF was matrix-bound. The addition of TGF-β markedly increased the amount of CTGF mRNA (Riser et al., 2000). In a separate study, CTGF has been shown to act as a mitogen in cultures of normal rat kidney fibroblasts, which is enhanced with the addition of either EGF or heparin. In the same study, CTGF also increased the mRNA transcripts for type I collagen, α5 integrin, and fibronectin (Frazier et al., 1996d). Thus, similarly to TGF-β, CTGF can induce connective tissue cell proliferation and ECM synthesis, differentiating it from EGF, FGF, and PDGF, which do not contribute significantly. These experiments show that CTGF was similar but not identical properties to TGF-β,

suggesting that it may function as a downstream mediator of some of the actions of TGF-β.

Limited information is available on the expression of CTGF in ocular tissues. One study showed the expression and localization of CTGF mRNA in human retrocorneal and subretinal fibrovascular membrane specimens using in situ hybridization (Wunderlich et al., 2000d;Meyer et al., 2002). Other studies show the expression of CTGF in human aqueous humor, human tear fluid, and pterygia samples, suggesting a possible involvement of CTGF in ocular pathology (van Setten et al., 2002b;van Setten et al., 2003;Van Setten et al., 2003). An additional study shows that the addition of TGF-β to cultures of rabbit corneal fibroblasts induces the expression of CTGF mRNA and protein although the properties of rabbit corneal fibroblasts in culture have proven to be quite different from human cultures (Folger et al., 2001a). Since the role of CTGF appears to be so crucial in the regulation of fibrosis in other tissues, its expression and role in the normal and fibrotic cornea needs to be assessed as a target for reducing fibrosis.

CTGF as a Mediator of TGF-β Action

The link between TGF-β and CTGF is clear in its role in the regulation of normal and fibrotic pathophysiology. The fact that TGF-β induces expression of CTGF in almost every mesenchymal cell type suggests that expression of CTGF is necessary to mediate some of the actions of TGF-β on inducing extracellular matrix synthesis and regulating cell proliferation. TGF-β is known to affect many genes that are involved in wound healing, but it is the effect it has on expression of CTGF that may be one of the most important factors in understanding the regulation of stromal scarring

CTGF Gene Regulation

CTGF is known to be induced by TGF-β but not by other related growth factors like EGF, PDGF, FGF, insulin or IGF (Grotendorst et al., 1996d). Most likely this is due to different signal transduction pathways induced upon activation by TGF-β, which activates a serine/threonine protein kinase receptor, as opposed to other growth factors like EGF, FGF, PDGF, insulin and IGF, which activate tyrosine kinase receptors (Ohtsuki and Massague, 1992;Ullrich and Schlessinger, 1990). The CTGF promoter has a TGF-β-inducible element, which is another mechanism for inducing the expression of CTGF mRNA by TGF-β. Examination of the CTGF promoter has revealed multiple consensus elements that are similar to other growth factor genes like the CArG box and AP-1/SP-1 sites. The sequences are present although they do not appear to be required for TGF-β induction of the CTGF gene (Grotendorst et al., 1996c). Other regions of the human CTGF promoter include nucleotide sequences that are related to two other reported TGF-β control elements, NF-1 and the TGF-β inhibitory element. Analysis of deletion mutants indicated that neither element was necessary for TGF-β induction, and that an important TGF-β regulatory element was located between positions –162 and –128 of the CTGF promoter sequence (Grotendorst et al., 1996b).

Extended expression of CTGF transcripts for 24-48 hours has been noted after only a brief one-hour exposure to TGF-β. In another experiment, brief treatment of human skin fibroblasts with TGF-β for 1 hour gave nearly the same fold induction of CTGF gene transcription as either 4 or 24 hours of treatment (Grotendorst et al., 1996a). The induction of CTGF mRNA in fibroblasts in response to TGF-β is not blocked by protein synthesis inhibitors such as cycloheximide, even after a brief exposure in

combination with TGF-β. These results confirmed that transcriptional regulation by TGF-β is a component of the mechanism for induction of CTGF expression.

CTGF-Mediated TGF-β Signaling

TGF-β is thought to influence CTGF by either direct or indirect pathways. With these hypotheses, TGF-β is believed to have an effect on cells via CTGF or synergistically with CTGF to induce a cellular response. TGF-β has the ability to stimulate the growth of fibroblasts in soft agar, which is a property typical of transformed cells. On the other hand CTGF cannot induce anchorage independent growth of NRK fibroblasts. Also, neutralizing antibodies to CTGF specifically blocked TGF-β-induced anchorage-independent growth (AIG), while other growth factors including PDGF, FGF or EGF were not effective as mitogens on cells in culture. In addition, clones of normal rat kidney (NRK) fibroblasts that express an antisense-CTGF gene blocked the expression of endogenous CTGF but do not respond to TGF-β in the AIG assay. In an identical assay the addition of pure recombinant CTGF to the media restored the growth of cells (Kothapalli et al., 1997a). These studies show that TGF-β stimulation of NRK fibroblast AIG acts via the synergistic pathway probably by CTGF downstream stimulation.

In the same study, the ability of CTGF to induce collagen synthesis (a component of the ECM) was examined. *In vitro* and *in vivo* studies were performed to determine whether CTGF was also essential for TGF-β-induced collagen synthesis (Duncan et al., 1999k). *In vitro* studies with NRK fibroblasts demonstrated that CTGF potently induced collagen synthesis and transfection. Additionally, an antisense to the CTGF gene blocked induction by TGF-β. Moreover, TGF-β induced collagen synthesis in NRK fibroblasts

and human foreskin fibroblasts was effectively blocked with specific anti-CTGF antibodies. A similar result was also observed by suppressing TGF-β- induced CTGF expression by elevating intracellular cAMP levels in the same report with either membrane-permeable 8-bromo-cAMP or an adenylate cyclase activator such as cholera toxin (Duncan et al., 1999). These data indicate that CTGF mediates TGF-β induced fibroblast collagen synthesis and that *in vivo* blockade of CTGF synthesis. TGF-β also induced granulation tissue formation via CTGF by inhibiting both collagen formation as well as fibroblast accumulation.

Study Design and Rationale

Although limited information is available on the role of CTGF in the cornea, most reports suggest that it might play a significant role in corneal fibrotic disorders (Wunderlich et al., 2000c;Folger et al., 2001b). Based on the reported effects of CTGF in other fibrotic conditions and initial experiments, it is the overall hypothesis that CTGF is a major regulator of corneal scar formation and mediates many of the fibrotic effects of TGF-β in corneal scarring. It is hypothesized that levels of CTGF mRNA and protein will increase in rat corneas during healing of excimer ablation wounds, and that all three TGF-β isoforms induce CTGF mRNA and protein in cultured human fibroblasts. It is also believed that CTGF will induce collagen synthesis, and most importantly, that inhibiting CTGF will block TGF-β-induced collagen synthesis in cultured human fibroblasts. Since limited information is available for the putative CTGF receptor (which will be addressed to greater detail in Chapter 4) characteristics of the receptors for CTGF on the surface of human corneal fibroblasts need to be obtained using a combination of

biochemical techniques that include chemical cross-linking of ^{125}I-CTGF to cultured fibroblasts, CTGF affinity column chromatography and immunoprecipitation.

The proposed model of CTGF induction of corneal scarring is illustrated in Figure 1-2. Epidermal growth factor (EGF) and transforming growth factor alpha (TGF-α) are produced by the lachrymal gland and are present in tears. Activated macrophages and neutrophils from the inflammation response also release TGF-β. The binding of TGF-β activates the synthesis and release of CTGF from the stromal fibroblasts within the cornea. These fibroblasts are also stimulated to produce even more TGF-β, which stimulates more cells to produce CTGF. When CTGF is released, it binds to receptors on the stromal fibroblasts or perhaps the epithelium and/or endothelium and signals the synthesis of collagen I, III, and IV, as well as fibronectin. CTGF also stimulates cell proliferation within the stroma so that the effect is amplified.

Although sufficient information is available showing that CTGF is a mitogen for fibroblasts and a strong inducer of collagen synthesis, very little is known its regulation of other genes. The most effective method to understand the broad actions of CTGF on corneal gene expression and wound healing is to use microarray GeneChip technology to initially identify genes that are changing. This technology can be used to identify a number of genes that are up-regulated or down-regulated by CTGF. This information will be used to test previous hypotheses about corneal wound healing and to generate new hypotheses about how CTGF influences scar formation. A long-term goal of this research is to develop agents that reduce corneal scarring by selectively reducing the expression of fibrotic genes such as TGF-β and CTGF. In this work, antisense

oligonucleotides and ribozymes to CTGF will be developed and optimized to evaluate the anti-scarring effects of these powerful agents on corneal wound healing animal models.

The general goal of this dissertation is to understand the molecular regulation of stromal scarring and the role that CTGF plays in regulating corneal scarring and to develop new anti-scarring agents, targeting CTGF and related genes.

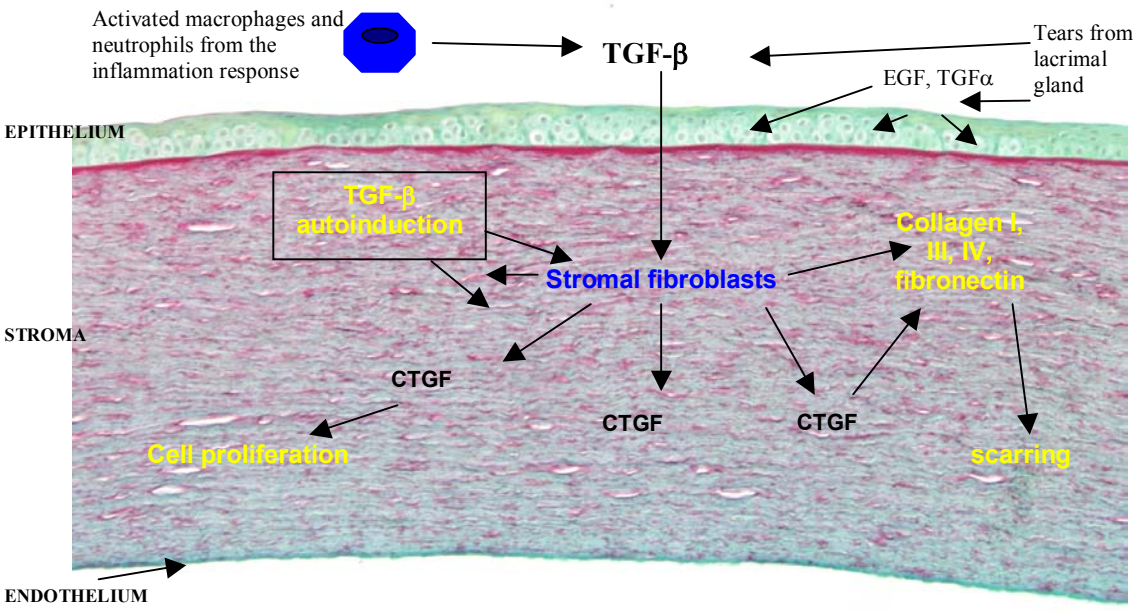

Figure 1-2. The proposed role of connective tissue growth factor (CTGF) in corneal fibrosis.

CHAPTER 2
GENERAL METHODS

Experimental Animals

Adult male Sprague-Dawley rats (200-250 g) were purchased from Harlan (Indianapolis, IN). All rats were housed in pairs in air-conditioned rooms (22-25° C) with 14 hours of lights per day. Constant food and water were available to all animals. Rats were euthanized at the end of the experiments with intraperitoneal injection of pentobarbital (Beuthanasia-D Special). Mice used for all experiments were housed four per cage in a similar environment. Mice were euthanized by cervical dislocation at the end of the experiments. All animal protocols were approved by the Institutional Animal Care and Use Committee (IACUC) at the University of Florida.

Photorefractive Keratectomy

Adult Sprague-Dawley male rats (200-250 g) with normal eyes were anesthetized with an intraperitoneal injection of sodium pentobarbital (30 mg/kg). Eyelashes and whiskers surrounding the eye were removed from the visual field. A drop of proparacaine-HCl (0.05%) was applied to the eye and the cornea was centered under the laser microscope. Bilateral excimer laser photorefractive keratectomy was performed (Chen et al., 2000h). Briefly, corneas were ablated in a 4.4-mm treatment zone with an excimer laser (Summit SVS Apex) in the phototherapeutic keratectomy mode. The corneal epithelium was ablated to a depth of 40 μm, followed by ablation of the stroma to a depth of 20 μm for a total ablation depth of 60 μm. After excimer laser treatment,

tobramycin (0.3%) ointment was applied to the corneal surface to prevent infection. No postoperative topical steroid was administered.

Sample Collection

On the appropriate day following excimer laser keratectomy, rats were euthanized as described earlier. The corneas were harvested with the aid of an operating microscope. Briefly, a 3-mm disposable biopsy punch was used to groove the cornea and enter the anterior chamber of the eye, followed by completion of tissue excision using Vannase scissors and Maumenee forceps. Corneal buttons were snap frozen in liquid nitrogen, placed in polypropylene 1.5-ml microcentrifuge tubes, and stored at -80° C until further analysis. Normal, unoperated rats were sacrificed at each of the time points to obtain control (Day 0) corneas.

Tissue Sectioning and Processing

After standard histological processing and embedding in paraffin blocks, 6 micrometer thick sections were cut with a microtome. Tissue sections were deparaffinized by two incubations in xylene for ten minutes, hydrated through absolute alcohol, 95% alcohol, 75% alcohol and 50% alcohol for ten minutes at each step followed by a 1 minute wash in distilled water. Endogenous peroxidase activity was quenched by incubation with 0.03% H_2O_2 for 60 minutes at room temperature. Tissue sections were gently rinsed in distilled water, washed for five minutes and wash buffer (5 mM Tris, 300 mM NaCl, 0.1% Tween 20, pH 7.4) containing 2% goat serum and 5% bovine serum albumin (BSA) was added and allowed to incubate for 60 minutes at room temperature.

Immunohistochemical localization was then achieved through affinity-purified primary and secondary antibodies followed by the appropriate detection reagents.

Microscopy

Tissue sections mounted on glass slides were photographed using either bright field illumination or fluorescence microscopy with excitation/emission wavelengths for Texas Red staining, and Nomarski phase-contrast microscopy at 200x magnification. Photographs were taken at a constant exposure using a Peltier-cooled Olympus digital camera. Cell cultures fixed with paraformaldehyde or methanol on glass slides were photographed in a similar fashion, using an inverted-phase microscope using either bright field illumination or fluorescence microscopy with excitation/emission wavelengths for Texas Red staining.

CHAPTER 3
CONNECTIVE TISSUE GROWTH FACTOR EXPRESSION AND ACTION IN THE CORNEA

Introduction

Connective tissue growth factor (CTGF) is a secreted, cysteine-rich monomer of about 38 kDa that was originally identified as a mitogen for fibroblast in conditioned media cultures from human umbilical vein endothelial cells (Bradham et al., 1991b;Ryseck et al., 1991;Frazier et al., 1996c). CTGF belongs to the CCN (CTGF, Cyr61/Cef10, Nov) family of secreted cysteine-rich proteins, which possess important growth regulatory functions and are involved in cell differentiation (Hashimoto et al., 1998a;Hurvitz et al., 1999;Albrecht et al., 2000). However, the most important biological action of CTGF may be in stimulating synthesis of extracellular matrix components. When added to cultured human skin fibroblasts, CTGF dramatically increased synthesis of collagen, integrin, and fibronectin, and subcutaneous injections of CTGF into mice produced granulation tissue and fibrosis in the skin (Frazier et al., 1996b). This finding led to investigations of the possible role of CTGF in fibrotic diseases. CTGF mRNA was significantly elevated in the left ventricles of rat hearts following myocardial infarction, which correlated well with concomitant increases in fibronectin, and type I and type III collagen mRNA levels and development of cardiac fibrosis in the animal hearts (Chen et al., 2000i). Significant upregulation of CTGF was detected in human heart samples derived from patients diagnosed with cardiac ischemia. Elevated CTGF protein and mRNA levels were found in sclerotic skin fibroblasts (Igarashi et al., 1995), specimens of

inflammatory bowel disease (Dammeier et al., 1998b), in retrocorneal membranes (Wunderlich et al., 2000b), and overexpression of CTGF was linked to human renal fibrosis (Ito et al., 1998b).

The transforming growth factor beta (TGF-β) system (Border and Noble, 1994b;Perkett, 1995;Perkett, 1995) has also been implicated in promoting scarring and fibrosis in numerous tissues including lung (Westergren-Thorsson et al., 1993), kidney (Border et al., 1992), liver (Castilla et al., 1991), and pancreas (Vogelmann et al., 2001). Furthermore, agents that reduced the activity of the TGF-β system by selectively targeting TGF-β or its receptors reduced scarring in several animal models of tissue fibrosis (Castilla et al., 1991;Border et al., 1990;Jester et al., 1997). Recently, two important links between CTGF and the TGF-β system were reported that added weight to the concept that CTGF plays important roles in scarring. First, TGF-β1 induced synthesis of CTGF in cultured normal rat kidney fibroblasts (Frazier et al., 1996a), and second, neutralizing antibodies to CTGF blocked collagen synthesis induced by TGF-β in rat and human fibroblasts (Duncan et al., 1999i). These results indicated that CTGF could be a downstream mediator of some of the scarring effects of TGF-β.

The CTGF system has not been investigated in corneal wound healing. To help assess the hypothesis that CTGF regulates corneal scarring, the influence of TGF-β isoforms on expression of CTGF in human corneal fibroblasts was investigated as well as the role of CTGF in mediating the effects of TGF-β on CTGF levels and collagen synthesis by cultured human corneal fibroblasts. Finally, the levels of CTGF protein and mRNA in rat corneas after PRK were measured and CTGF protein was localized in healing rat corneas.

Materials and Methods

Cell Culture

Cultures of human corneal fibroblasts were established by outgrowth from corneal explants as described previously (Woost et al., 1992). Briefly, epithelial and endothelial cells were removed from corneas that were unsuitable for corneal transplantation, the stroma was cut into cubes approximately 1 mm^3, placed in culture medium consisting of equal parts Dulbecco's Modified Eagle Medium (DMEM), Medium 199 (Gibco BRL), Ham's F_{12} nutrient mixture (Gibco BRL) containing 1 mM $NaHCO_3$, and buffered with 25 mM HEPES at pH 7.4. The medium was supplemented with 10% heat-inactivated normal calf serum and 1x antibiotic-antimycotic (Gibco BRL). Cell cultures used between passages 2 and 5 for all experiments.

Induction of CTGF by TGF-β Isoforms in Human Corneal Fibroblast Cultures

Cultures of corneal fibroblasts were washed and placed in serum-free medium for 24 hours then the medium was replaced by three different concentrations of TGF-β1, TGF-β2, and TGF-β3 isoforms (0.1, 1.0, and 10 ng/ml) (R&D Systems, Minneapolis, MN). After 48 hours of incubation, the conditioned medium was removed, centrifuged, the supernatant solution frozen at -80°C until the samples were assayed for CTGF using the ELISA described below. The cells in each well were also collected by scraping and frozen at -80°C and total RNA was isolated as described below for measurement of mRNA levels using TaqMan quantitative RT-PCR as described below. Each level of TGF-β was assayed in three replicate wells, and results were analyzed using ANOVA/MANOVA and Tukey's HSD post-hoc test.

CTGF Immunocytochemistry in Human Fibroblast Cultures

Human corneal fibroblasts were seeded into 48-well plates and grown to confluence in serum-supplemented medium. After incubation in serum-free medium containing insulin, transferrin, and selenious acid for 72 hours, fibroblasts were then cultured for an additional 48 hours with or without 5 ng/mL TGF-β. Cells expressing CTGF were then detected immunohistologically using a standard avidin-biotin amplification method. Briefly, cells were fixed in cold 4% paraformaldehyde, permeabilized with Triton-X-100, and blocked with 2% milk / 10% horse serum. Fibroblasts were then sequentially incubated with goat anti-human CTGF for 1 hour at room temperature, washed three times with Tris buffer saline (TBS, pH =7.4), incubated with biotinylated horse anti-goat IgG secondary antibody (Vector Labs, Burlingame, CA), washed, incubated with alkaline phosphatase conjugated streptavidin (Dako, Carpinteria, CA), washed, then incubated with Vector Red alkaline phosphatase visualization substrate. The goat anti-human CTGF antibody was raised against recombinant human CTGF protein and was purified with a CTGF-affinity column as described previously (Duncan et al., 1999h). The antibody predominately recognizes antigenic determinants on the N-terminal sequence of CTGF.

Photorefractive Keratectomy

Animal Procedures were performed in accordance with the ARVO statement for the Use of Animals in Ophthalmic and Vision Research and was approved by the University of Florida Animal Care and Use Committee. Twenty adult Sprague-Dawley male rats (250 g) with normal eyes were anesthetized with an intraperitoneal injection of sodium pentobarbital (30 mg/kg). Eyelashes and whiskers surrounding the eye were removed from the visual field. A drop of proparacaine-HCl (0.05%) was applied to the

eye and the cornea was centered under the laser microscope. Bilateral excimer laser photorefractive keratectomy was performed.(Chen et al., 2000g) Briefly, corneas were ablated in a 4.4-mm treatment zone with an excimer laser (Summit SVS Apex) in the phototherapeutic keratectomy mode. The corneal epithelium was ablated to a depth of 40 μm, followed by ablation of the stroma to a depth of 20 μm for a total ablation depth of 60 μm. After excimer laser treatment, tobramycin (0.3%) ointment was applied to the corneal surface to prevent infection. No postoperative topical steroid was administered. At 1, 3, 7, 11, 14, and 21 days after excimer laser ablation, rats were euthanized by peritoneal injection of pentobarbital. The corneas were excised using an operating microscope and snap-frozen in liquid nitrogen followed by storage at -80° C until analysis. Four rats were euthanized at each time point. Three rats from each time point were used for protein and RNA analysis. Corneas from the left eyes were used for protein analysis. Corneas from the right eyes were pooled and used to measure mRNA for CTGF. One rat from each time point was used for immunohistochemistry. Eight corneas from four rats that did not undergo excimer ablation were used as normal controls (Day 0).

Protein and RNA extraction

Whole corneas or epithelial scrapings were homogenized in 200 μL PBS/0.1% Triton-X-100 using a frosted glass-on-glass tissue grinder (Duall 22). Tissue extracts were centrifuged at 4° C at 15,000 x g for 15 minutes to remove cellular debris and membranes. The supernatants were measured for CTGF protein levels using an enzyme-linked immunosorbent assay (ELISA). Total RNA was extracted from pooled corneas by homogenization in TRIzol reagent (Invitrogen Life Technologies, Carlsbad, CA) using a frosted glass-on-glass tissue grinder. Total RNA was extracted from each sample using

chloroform, RNA was precipitated with 70% isopropanol at -20° C and washed with 70% ethanol. RNA pellets were dissolved in diethylpyrocarbonate (DEPC)-treated water and stored at -80° C. RNA concentrations isolated from each group were measured using a spectrophotometer (GeneQuant, Amersham/Pharmacia Biotech).

CTGF Sandwich ELISA

CTGF was measured in the conditioned medium of cultured cells and in tissue extracts using a capture sandwich ELISA with biotinylated and non-biotinylated affinity purified goat polyclonal antibodies to human CTGF which was produced using a baculovirus expression system as described previously (Duncan et al., 1999g). Briefly, a flat-bottom ELISA plate (Costar 96-well) was coated with 50 μL of goat anti-human CTGF antibody, which recognizes predominately epitopes in the N-terminal half of the CTGF molecule at a concentration of 10 μg/mL in PBS/0.02% sodium azide for 1 hour at 37° C. Wells were washed four times and incubated with 300 μL of blocking buffer (PBS/0.02% sodium azide/1% bovine serum albumin) for 1 hour at room temperature. This polyclonal antibody is appropriate for detection of rat CTGF because there is a 92% amino acid identity between the sequences of rat and human CTGF in the N-terminal half of the peptide (Moussad and Brigstock, 2000). The wells were washed four times and 50 μL of recombinant human CTGF protein (from 0.1 ng/ml to 100 ng/ml) or sample was added and incubated at room temperature for 1 hour. After washing, 50 μL of biotinylated goat anti-human CTGF (2 μg/mL) was added and incubated at room temperature in the dark for 1 hour, then washed, and 50 μL of alkaline phosphatase-conjugated streptavidin (1.5 μg/ml, Zymed, South San Francisco, CA) was added and incubated at room temperature for 1 hour. The wells were washed again and incubated

with 100 μL of alkaline phosphatase substrate solution (1 mg/mL p-nitrophenyl phosphate, Sigma Chemicals, St. Louis, MO) in sodium carbonate/bicarbonate buffer/0.02% sodium azide, pH = 9.6. Absorbance at 405 nm was measured using a microplate reader (Molecular Devices, Sunnyvale, CA). CTGF levels were normalized for total protein content of samples using bicinchoninic acid (BCA) protein assay reagent (Pierce Chemical, Rocckford, IL) and were expressed as ng/mg protein for three replicate samples for each condition. Sensitivity of the ELISA was 0.1 ng/ml with an intra-assay variability of 3%, which is similar to a previously published ELISA for CTGF (Tamatani et al., 1998).

CTGF TaqMan Assay

CTGF mRNA transcripts were detected using the TaqMan real-time quantitative RT-PCR procedure (Heid et al., 1996). The TaqMan technique for measuring mRNA levels is based on the 5' exonuclease activity of Taq polymerase on DNA/DNA oligonucleotide complexes (Holland et al., 1991). In addition to gene specific PCR primers, TaqMan uses a reporter probe that is coupled to two fluorescent dye molecules at the 5' and 3' ends of the probe (Livak et al., 1995). A standard curve was generated using CTGF mRNA transcripts that were transcribed *in vitro* from a plasmid containing CTGF cDNA. Briefly, electrocompetent *E. coli* cells (Stratagene, La Jolla, CA) were transformed with a plasmid (pRc/CMV, Invitrogen, Carlsbad, CA) containing the full length cDNA for human CTGF, colonies were selected with ampicillin, and 1 μg of isolated plasmid was transcribed using an *in vitro* transcription kit (Ambion, Houston, TX). CTGF mRNA was precipitated with ethanol and dissolved in DEPC-treated water. Reactions were assembled in a 96-well optical reaction plate. Each reaction contained 1x

TaqMan One-step RT-PCR Master Mix, 900 nM forward primer (5'-AGCCGCCTCTGCATGGT-3'), 900 nM reverse primer (5'-CACTTCTTGCCCTTCTTAATGGTTCT-3'), 2 μM fluorescent TaqMan probe (5'-6FAM-TTCCAGGTCAGCTTCGCAAGGCCT-TAMRA-3'), and RNA sample (CTGF mRNA standard or 500 ng of sample RNA) to a final volume of 25 μL per reaction. The plate was analyzed on the ABI Prism 5700 Sequence Detection System (Applied Biosystem, Foster City, CA), which simultaneously performs the RT-PCR and detects fluorescence signal. A standard curve was generated using the transcribed CTGF mRNA samples (2.3×10^{-2} to 2.3×10^{-6} pmol). The level of glyceraldehyde phosphate dehydrogenase (GAPDH) mRNA was also measured in each sample using the TaqMan GAPDH Control Kit (Applied Biosytems, Foster City CA), and the number of CTGF mRNA molecules in samples was expressed as pmol CTGF mRNA per pmol of GAPDH mRNA. Levels of mRNA were expressed as mean ± standard error of 3 replicate samples for each condition, and ANOVA and Tukey's HSD post-hoc test were used to assess statistical significance between times and groups.

Collagen synthesis assay

Collagen synthesis by human corneal fibroblasts was measured using ^{3}H-proline incorporation as described previously (Duncan et al., 1999f;Webster and Harvey, 1979). Briefly, cultures of human corneal fibroblasts were grown to confluence in serum supplemented medium, incubated in serum-free medium for 24 hours, then incubated 24 hours with eight different supplements: (1) serum-free medium; (2) 10% serum; (3) serum-free medium with 5 ng/mL TGF-β1; (4) 25 ng/mL CTGF; (5) 5 ng/mL TGF-β1 + 50 μg/mL goat anti-CTGF; (6) 5 ng/mL TGF-β1 + 50 μg/mL non-immune goat IgG; (7)

5 ng/mL TGF-β1 + 10 μM CTGF antisense oligonucleotide; (8) 5 ng/mL TGF-β1 + 10 μM control scrambled oligonucleotide (Dou et al., 1997). All treatments contained 50 μg/mL ascorbic acid and 1x insulin, transferrin, and selenious acid (ITS, Invitrogen Life Technologies, Carlsbad, CA) and 1 μCi tritiated proline (Amersham Biosciences, Piscataway, NJ). The CTGF antisense oligonucleotide was a 20-mer with the sequence GCCAGAAAGCTCAAACTTGA that contained phosphorothioate ester backbone modifications with 2-O-methoxyethylribose groups coupled at base positions 1 – 6 and 16 – 20, and 5-methylcytosine substituted for all cytosines (Dean and Griffey, 1997). The CTGF antisense oligonucleotide was identified by screening 81 separate 20-mer nucleotide sequences that span the mRNA sequence for reduction of CTGF mRNA in cultured mouse cells using RNase protection assay (data not shown). The scrambled 20-mer oligonucleotide control was a random mixture of AGCT bases. Addition of oligonucleotides into the culture medium penetrated membranes, accessed cellular mRNA and reduce levels of target gene mRNA (Dou et al., 1997). Wells were incubated overnight with pepsin in 0.5 M acetic acid, carrier collagen was then added and the solution was centrifuged, the collagen was precipitated and washed with 0.1 M sodium chloride in 0.1 M acetic acid and the radioactivity was measured with beta scintillation counter (Duncan et al, 1999). Results were expressed as cpm/well ± standard error for six replicate wells.

Reverse transcriptase polymerase chain reaction (RT-PCR)

Total RNA was extracted from epithelial cells obtained from *ex vivo* corneal scrapings from 6 rat corneas using Trizol as described above, and RT-PCR was performed using the one-step RT-PCR kit (Invitrogen Life Technologies, Carlsbad, CA)

to detect CTGF mRNA expression. Briefly, 10 μM of CTGF-specific forward primer (5'-AGTGTGCACTGCCAAAGATG-3') and reverse primer (5'-TTAGGTGTCCGGATGCACT-3') were added to 1 μg of total RNA isolated from the pooled rat epithelial cells along reverse transcriptase, nucleotides and buffer and 35 cycles of amplification were completed using an annealing temperature of 58° C, an extension temperature of 72ºC, and a dissociation temperature of 94ºC. Controls included omitting the sample RNA, reverse transcriptase, or both reverse transcriptase and Taq polymerase. PCR products were visualized on a 1.5% agarose gel with ethidium bromide and isolated using a PCR purification kit (Qiagen, Valencia, CA). The predicted 503-bp product was cleaved using a unique restriction site (*PstI*) into 405 and 98 bp fragments and were visualized on a 1.5% agarose gel with ethidium bromide.

CTGF Immunohistochemistry in Corneal Sections

Excised corneas from each time point were incubated in 4% para-formaldehyde / PBS overnight at 4° C and transferred to 70% ethanol. Paraffin sections were prepared and 5-micron thick sections were mounted on Superfrost/Plus microscopic slides (Fisher Chemicals, Pittsburgh, PA). Slides were deparaffinized and rehydrated using xylene and a graded series of ethanol. Slides were blocked for 30 minutes at room temperature in TBS/10% rabbit serum, incubated with affinity purified goat anti-human CTGF (14 μg/ml) in TBS/10% rabbit serum overnight at 4°C, washed and incubated with biotinylated rabbit anti-goat IgG in TBS/10% rabbit serum, washed then incubated with alkaline phosphatase conjugated streptavidin followed by Vector Red alkaline phosphatase visualization substrate (Vector Labs, Burlingame, CA). Sections were photographed using bright field illumination, fluorescence microscopy with

excitation/emission wavelengths for Texas Red staining, and Nomarski phase-contrast microscopy at 200x magnification. Photographs were taken at a constant exposure (430 ms) using a Peltier-cooled Olympus digital camera.

Results

Increased CTGF Expression by TGF-β Isoforms

All three TGF-β isoforms induced significantly higher levels of CTGF protein in conditioned medium and mRNA in cultures of human corneal fibroblasts (Figure 3-1). Furthermore, the levels of induction of CTGF mRNA and protein were dependent on the dose of the TGF-β isoforms. For example, the highest dose (10 ng/mL) of TGF-β1, TGF-β2, and TGF-β3 increased CTGF protein production 70-fold, 200-fold, and 160-fold, respectively, compared to cells cultured in serum-free medium ($p < 0.001$). Also, increasing concentrations of each isoform significantly increased higher levels of CTGF ($p < 0.05$). The largest increase in CTGF protein was produced by TGF-β2, which was significantly higher than TGF-β1 ($p < 0.05$).

All three TGF-β isoforms also significantly increased levels of CTGF mRNA when compared to control cells incubated with serum-free medium. CTGF mRNA transcripts were detected at 10- to 45-fold increased levels upon stimulation by TGF-β isoforms ($p < 0.001$). The results of these experiments suggest that TGF-β isoforms regulate CTGF expression at both the levels of transcription and translation. No significant difference between CTGF mRNA induced by the highest concentration of the three isoforms is noted. These data suggest that CTGF is regulated by TGF-β isoforms at both the transcriptional and translational level.

CTGF Mediated TGF-β-Induced Collagen Synthesis

The addition of 5 ng/mL of either TGF-β1 or CTGF increased collagen synthesis approximately 4-fold, (Figure 3-2). However, the increase in collagen synthesis produced by TGF-β1 was blocked 80% by a neutralizing goat anti-CTGF antibody, and was blocked 92% by an antisense oligonucleotide directed to human CTGF ($p < 0.001$). The antibody was shown to be neutralizing using the appropriate controls as shown previously (Duncan et al., 1999e). Blockage of collagen synthesis did not occur with addition of an irrelevant goat IgG or by scrambled oligonucleotides ($p < 0.001$). These experiments demonstrate that CTGF induced by TGF-β mediates the increase in collagen synthesis when TGF-β is added to cultures of human corneal fibroblasts. Because the antisense oligonucleotide and neutralizing antibody to CTGF did not reduce collagen synthesis to levels below that for serum-free, CTGF does not appear to mediate the basal level of collagen synthesis of corneal fibroblasts grown on plastic. Furthermore, the effects of the neutralizing antibody and the antisense oligonucleotide are not due to non-specific toxicity of the reagents.

Increased CTGF Immunostaining in Human Corneal Fibroblast Cultures

Intensity of immunostaining for CTGF was markedly increased in human corneal fibroblasts cultured for 48 hours with 5 ng/mL TGF-β1, especially in the perinuclear region when compared to non-stimulated cells (Figure 3-3). This localization is most likely due to increased levels of newly CTGF protein in the Golgi and secretory pathway. Furthermore, CTGF immunostaining is detected in essentially all the fibroblasts

indicating that TGF-β-induced CTGF synthesis is not restricted to a subpopulation of corneal fibroblasts.

CTGF Expression in Rat Corneas after PRK

The experimental *in vitro* data described above established that TGF-β induces CTGF synthesis, and that CTGF mediates the effects of TGF-β on collagen synthesis in cultures of human corneal fibroblasts. However, it is important to assess changes in levels of CTGF mRNA and protein change during healing of corneal wounds. As shown in Figure 3-4, levels of CTGF mRNA and protein significantly increased in rat corneas at several time points following PRK. Specifically, levels of CTGF mRNA increased in the corneas beginning at Day 3 following surgery after PRK when compared to non-operated control corneas. Furthermore, the mRNA levels progressively increased and remained statistically higher than normal corneas through Day 21, reaching approximately 1,000-fold higher levels than non-injured corneas.

Levels of CTGF protein tended to decrease during the first 3 days after PRK, perhaps reflecting fewer epithelial cells in the healing corneas. Beginning at Day 7 following surgery, levels of CTGF protein increased dramatically, which was slightly after mRNA levels begin to increase in the corneas, and continued to increase through Day 21 following surgery reaching approximately 10-fold higher levels than non-injured corneas. By Day 21, all corneas showed significant corneal haze, corresponding with elevated levels of CTGF. These data suggest that CTGF expression in rat corneas increases after PRK in a similar fashion as seen in the TGF-β stimulated corneal fibroblasts.

CTGF Immunohistochemistry in Rat Corneas Following PRK

CTGF was also immunolocalized in paraffin sections of rat corneas harvested at the same time points after surgery used for protein and RNA measurements. As shown in Figure 3-5, CTGF was detected in epithelial cells and stromal fibroblasts, with light staining in the stromal matrix of normal corneas before PRK ablation (Day 0). The fluorescence image (inset) emphasizes the intense staining of the epithelium. At Day 3 after injury, there was generally less intense staining in the epithelium and stroma. On Day 7, numerous fibroblast-like cells and inflammatory cells were present, which stained strongly for CTGF. On Days 11, 14, and 21, the epithelium continued to immunostain strongly for CTGF, corresponding to the increase in CTGF protein measured in corneal homogenates (Figure 3-4). On Day 21, intense immunostaining was present on the endothelium/Descemet's membrane. Negative controls that omitted the primary anti-CTGF antibody showed faint immunostaining when viewed in Nomarski-phase contrast, bright field, and fluorescence microscopy.

CTGF Expression in Corneal Epithelium

The immunostained corneas indicated high levels of CTGF protein were present in corneal epithelial cells and fibroblasts. To assess whether corneal epithelial cells synthesize CTGF mRNA and protein, CTGF ELISA and RT-PCR was performed on *ex vivo* corneal epithelium scrapings from normal rats, since corneal epithelial cell cultures were not available. CTGF ELISA detected substantial levels (1.5 ng/mg of total detergent-extracted protein) of CTGF protein in the corneal scrapings. In addition, RT-PCR generated an intense amplicon band of the predicted size (503 bp) using primers specific for rat CTGF cDNA. Furthermore, endonuclease restriction digestion using *PstI* generated two fragments with the predicted sizes (405 bp and 98 bp), indicating that the

amplicon contained the correct cDNA nucleotide sequence corresponding to rat CTGF mRNA (Figure 3-6).

Discussion

Multiple growth factors have been detected in the cornea, including epidermal growth factor (EGF), transforming growth factor alpha (TGF-α, basic fibroblast growth factor (bFGF), and interleukin-1 alpha (IL-1α), platelet derived growth factor (PDGF), and TGF-β, where they appear to play different and important roles in corneal wound healing (Wilson et al., 1994a;Hoppenreijs et al., 1993;Hoppenreijs et al., 1992). For example, Chen et al.(Chen et al., 2000f) reported that levels of mRNAs for TGF-β isoforms rapidly increased and remained elevated 90 days in rat corneas after PRK, which correlated with increases in mRNAs for Type I and Type III collagen and fibronectin and the development of corneal haze after PRK in rats. They also reported the clinical status of the rat corneas. Epithelial healing was complete by Day 7, and corneal edema increased on Day 1.5 but returned to normal by Day 7. Corneal haze progressively increased from Day 7 through Day 91 following PRK, with all corneas showing significant corneal haze on Day 21 (average clinical grade 0.83 on a 0 to 4 scale). The clinical evaluations reported previously by Chen et al (Chen et al., 2000e). correlated well with the progressive increases in levels of CTGF mRNA and protein measured in the corneas. Inhibition of TGF-β by repeated topical applications of neutralizing antibody reduced corneal haze in rabbits following lamellar keratectomy (Jester et al., 1997).

TGF-β also is a key regulator of conjunctival scarring. For example,

subconjunctival injections of TGF-β caused a rapid-onset and exaggerated scarring response in a mouse model of conjunctival scarring (Cordeiro et al., 1999c). Reducing TGF-β activity by repeated subconjunctival injections of a recombinant humanized mouse monoclonal antibody to TGF-β2 significantly reduced conjunctival scarring and improved glaucoma filtration surgery outcome in an aggressive rabbit model of filtration surgery scarring (Cordeiro et al., 1999b). These data led to a prospective, randomized, placebo-controlled, phase I/IIa clinical trial evaluating four subconjunctival injections of a neutralizing, humanized, mouse monoclonal antibody to TGF-β2 into the filtering bleb of trabeculectomy patients (Siriwardena et al., 2002a). Analysis of outcomes indicated the anti-TGF-β2 antibody produced greater declines in intraocular pressures at 3 and 6 months and fewer interventions than control injections without causing serious adverse events or complications (Siriwardena et al., 2002b).

One important finding demonstrates the upregulation of CTGF by TGF-β in cultured rabbit corneal fibroblasts (Folger et al., 2001c). However, the interactions between the TGF-β and CTGF systems in human corneal fibroblasts, and the alterations of CTGF expression during corneal wound healing have not been investigated previously. As shown in Figure 3-1, all three isoforms of TGF-β significantly increased CTGF mRNA and protein levels compared to fibroblasts in serum free medium. Although there was no significant difference in the levels of CTGF mRNA induced by the highest concentration of the TGF-β isoforms, the highest concentrations TGF-β2 and TGF-β3 (10 ng/ml) induced significantly higher levels of CTGF protein than TGF-β1. This suggests that all three TGF-β isoforms regulate CTGF synthesis by transcription of mRNA, but regulation of CTGF synthesis by TGF-β1 may also involve some post-

transcriptional regulation. Thus, during healing of wounds, corneal fibroblasts should respond to both TGF-β1 and TGF-β2 isoforms by increasing CTGF synthesis, even though TGF-β1 isoform predominates in human tears(Gupta et al., 1996) and TGF-β2 isoform predominates in aqueous humor (Jampel et al., 1990). Interestingly, corneal fibroblasts also increased CTGF synthesis in response to TGF-β3 isoform, which was reported to oppose the scarring effects of TGF-β1 and TGF-β2 isoforms in a rat skin incision model (Shah et al., 1994a).

Another important interaction between the TGF-β and CTGF systems is shown in Figure 3-2. Specifically, addition of CTGF antisense oligonucleotide or CTGF neutralizing antibody blocked over 85% of the increased collagen synthesis induced by TGF-β1. This demonstrates that synthesis of CTGF is required for TGF-β to increase collagen synthesis. However, neither antisense oligonucleotide nor neutralizing antibody totally suppressed the effect of TGF-β nor was collagen synthesis reduced below basal levels for fibroblasts cultured in serum free medium. This may be due to suboptimal levels of the antisense oligonucleotide and antibody, the presence of other autocrine factors that stimulate collagen synthesis such as PDGF, or to a low constitutive level of collagen synthesis by fibroblasts grown on plastic, perhaps through activation of integrin receptors. Nevertheless, antisense oligos or ribozymes targeting CTGF might be effective therapies for selectively reducing corneal scarring.

The *in vitro* experiments shown in Figures 3-1 and 3-2 strongly indicated that TGF-β and CTGF systems are linked and that CTGF is an important inducer of collagen synthesis. If the hypothesis that CTGF is a major promoter of corneal scarring *in vivo* is correct, levels of CTGF mRNA and protein should increase in corneas during wound

healing and scar formation. As shown in Figure 3-4, analysis of rat corneas showed little change in levels at 1 day after PRK, followed by a sharp increase in mRNA at Day 3 with a continual and almost exponential increase in mRNA levels, reaching a 1,000-fold increase on Day 21. Protein levels slightly lagged mRNA levels, with a slight decrease on Day 3 followed by a nearly 10-old linear increase to Day 21. Since CTGF is a secreted protein, it is expected that the levels of CTGF measured in the detergent extracts of the corneal homogenates to represent only a small portion of the total CTGF protein that was synthesized by corneal cells.

Immunostaining indicated the sources of CTGF protein appeared to be the fibroblasts, inflammatory cells and epithelial cells, which stained intensely. Previous reports suggested that synthesis of CTGF was limited to cells of mesenchymal origin (Grotendorst, 1997c). However, corneal epithelial cells are derived from surface ectoderm (Barishak, 1992). CTGF immunostaining in the epithelial cells could be due to synthesis of CTGF or to other sources of CTGF such as the tears. Unpublished findings showed that CTGF was detected in human tears at an average level of 6.2 ng/ml. RT-PCR analysis performed on samples of total RNA isolated from corneal epithelial cells scraped from rat corneas generated a single amplicon with the predicted size, which was cleaved into the unique fragments predicted by endonuclease digestion, which strongly supports the concept that corneal epithelial cells synthesize CTGF (Figure 3-6). The intensity of CTGF immunostaining roughly followed the levels of CTGF protein measured by ELISA in rat corneas, with intense staining observed in the epithelium at Day 21 and strong staining in fibroblasts and endothelial cells/Descemet's membrane. It was recently reported that CTGF protein was present in aqueous humor at an average

concentration of 1.24 ng/ml (van Setten et al., 2002a). CTGF may be bound to extracellular matrix proteins and glycosoaminoglycans in basement membrane since CTGF possesses a heparin-binding domain (Grotendorst, 1997b).

In summary, the interaction between TGF-β and CTGF systems in corneal fibroblast cultures, their regulation of collagen synthesis, and the expression and localization of CTGF in the cornea during wound healing after PRK was investigated. Collectively, the data strongly support the hypothesis that CTGF is induced by TGF-β, mediates the effects of TGF-β on collagen synthesis, increases dramatically during corneal wound healing and is likely to be a key regulator of corneal wound healing. These results suggest that CTGF may be a key target for therapies that reduce scarring by selectively reducing expression of CTGF.

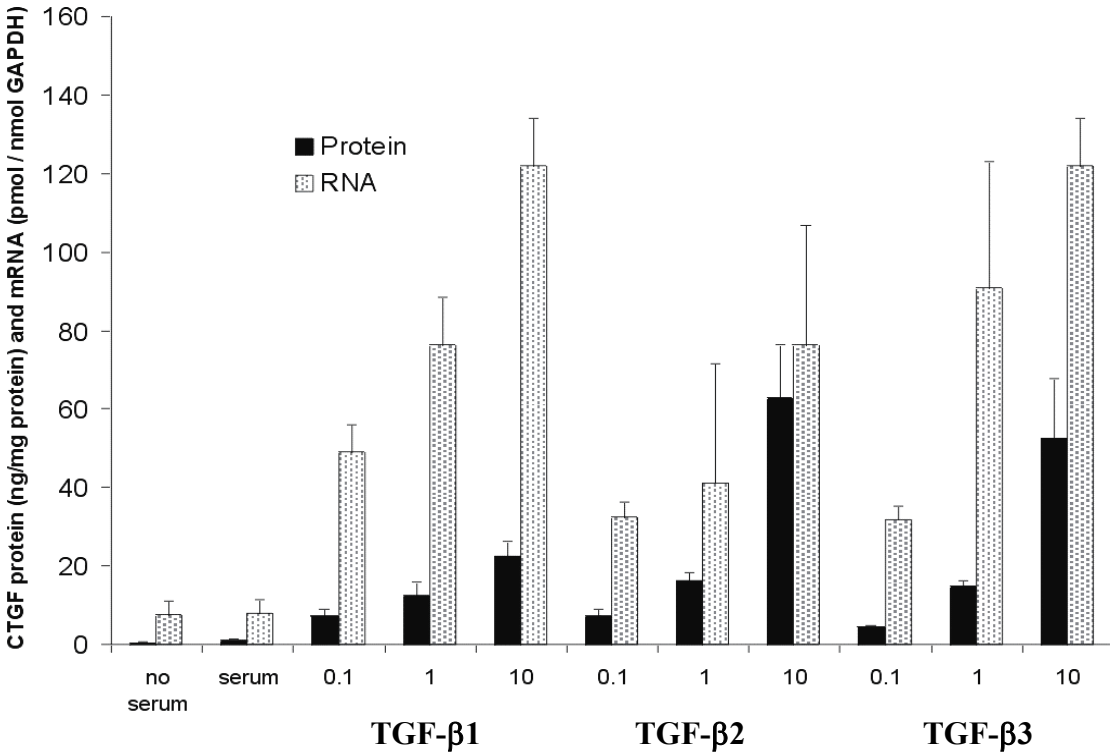

Figure 3-1. Expression of CTGF by human corneal fibroblasts. CTGF protein expression was detected by ELISA and mRNA was detected using TaqMan quantitative RT-PCR assay. Cells were cultured in a 96-well plate with each group performed in triplicate. The cells were grown to confluence and starved of serum for 24 hours followed by 48-hour treatments as shown on the graph. Results are shown as ng CTGF per total mg of protein in conditioned medium for normalization or in pmol of CTGF mRNA per nmol GAPDH mRNA. Results are expressed as the mean ± SE.

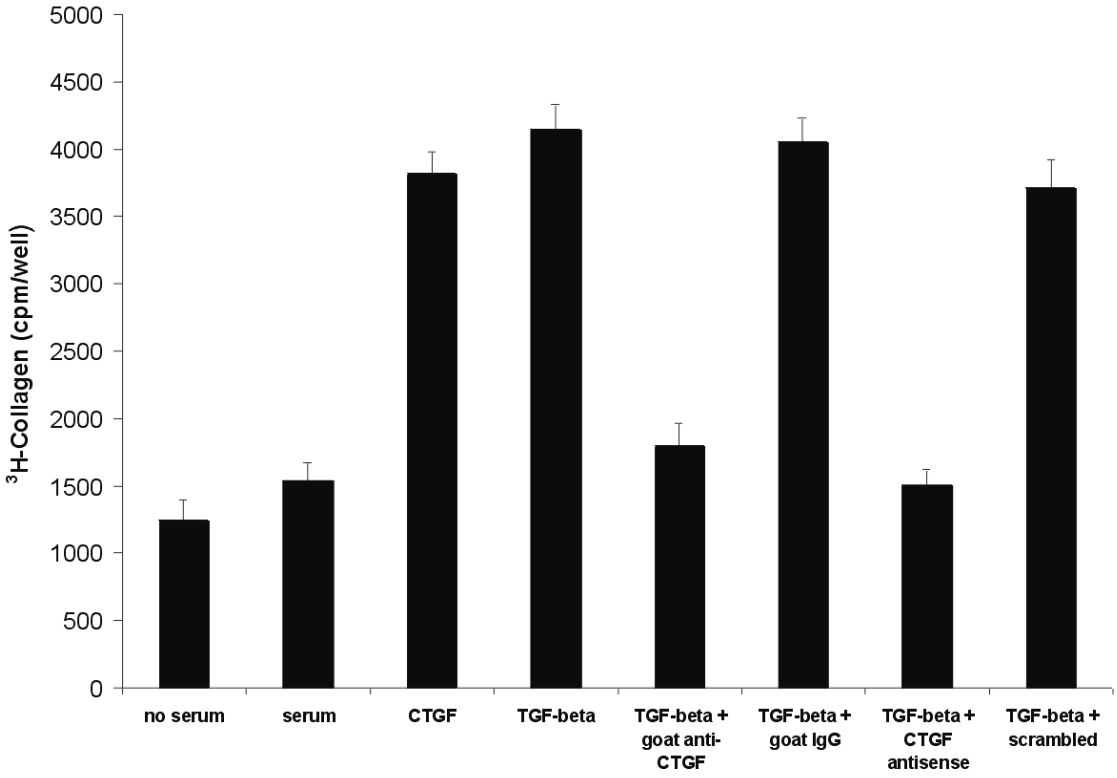

Figure 3-2. Collagen synthesis stimulation in human corneal fibroblasts by CTGF and TGF-β. Collagen synthesis was examined by measuring ^{3}H-proline incorporation. Cells were cultured in a 48-well plate with each group performed six times. The cells were grown to confluence for 5-7 days and starved of serum for 24 hours followed by 24-hour treatments as shown on the graph. Amount of ^{3}H-collagen is expressed as cpm/well. Results are expressed as the mean ± SE.

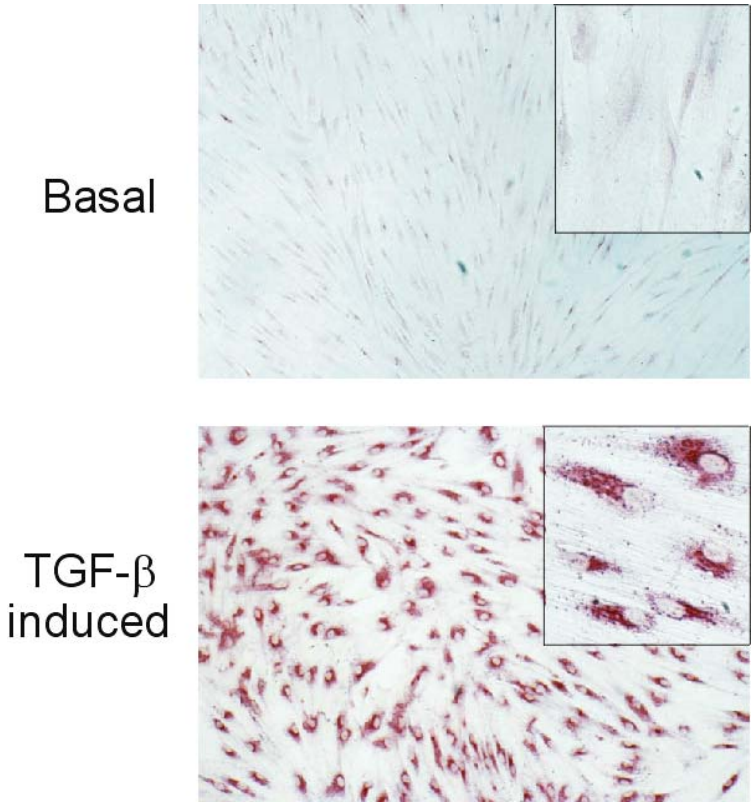

Figure 3-3. Immunolocalization of CTGF in human corneal fibroblasts. Human corneal fibroblasts were grown to confluence and then rested in serum-free medium for 72 hours before stimulation with 5 ng/mL TGF-β1 for 48 hours. The cells were fixed followed by localization of CTGF using immunocytochemistry. Original photographs were taken at 100x magnification with 400x magnifications in the insets.

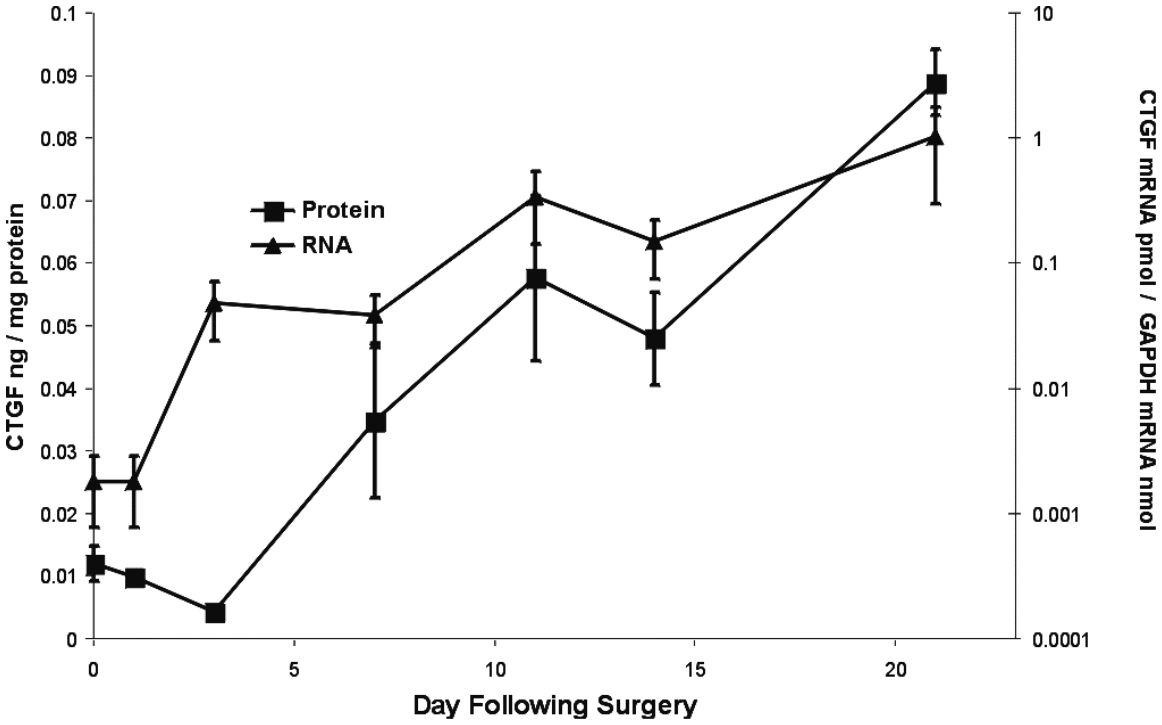

Figure 3-4. Expression of CTGF protein and mRNA in rat corneas after PRK. CTGF protein expression was detected by ELISA and mRNA was detected using TaqMan quantitative RT-PCR assay. Three corneas were analyzed for both protein and RNA at days 0, 1, 3, 7, 11, 14, 21 after PRK. Results are shown as ng CTGF per total mg of protein in the sample for normalization or as pmol of CTGF mRNA per nmol GAPDH mRNA. Results are expressed as the mean ± SE.

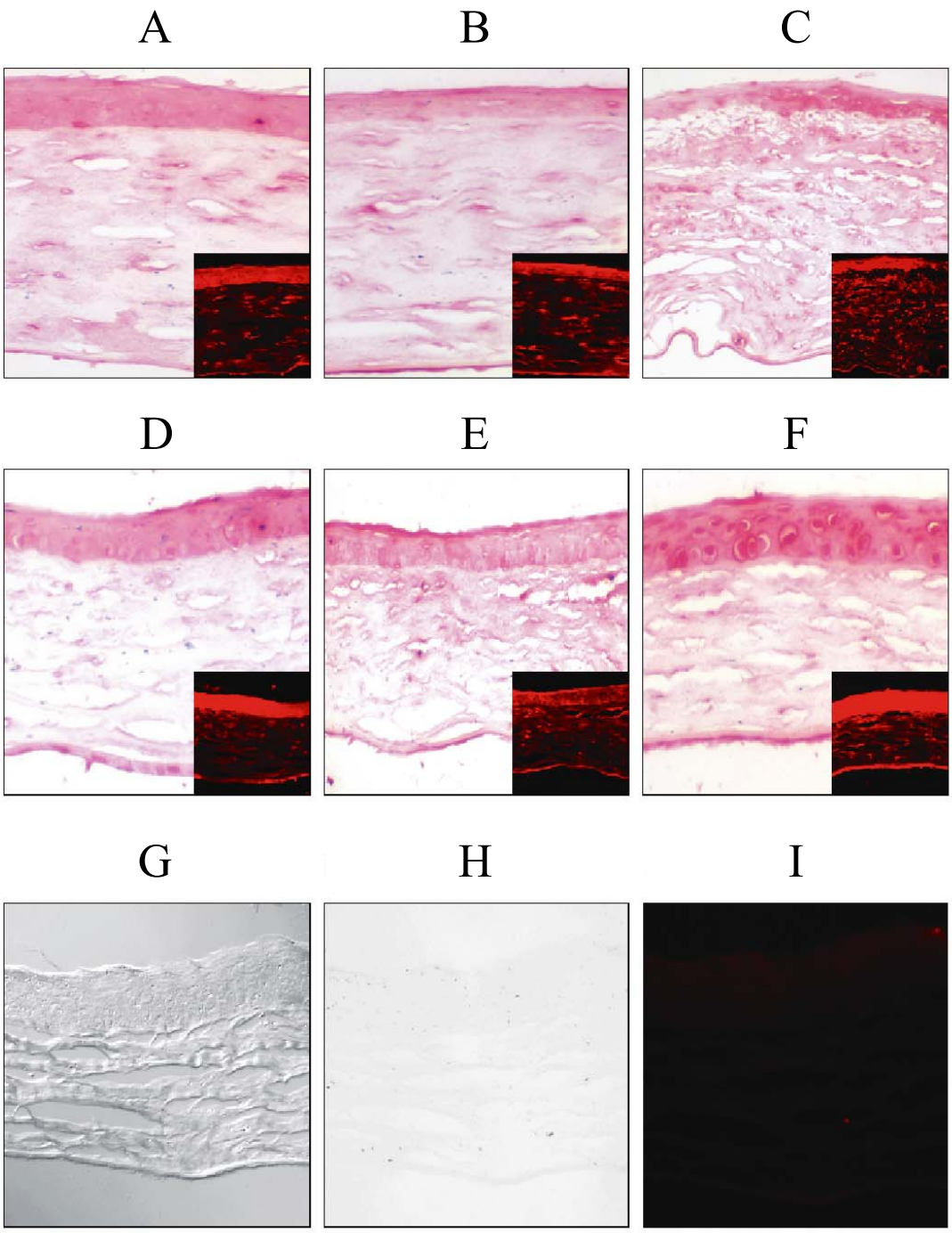

Figure 3-5. Immunolocalization of CTGF in rat corneas after PRK. A-F) Rat corneas were excised at day 0, 3, 7, 11, 14, and 21 after PRK. The corneas were fixed, paraffin sections were prepared, and CTGF was localized using immunohistochemistry. CTGF was localized using Vector Red reagent (see Materials and Methods). Sections were photographed at 200x magnification using bright field microscopy. Images of the same field using fluorescence microscopy are shown in the insets. G-I) Control images in Nomarski, bright field, and fluorescence microscopy are shown which lack the primary antibody.

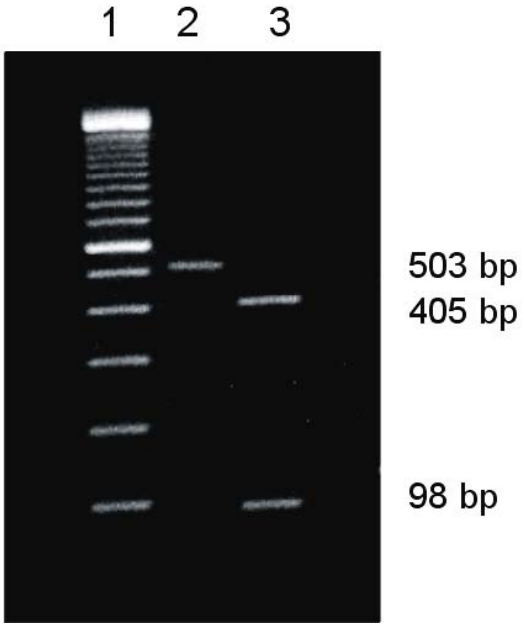

Figure 3-6. Detection of CTGF mRNA in rat corneal epithelium using RT-PCR. Corneal epithelium scrapings were isolated from rats and total RNA was isolated using TRIzol reagent. Reverse transcriptase polymerase chain reaction (RT-PCR) was performed using primers that amplify a 503 bp region of rat CTGF. The PCR product was cleaved with a unique restriction site (*PstI*) into 405 and 98 bp fragments and visualized on a 1.5% agarose gel with ethidium bromide. Lane 1 – 100 bp ladder, Lane 2 – 503 bp PCR product, Lane 3 – *PstI* digestion of PCR product.

CHAPTER 4
BIOCHEMICAL CHARACTERIZATION OF THE CONNECTIVE TISSUE GROWTH FACTOR RECEPTOR IN CORNEAL FIBROBLASTS

Introduction

CTGF mediates the effects of transforming growth factor beta (TGF-β) on activity in fibroblast cell types in a cycloheximide-independent manner, indicating a direct signaling pathway (Pelton et al., 1990;Igarashi et al., 1993;Kikuchi et al., 1995b). CTGF alone does not induce anchorage-independent growth of fibroblasts, which distinguishes its actions distinctly from that of TGF-β (Kothapalli et al., 1997b). However, little information is known about the characteristics and identity of the CTGF receptor. CTGF was shown to cross-link to a cell-surface protein of about 250 kDa in a chondrosarcoma cell line (Nishida et al., 1998b). Other studies suggest that CTGF binds to the low-density lipoprotein receptor-related protein (LRP) / alpha-2-macroglobulin receptor in bone marrow-derived stromal cells (Segarini et al., 2001a).

Insulin-like growth factors I and II (IGF-I and IGF-II) are peptides with diverse functions and effects on many tissues (Stewart et al., 1996b). IGF-I and IGF-II have a tremendous impact on many tissues since they exhibit mitogenic and anti-apoptotic properties on cells (Jones and Clemmons, 1995;Sara and Hall K, 1990;Stewart et al., 1996a). Both IGF-I and IGF-II bind to the insulin receptor, the type I IGF receptor and the type II IGF receptor with differing affinities (Andersen et al., 1990;Gustafson and Ritter, 1990;Schumacher et al., 1991). The overexpression and/or activation of type I

IGF receptor has been shown to induce ligand-dependent neoplastic transformation (Kaleko et al., 1990). The type II IGF receptor is a single chain, membrane-spanning glycoprotein, which is identical to the cation-independent mannose-6-phosphate receptor (Kornfeld, 1992), however IGF-II and mannose-6-phosphate bind to distinct domains on the extracellular region of the receptor (Marron-Teraga et al., 1998). IGF-II is a bifunctional ligand that is able to stimulate both insulin and IGF-I receptor signaling, although with different potencies. In addition, the type II IGF receptor/cation-independent mannose-6-phosphate receptor regulates IGF-II clearance (Nakae et al., 2001).

Elevated expression of CTGF has been shown in fibrotic and inflamed tissue, especially in the cornea after phototherapeutic keratectomy (PRK), where scarring is prevalent (Blalock et al., 2003;Sutton et al., 1995). Significant levels of other growth factors have been detected in the cornea (Wilson et al., 1994b) such as epidermal growth factor (EGF), TGF-β, TGF-α, basic fibroblast growth factor (bFGF), and interleukin-1 alpha (IL-1α), suggesting a role for CTGF in the process of corneal fibrosis. CTGF is regulated by TGF-β, and increasing evidence shows that it is most likely an important component of corneal wound healing. Investigation of the role of the CTGF receptor in corneal wound healing can provide insight into treating corneal defects as well as applications to other tissues. Thus, it is crucial to investigate the biochemical properties of the CTGF receptor and binding to human corneal fibroblasts, a valid cell culture model for corneal wound healing. Evidence in this work suggests that CTGF is a ligand for the type II IGF receptor.

Materials and Methods

Iodination of Recombinant Human CTGF

Recombinant human CTGF was labeled with iodine-125 using a modified Chloramine-T method (Iodobead method, Pierce). One Iodobead (Pierce) was added to 200 μL of reaction buffer (10 mM phosphate buffer, 0.5 M NaCl, pH = 7.4) along with 1 mCi of $Na^{125}I$ with constant agitation for 5 minutes at room temperature. Five micrograms of recombinant CTGF were added and the reaction was carried out at room temperature for 10 minutes with constant stirring. The labeling reaction was applied to a PD-10 G-25 Sephadex column (Pharmacia) which was pre-equilibrated with reaction buffer containing 0.1% bovine serum albumin and 0.05% Tween-20 to reduce non-specific binding to the column. Fractions were collected and aliquots were measured in a gamma counter. A representative iodination profile of recombinant human CTGF is shown in Figure 4-1. Two-microliter fractions were separated on a 15% SDS-PAGE gel followed by exposure of the gel to X-ray film overnight. Quality of labeled CTGF was also assessed by Western blot. Fractions with the highest specific activity were pooled for use in these experiments. Specific activity was approximately 33 μCi/μg.

Cell Culture

Cultures of human corneal fibroblasts were established by outgrowth from corneal explants as described previously (Woost et al., 1992). Briefly, epithelial and endothelial cells were removed from corneas that were unsuitable for corneal transplantation, the stroma was cut into cubes approximately 1 mm^3, placed in culture medium (equal parts Dulbecco's Modified Eagle Medium (DMEM), Medium 199 (Gibco BRL), Ham's F_{12} nutrient mixture (Gibco BRL) containing 1 mM $NaHCO_3$, and buffered with 25 mM

HEPES at pH 7.4). The medium was supplemented with 10% heat-inactivated normal calf serum and 1x antibiotic-antimycotic (Gibco BRL). Cultures of type II IGF receptor knockout cells were established in a similar fashion by outgrowth from lung tissue from knockout mice. Lung fibroblasts from normal tissue in C57BL/6 mice were used as a control.

Cell Binding Experiments

Human corneal fibroblasts were grown to confluence in 48-well plates. Cells were washed and incubated with chilled binding buffer alone (serum-free culture medium plus 1 mg/mL bovine serum albumin) or binding buffer with unlabeled CTGF (2 μg/mL) at 4°C for 1 hour. 25,000 cpm of ^{125}I-CTGF was added to the wells and allowed to bind at 4°C or 37°C for the time points (0 min, 15 min, 30 min, 1, 2 and 4 hours). Cell layers were washed five times with chilled phosphate-buffered saline containing 1 mg/mL BSA and solubilized in 1 N NaOH. Radioactivity was measured by gamma scintillation counter. Specific binding of ^{125}I-CTGF was measured by subtracting non-specific binding (wells with unlabeled CTGF present) from total binding (wells with unlabeled CTGF absent). Each time point was performed in triplicate.

To measure the specificity of CTGF binding to cell surface receptors, human corneal fibroblasts were grown to confluence in a 48-well plate. Cells were washed as described above and incubated with 1 μg/mL of the unlabeled competitor (CTGF, TGF-β1, TGF-α, PDGF, EGF, FGF, or insulin) for 1 hour at 4° C. 25,000 cpm of ^{125}I-CTGF was added to each well and incubated for 1 hour at 37° C. Cells were washed five times as described above and solubilized in 1 N NaOH. Each experimental condition was performed six times.

Scatchard analysis was performed (Scatchard, 1949) on human corneal fibroblasts cultures grown to confluence in a 48-well plate. Cells were washed and incubated with increasing concentrations of unlabeled CTGF (10^{-11} M to 10^{-6}) for 1 hour at 4° C. 50,000 cpm of ^{125}I-CTGF was added to each well and incubated at 37° C for 1 hour. Cells were washed five times and solubilized in 1 N NaOH. Each condition was performed six times. A saturation curve was constructed by plotting bound pM of ^{125}I-CTGF versus free pM ^{125}I-CTGF. Then, a Scatchard plot was constructed using the saturation curve data and the dissociation constants were calculated.

Triton-X-100 soluble membrane extracts from human corneal fibroblasts were applied to a CTGF-coupled affinity column and eluted with 0.1 M glycine (pH = 2.5). Eluted fractions were bound with ^{125}I-CTGF in the presence or absence of unlabeled CTGF and precipitated with gamma globulin as carrier and 15% polyethylene glycol. Pellets were washed with 20% ethanol and radioactivity measured by gamma scintillation counter. Specific binding was calculated by subtracting non-specific binding from total binding.

Cell Proliferation Assay

Control lung fibroblasts from normal mouse lung and type II IGF receptor knockout lung fibroblasts were seeded in a 48-well plate (5000 cells per well) and cultured for 48 hours in serum-supplemented medium. The cultures were held in serum-free medium for 48 hours followed by stimulation with 10% normal calf serum, 5 ng/mL recombinant human TGF-β1 (R&D Systems; Minneapolis, MN), 25 ng/mL CTGF, 25 ng/mL CTGF + 6.5 μg/mL RAP, 6.5 μg/mL RAP, 1 mg/mL IGF-I or IGF-II (R&D Systems; Minneapolis, MN), or 5 ng/mL TGF-β in the presence of 10 μM CTGF

antisense or scrambled control oligonucleotides following 48 hours of serum-starvation. Cell proliferation was measured using a non-radioactive MTS cell proliferation assay (Promega; Madison, WI). Absorbance readings corresponding to cell proliferation were expressed as mean ± standard error of six replicate samples for each condition, and ANOVA and Tukey's HSD post-hoc test were used to assess statistical significance between times and groups.

Cross-Linking of ^{125}I-CTGF to Human Corneal Fibroblast Receptors

Human corneal fibroblasts were grown to confluence in two T-75 flasks. The cells were stimulated for 24 hours with 5 ng/mL transforming growth factor beta-1 (TGF-β1). One flask was incubated with 2 μg/mL CTGF for one hour at 4°C. Then 4,000,000 cpm of ^{125}I-CTGF was added to each flask and incubated for 2 hours at 4°C. The cells were washed three times with chilled binding buffer (128 mM NaCl, 5 mM KCl, 5 mM $MgSO_4$, 1.2 mM $CaCl_2$, 50 mM HEPES, 0.1% bovine serum albumin, pH = 7.5). The cells were then incubated with 10 mg/mL disuccinimidyl suberate (DSS, dissolved in dimethyl sulfoxide) for 15 minutes at 4°C. The reaction was terminated with quenching buffer at 4°C (0.25 M sucrose, 10 mM Tris HCl, 1 mM EDTA, 0.3 mM PMSF, pH = 7.4). One milliliter of quenching buffer was added to each flask and the cells were detached using a cell scraper. The two cell suspensions were centrifuged at 14,000 *x g* for 2 minutes at 4°C to pellet the cells. The supernatants were removed and 100 μL of solubilizing buffer was added to each pellet (125 mM NaCl, 10 mM Tris, 1 mM EDTA, 1% Triton-X-100, pH = 7.0, with protease inhibitor cocktail). The cell pellets were incubated overnight with the solubilizing buffer at 4°C with constant rocking. The samples were centrifuged at 14,000 *x g* for 15 minutes to remove insoluble cell debris.

The protein-containing supernatants were added to an equal volume of electrophoresis buffer (100 mM Tris, pH = 6.8, 20% glycerol, 3% SDS, 0.05% bromophenol blue, 180 mM 2-mercaptoethanol). The samples were heat-denatured and run on a 3-8% Tris-Acetate SDS-PAGE gel (Novex). The gel was fixed, dried, and exposed to X-ray film overnight at -80°C. The molecular weights of the bands were determined by comparing to Multi-Mark molecular weight protein standards (Novex).

Time Course of Binding to Rat Corneas following PRK

Photorefractive keratectomy (PRK) was performed on 28 male rats as described previously (Chen et al., 2000d). Adult Sprague-Dawley male rats (250 g) with normal eyes were anesthetized with inhaled isofluorane anesthetic. Eyelashes and whiskers surrounding the eye were removed from the visual field. A drop of proparacaine-HCl (0.05%) was applied to the eye and the cornea was centered under the laser microscope. Excimer laser photorefractive keratectomy was performed. Bilateral ablation of the corneas was performed in a 4.4-mm treatment zone with an excimer laser (Summit SVS Apex) in the phototherapeutic keratectomy mode. The corneal epithelium was ablated to a depth of 40 μm, followed by ablation of the stroma to a depth of 20 μm for a total ablation depth of 60 μm. After excimer laser treatment, tobramycin (0.3%) ointment was applied to the corneal surface to prevent infection. No postoperative topical steroid was administered. Eight corneas from four rats were harvested on Days 0, 1, 3, 5, 7, 14, and 21 after surgery. Four corneas on each day were diced with scalpels and each was placed in 1 ml of binding buffer (phosphate-buffered saline containing 1 mg/ml BSA) with 2 μg/ml unlabeled CTGF and four corneas were placed in binding buffer lacking CTGF. After incubation for 1 hour at 4° C, 50,000 cpm of ^{125}I-CTGF were added to each cornea

and incubated for 1 hour at 37° C. The corneas were then washed five times in binding buffer with BSA and radioactivity measured by gamma scintillation counter. Specific binding was calculated by subtracting non-specific binding from total binding. Values were normalized to the total mass of each cornea and expressed as cpm/10 mg tissue.

Immunoprecipitation of Type II IGF Receptor

To further confirm the identity of the CTGF receptor as the type II IGF receptor, affinity chromatography and immunoprecipitation was performed. Briefly, Recombinant human CTGF was covalently cross-linked to Ultra-link Support Medium (Pierce) and a column was prepared. Triton-X-100 solubilized membrane protein extracts were prepared from cultures of human corneal fibroblasts and applied to the resin. Bound protein was eluted from the resin by a drop in pH to 2.5. Fractions were tested for protein concentration. Fractions were also tested for binding of ^{125}I-CTGF for 1 hour at 4° C, followed by precipitation with 15% polyethylene glycol (PEG) and γ-globulins as carrier proteins. Fractions from the CTGF affinity column exhibiting the highest binding activity to ^{125}I-CTGF were pooled. A portion of the sample was bound to ^{125}I-CTGF following binding by a goat antibody to the type II IGF receptor. The complex was run through a Protein G affinity column. The complex was eluted from the column with a shift in pH to 3.0 with 0.1 M glycine. The amount of binding was measured by counting the samples in the gamma counter. Two controls were used: 1) competition by unlabeled CTGF and 2) non-specific binding of ^{125}I-CTGF alone to Protein G column.

Immunoprecipitation of Binding Reactions

To assess the interaction between CTGF and the type II IGF receptor, *in vitro* binding reactions were performed followed by immunoprecipitation of the complexes.

1.5-mL microcentrifuge tubes were coated with buffer containing 0.1% BSA to reduce non-specific binding to the walls of the tubes. Reactions were assembled in the presence of 10 μL of 1 mg/mL BSA and 75,000 cpm ^{125}I-CTGF according to the scheme shown in Figure 4a overnight at 4°C. The reactions were precipitated by adding 150 mL of 10 mg/mL gamma-globulin and 150 mL of 20% polyethylene glycol (molecular weight = 8000). The samples were centrifuged at 14,000 x g for 15 minutes at 4°C. Pellets were washed with 20% ethanol and radioactivity was measured by gamma scintillation counter. Each reaction was repeated in triplicate. Specificity of the reaction was measured by adding various, related unlabeled competitors (CTGF, TGF-β1, TGF-α, PDGF, EGF, FGF, insulin, RAP, IGF-II, and mannose-6-phosphate) to the binding reactions and precipitated as described.

Immunoprecipitation of Cross-linked Human Corneal Fibroblast Receptors

Reactions were assembled in the presence of 10 μL of 1 mg/mL BSA, 1000 cpm of ^{125}I-CTGF cross-linked human corneal fibroblast extracts and either affinity purified goat anti-human CTGF or goat anti-human sMPR (soluble cation-independent mannose-6-phosphate receptor) and incubated overnight at 4°C. The reactions were precipitated and measured as described above.

Results

Binding of CTGF to Receptors on Human Corneal Fibroblasts

Recombinant CTGF binds to receptors on human corneal fibroblasts. Specific binding to the receptors reaches maximum at about two hours at 4º C and by one hour at 37º C (Figure 4-2). Specific binding is measured by calculating the difference between total binding of ^{125}I-CTGF and binding in the presence of excess unlabeled ligand.

Binding of CTGF to cell-surface receptors at 4º C is not inhibited by the addition of other closely related growth factors ($P < 0.01$, Figure 4-3). Scatchard analysis of CTGF binding to human corneal fibroblasts at 4º C reveals two classes of cell-surface receptors (Figure 4-4). One high affinity, low abundance class is observed (Kd = 3.3 nM at 18,000 receptors per cell). A second lower affinity, high abundance class is also measured (Kd = 133.3 nM at 83,000 receptors per cell). ^{125}I-CTGF cross-links to a protein of approximately 250 kDa on human corneal fibroblasts. The interaction is not observed in the presence of excess unlabeled ligand (Figure 4-5). To confirm this interaction further, corneal fibroblast cell membrane extracts were applied to a CTGF-coupled affinity column. Fractions that were eluted from the column exhibit a significantly higher amount of CTGF specific binding (approximately 330%) when compared to total cell membrane extract (Figure 4-6).

Binding of CTGF to Rat Corneas Following PRK

Levels of inflammatory cytokines and growth factors are known to increase in rat corneas following laser photorefractive keratectomy (PRK) and in cultures of corneal fibroblasts, which comprise the majority of the structure of the cornea. It has been shown that the expression of CTGF is induced by PRK in rat corneas and by TGF-β in cultured cells (Blalock et al., 2003). To assess the possibility of up-regulation or increased availability of the putative CTGF receptor, surgery was performed to induce the corneal scarring response and its relationship with measured specific CTGF binding. Specific binding was measured by calculating the difference between total binding of ^{125}I-CTGF and binding in the presence of excess unlabeled ligand. Specific binding of CTGF

increased significantly, peaking at 5 days after surgery ($P < 0.01$, Figure 4-7). Data was analyzed using ANOVA/MANOVA and Tukey's HSD post-hoc statistical tests.

CTGF Binding to the Type II Insulin-like Growth Factor Receptor

When iodinated CTGF was bound to the type II insulin-like growth factor receptor and immunoprecipitated using a protein G column, over 80% of the labeled CTGF eluted from the column (Figure 4-8). It was also shown that CTGF has a specific affinity for the type II IGF receptor and is blocked by unlabeled CTGF in these fractions. *In vitro* binding reactions were performed to measure the amount of binding of CTGF to the type II insulin-like growth factor (IGF) receptor / cation-independent mannose-6-phosphate receptor. The interaction of ^{125}I-CTGF with soluble mannose-6-phosphate receptor (sMPR) is inhibited in the presence of unlabeled CTGF (Figure 4-9, #1-2). An affinity-purified antibody to CTGF precipitates ^{125}I-CTGF alone and is inhibited by the addition of unlabeled CTGF (#3 and #4). These binding complexes are also precipitated by affinity-purified antibody to human sMPR (#5 and #6) or to CTGF (#7 and #8). The amount of trace ^{125}I-CTGF precipitated by PEG alone is much lower than the binding reactions ($P < 0.01$, #9).

Figure 4-10 shows that the inhibition of ^{125}I-CTGF binding to sMPR by unlabeled CTGF is not seen upon addition of closely related growth factors and IGF family members. Insulin-like growth factor II (IGF-II) competes for binding somewhat ($P = 0.09$) but not to the degree of CTGF competition ($P < 0.01$). Human corneal fibroblast cell membrane extracts that are covalently cross-linked with ^{125}I-CTGF are immunoprecipitated by affinity-purified antibodies to either sMPR or to CTGF. The

amount of precipitated counts is significantly higher ($P < 0.01$) when compared to control antibody or the addition of no antibody (Figure 4-11).

Response to Exogenous TGF-β in Type II IGF Receptor Knockout Cells

To confirm that CTGF binds to the type II IGF receptor in cell cultures, binding and cell proliferation experiments were performed in knockout cells lacking the receptor. Figure 4-12 shows that there is no significant binding to cells lacking the type II IGF receptor when compared to normal mouse lung fibroblasts ($n = 6$, $P < 0.01$).

The same two cell cultures were used to measure cell proliferation in response to exogenously added growth factors and agents (Figure 4-13). Both cell types showed increased cell proliferation in response to serum but a reduced response was seen to both TGF-β and CTGF ($P < 0.01$). This suggests that TGF-β-induced cell proliferation is hindered due to the absence of a cell-surface receptor for CTGF. The presence of RAP appeared to have no effect on cell proliferation, suggesting that the low-density lipoprotein receptor-related protein (LRP) is not responsible for CTGF-mediated TGF-β signaling in this cell type. A marked difference between IGF-II- and IGF-I-induced cell proliferation is evident between the knockout and wild type cells ($P < 0.01$), which is expected due to absence of the type II receptor. Finally, CTGF antisense oligonucleotides blocked TGF-β-induced cell proliferation in both cell types, suggesting that CTGF synthesis is required and acts as a mediator of TGF-β's effects on the cells ($P = 0.17$). This blockage is not seen in the presence of scrambled control oligonucleotides.

Discussion

The presence of CTGF-specific receptors was demonstrated on the surface of human corneal fibroblasts in this study. The addition of unlabeled CTGF inhibited the binding of ^{125}I-CTGF whereas unlabeled TGF-β, TGF-α, PDGF-BB, bFGF, EGF, insulin, IGF-I, IGF-II, or mannose-6-phosphate did not (Figure 4-3). This suggests that CTGF binds to its receptor specifically on the cell surface of human corneal fibroblasts. Scatchard analysis reveals the presence of two classes of receptors on human corneal fibroblasts with K_d values of 1.3 nM and 133.3 nM and receptor numbers per cell of 18,000 and 83,000, respectively (Figure 4-4). Previous reports have shown that CTGF binds to PDGF receptors on fibroblasts (Bradham et al., 1991a), in which ^{125}I-labeled CTGF was not used. However, two reports using labeled CTGF have been reported (Nishida et al., 1998a;Segarini et al., 2001b) in which CTGF bound to chondrosarcoma and bone marrow-derived stromal cell lines. In the chondrosarcoma cell line study a cross-linking experiment was performed revealing a major band at 280 kDa (Figure 4-5). The molecular weight of the ligand-receptor complex indicated that the molecular weight of CTGF receptors on human corneal fibroblasts is about 242 kDa. This molecular weight is similar to the study performed in a human chondrosarcoma cell line (Nishida et al., 1998c). The addition of unlabeled CTGF resulted in a disappearance of the cross-linked band at 280 kDa, suggesting that this band is a result of a direct interaction between CTGF and its receptor. Immunoprecipitation of CTGF affinity chromatography experiments reveal that a protein or proteins present in cell membrane extracts specifically bind to CTGF (Figure 4-6).

CTGF binding also increased in rat corneas following photorefractive keratectomy (Figure 4-7). Expression of CTGF (Blalock et al., 2003), TGF-β I, II, and III, fibronectin, and collagen (Chen et al., 2000c) has been previously shown to increase in rat corneas following PRK. Expression of TGF-β receptors type I and II increases in corneal epithelium following surgery (Zieske et al., 2000), but has not been studied extensively in corneal fibroblasts. The increase in CTGF binding to corneal tissue following surgery could be due to upregulation of the CTGF receptor or increased migration of the receptors via vesicles to the cell membrane surface. This suggests a crucial involvement of CTGF and its receptor during the course of corneal wound healing.

Evidence from this report suggests that CTGF binds to the type II IGF receptor in human corneal fibroblasts. *In vitro* binding followed by immunoprecipitation using antibodies specific for CTGF or the soluble mannose-6-phosphate receptor show that CTGF specifically interacts with the sMPR (Figure 4-9) and that this interaction is not inhibited by the addition of other growth factors (Figure 4-10). In addition, the same antibodies precipitated the majority of ^{125}I-CTGF cross-linked cell membrane extracts present in the *in vitro* binding reactions (Figure 4-11). These experiments prove that CTGF interacts specifically with the type II IGF receptor on the surface of human corneal fibroblasts. CTGF was previously shown to bind to the low-density lipoprotein-related receptor (LRP) / alpha-2 macroglobulin receptor in bone marrow-derived stromal cells (Segarini et al., 2001c). This interaction was inhibited by the addition of unlabeled CTGF, lactoferrin, ApoE, LPL, and methionine-activated alpha-2 macroglobulin, all ligands for this receptor (Gliemann, 1998). However, previous studies have shown that

LRP is a multi-functional scavenger receptor (Herz and Strickland, 2001), so the interaction of CTGF may be rather non-specific and not confer any real biological activity. It is likely that the binding of CTGF, which is an IGF-binding protein related molecule (Kim et al., 1997b), to the type II IGF receptor on corneal fibroblasts confers biological responses and is responsible for signal transduction activity. The data presented in Figures 4-12 and 4-13 show additional evidence of the importance of CTGF binding to the type II IGF receptor. It is clear that the ability of CTGF to bind to this receptor is necessary for TGF-β to transmit a biological response such as cell proliferation to cells. Also, Figure 4-12 gives further evidence that CTGF binding to the LRP does not account for a significant amount of TGF-β-induced cell proliferation.

Many growth factor membrane receptors are composed of several different subunits. For example, it has been previously shown that FGF and hepatocyte growth factor (HGF) bind to their signaling receptors which possess tyrosine kinase activities with high affinity (Schlessinger et al., 1995;Lyon et al., 1994). However, the same growth factors also bind with low affinity to cell surface proteoglycans that cannot transmit signals alone. These experiments demonstrate the presence of two classes of receptors on human corneal fibroblasts. The low affinity class of receptor may be a proteoglycan, or even LRP, while the high affinity class is most likely due to specific binding of CTGF to the type II IGF receptor. This study shows that binding of CTGF and its receptor have a clear role in corneal fibroblasts and their interaction is likely to be crucially involved in corneal wound healing.

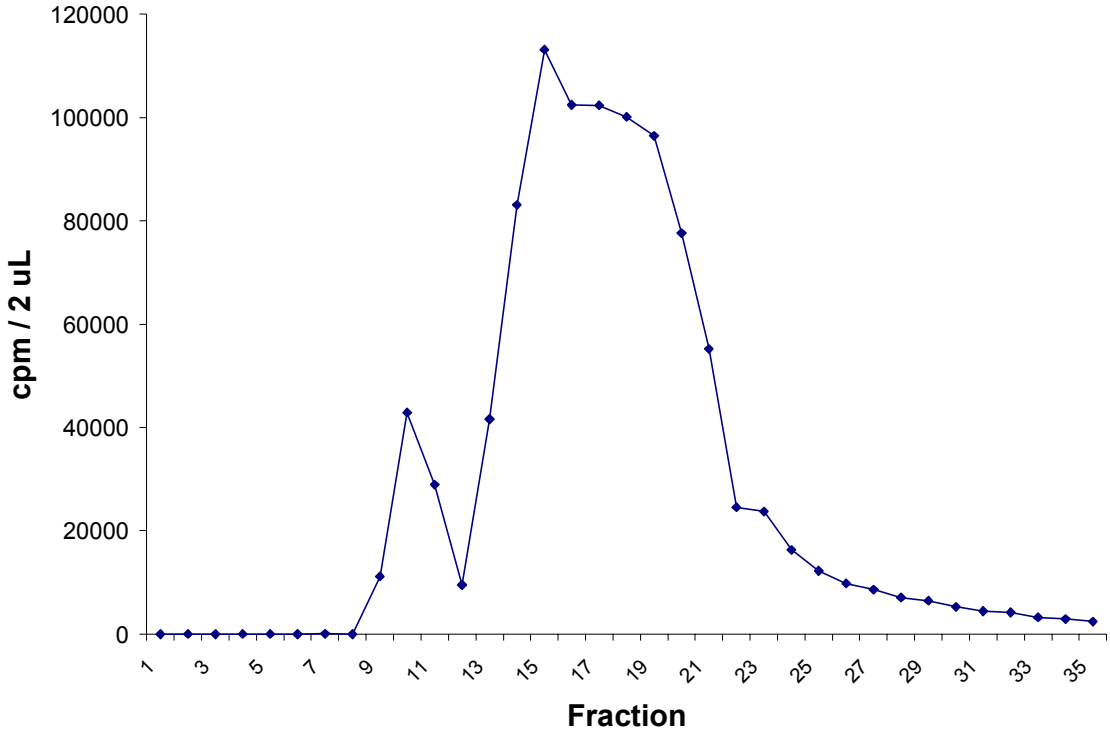

Figure 4-1. Iodination of recombinant human CTGF. Recombinant human CTGF was iodinated using a modified chloramine-T method (Iodobead, Pierce) and applied to a G-25 Sephadex column. 2 μL of each fraction was counted in a scintillation counter. Labeled protein was contained in fractions 10, 11, 12 and pooled together for use in further experiments. Presence of intact CTGF was verified by Western blot (data not shown)

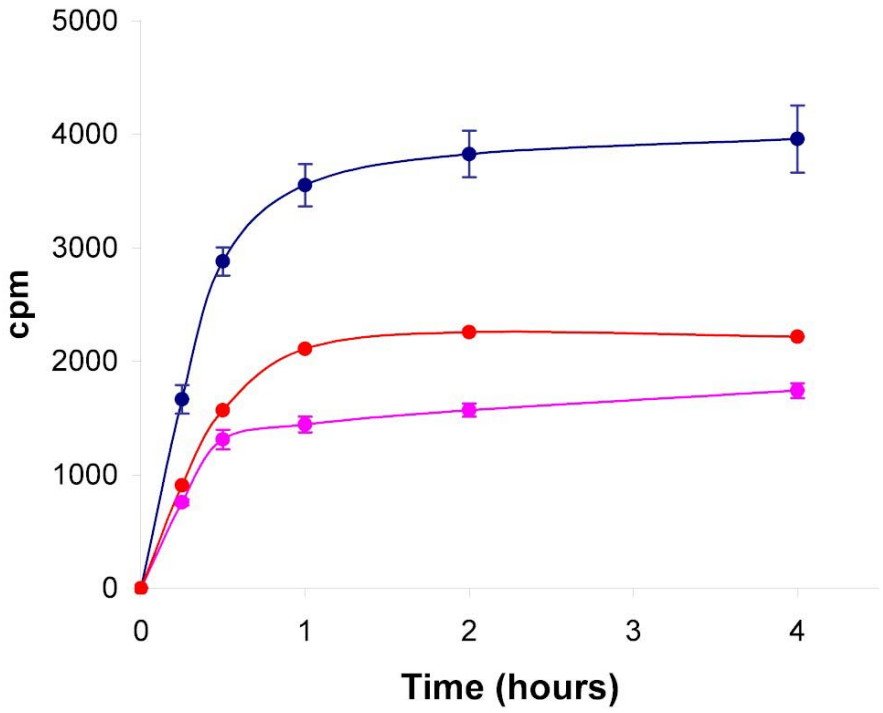

Figure 4-2. Time course of CTGF binding to human corneal fibroblasts. Human corneal fibroblasts were bound with ^{125}I-CTGF in the presence of absence of excess unlabeled CTGF at 4°C for the time points shown (n = 3). Blue – total binding, pink – non-specific binding, red – specific binding.

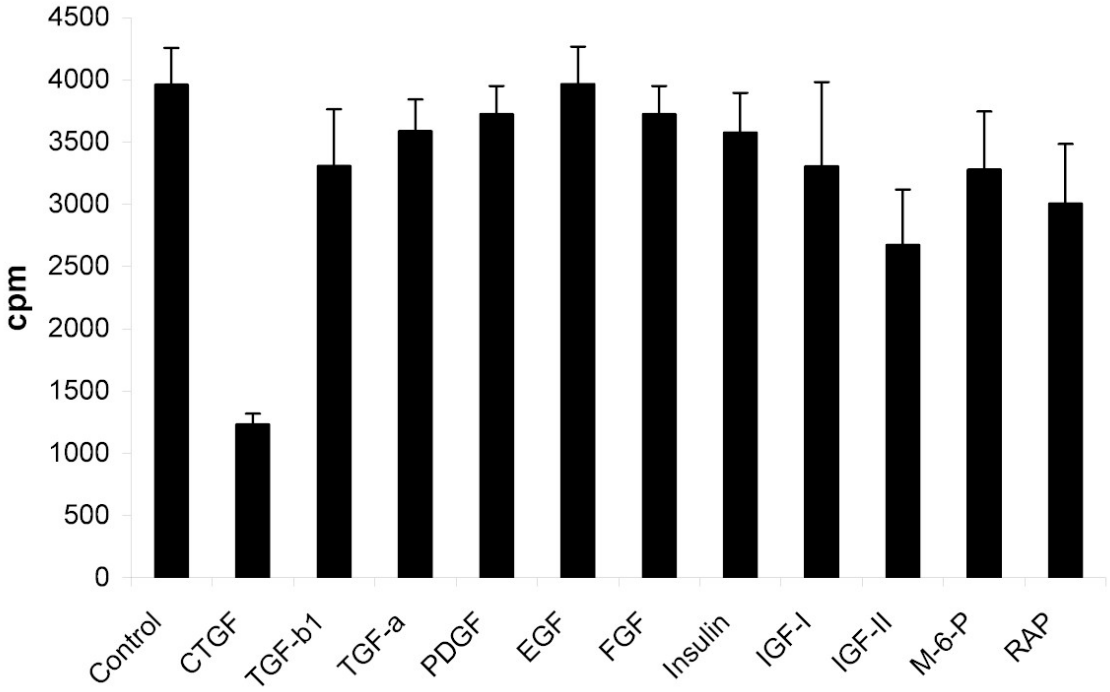

Figure 4-3. Specificity of CTGF binding to human corneal fibroblasts. Human corneal fibroblasts were incubated with ^{125}I-CTGF in the presence of absence of excess unlabeled growth factors at 4°C (n = 6)

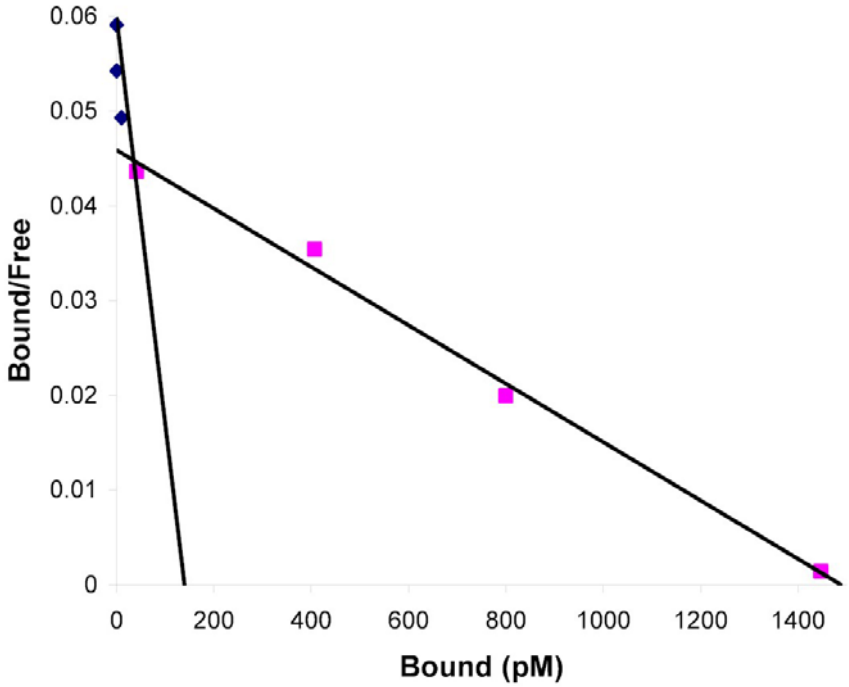

Figure 4-4. Scatchard analysis of CTGF binding to human corneal fibroblasts. Analysis of CTGF binding to human corneal fibroblasts at 4° C in the presence of increasing concentrations of excess, unlabeled CTGF (n = 6).

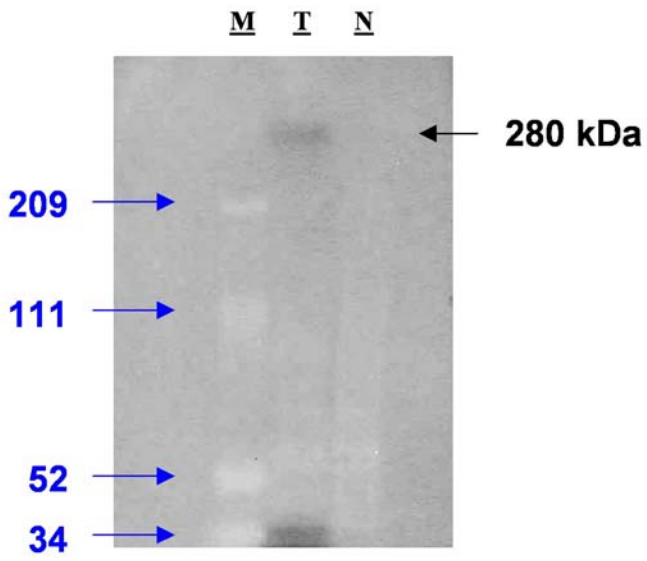

Figure 4-5. Cross-linking of CTGF to human corneal fibroblasts. ^{125}I-CTGF was covalently cross-linked to human corneal fibroblasts at 4°C in the presence or absence of excess, unlabeled CTGF. Cells were solubilized and Triton-X-100 soluble fractions were separated using SDS-polyacrylamide gel electrophoresis followed by autoradiography. M – molecular weight markers in kDa, T – total binding, N – non-specific binding.

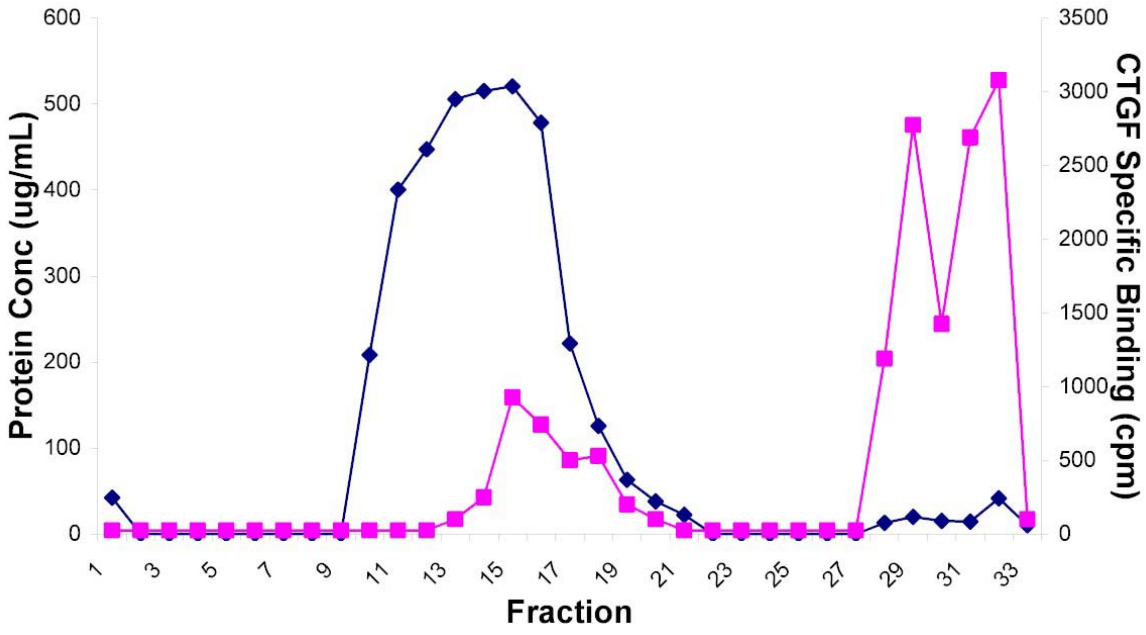

Figure 4-6. CTGF affinity chromatography and specific binding. Triton-X-100 soluble human corneal fibroblast extract was applied to a CTGF-coupled affinity column. CTGF bound material was eluted at fraction 28 by shifting the pH to 2.5. Eluted fractions were bound with ^{125}I-CTGF in the presence or absence of CTGF and precipitated with 15% polyethylene glycol. The blue line represents total protein concentration and the pink line represents specific CTGF binding.

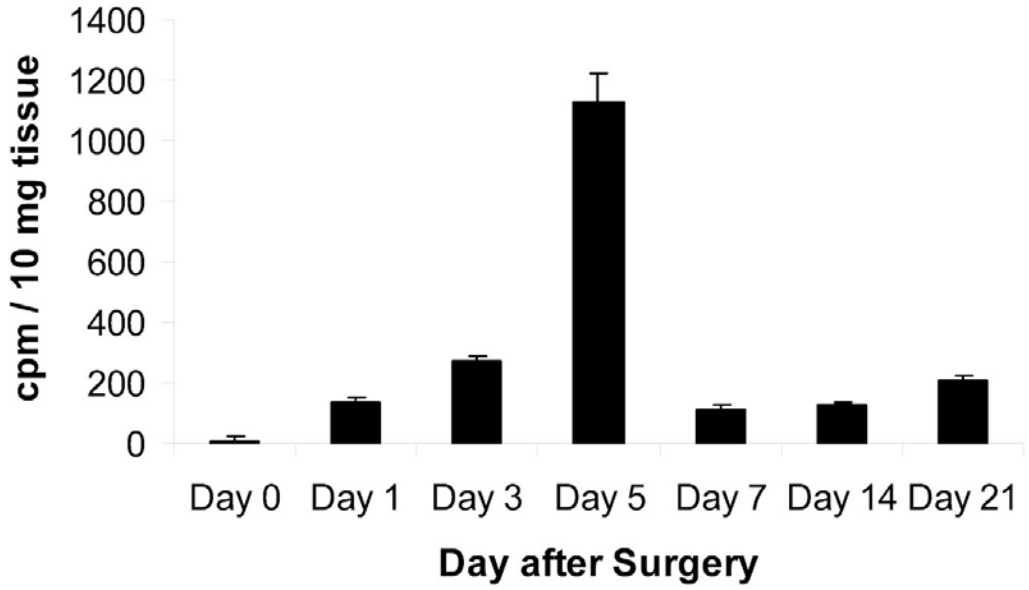

Figure 4-7. Specific binding of CTGF to rat corneas following PRK. Phototherapeutic keratectomy (PRK) was performed on male Sprague-Dawley rats. Whole corneas were removed at the time points indicated and bound with ^{125}I-CTGF in the presence or absence of unlabeled CTGF at 4°C (n = 3).

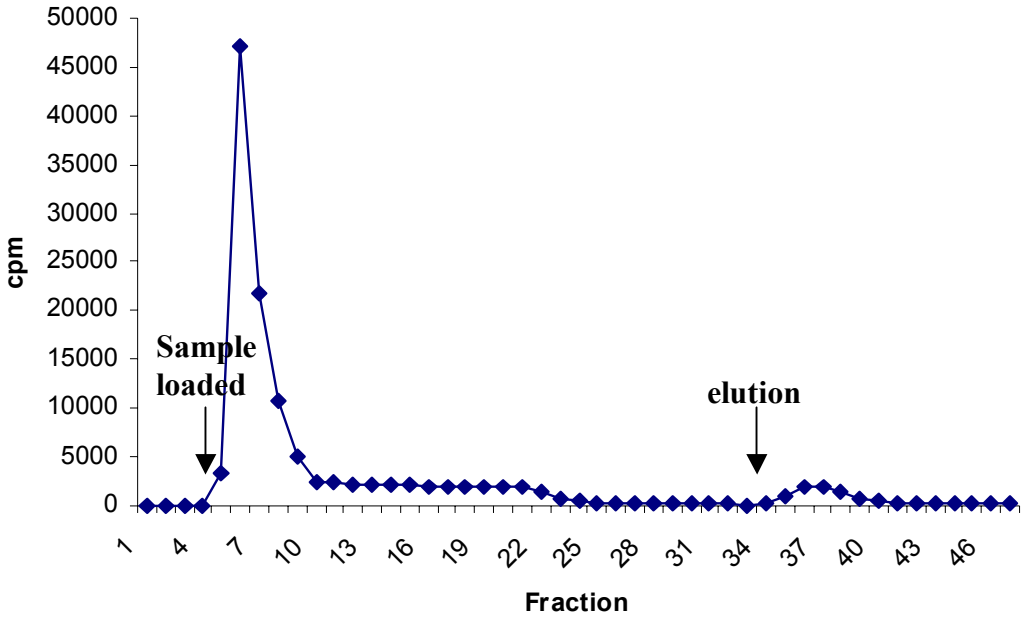

Figure 4-8. Immunoprecipitation of CTGF Bound to the Type II IGF Receptor. Iodinated CTGF was bound to soluble recombinant type II IGF receptor and bound to an affinity purified goat antibody to the type II IGF receptor. The complexes were applied to a Protein G column. Fractions bound to the column were eluted by a shift in pH to 3.0 with 0.1 M glycine

	1	2	3	4	5	6	7	8	9
^{125}I-CTGF	+	+	+	+	+	+	+	+	+
CTGF		+		+		+		+	
sMPR	+	+			+	+	+	+	
Goat anti-sMPR					+	+			
Goat anti-CTGF			+	+			+	+	

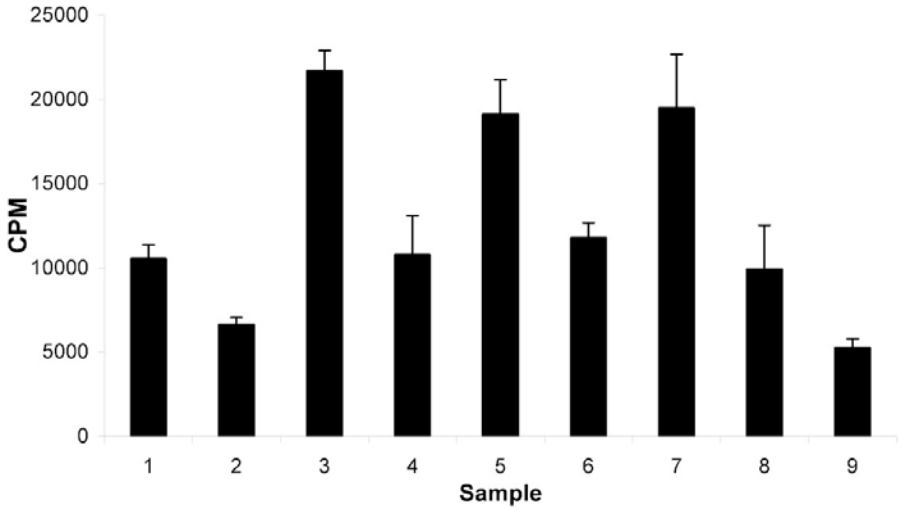

Figure 4-9. Immunoprecipitation of CTGF/Type II IGF receptor complexes. Reactions were assembled according to the scheme shown above. Reactions were precipitated in the presence of gamma globulin as a carrier protein and 15% polyethylene glycol (n = 3). Reactions were assembled in the presence of 10 μL of 1 mg/mL BSA and 75,000 cpm ^{125}I-CTGF according to the scheme shown above overnight at 4°C. The reactions were precipitated by adding 150 mL of 10 mg/mL gamma-globulin and 150 mL of 20% polyethylene glycol (molecular weight = 8000). The samples were centrifuged at 14,000 x g for 15 minutes at 4°C. Pellets were washed with 20% ethanol and radioactivity was measured by gamma scintillation counter. Total precipitated cpm are shown on the graph.

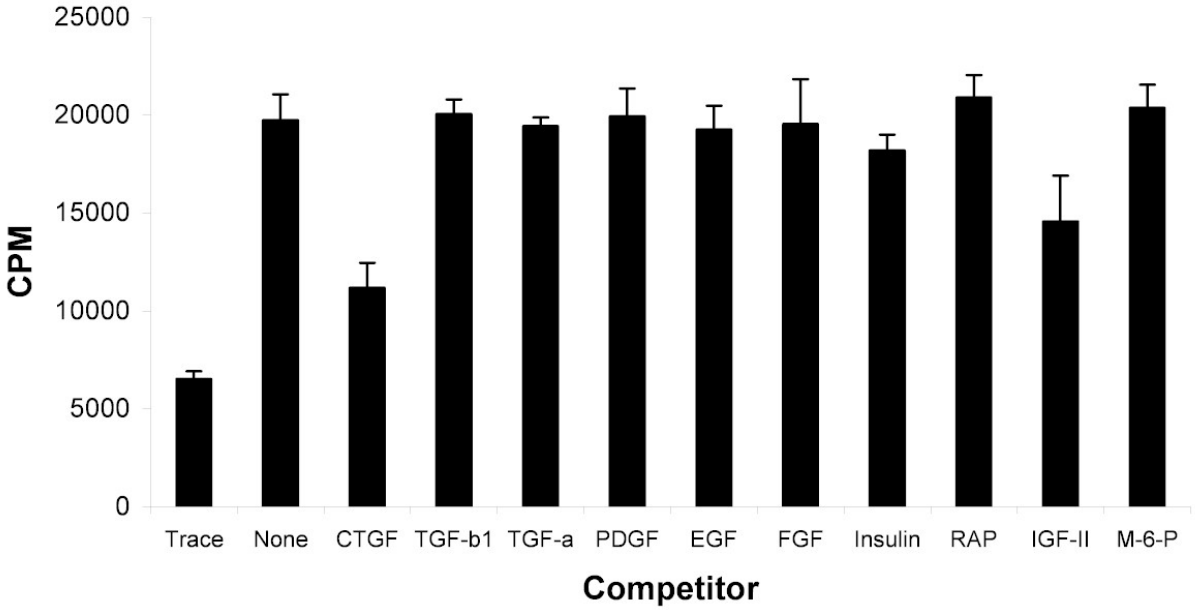

Figure 4-10. Specificity of CTGF binding to immunoprecipitated complexes. Reactions were assembled in the presence of various unlabeled growth factors shown and precipitated as in Figure 4-7 (n = 3).

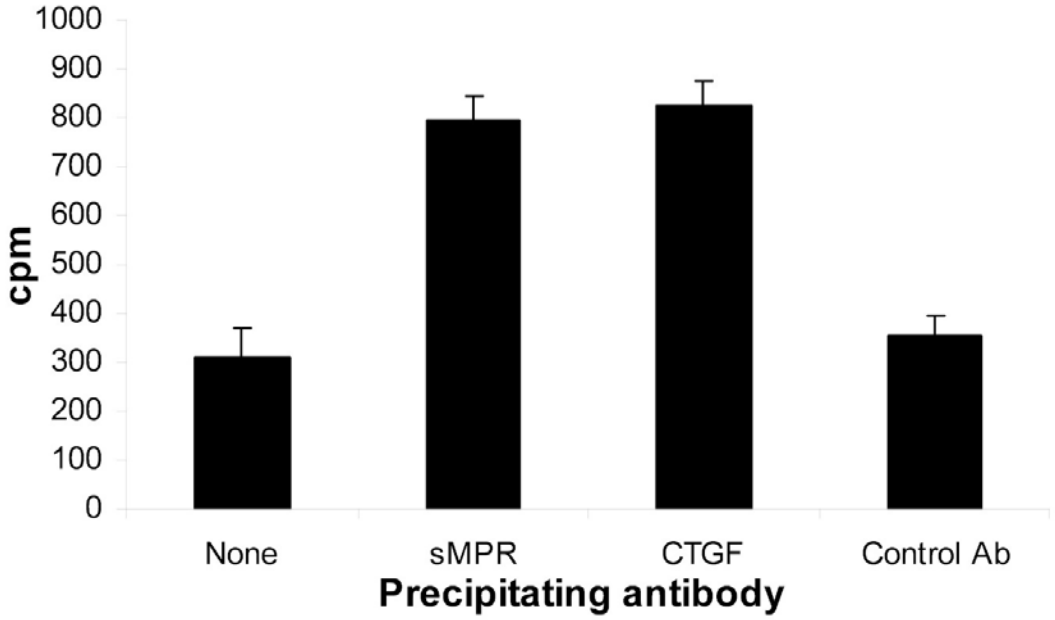

Figure 4-11. Immunoprecipitation of membrane proteins cross-linked with CTGF. ^{125}I-CTGF was covalently cross-linked to human corneal fibroblasts at 4°C in the presence or absence of excess, unlabeled CTGF. Cells were solubilized and Triton-X-100 soluble fractions were immunoprecipitated with goat anti-sMPR, goat anti-CTGF, or irrelevant goat IgG (n = 3).

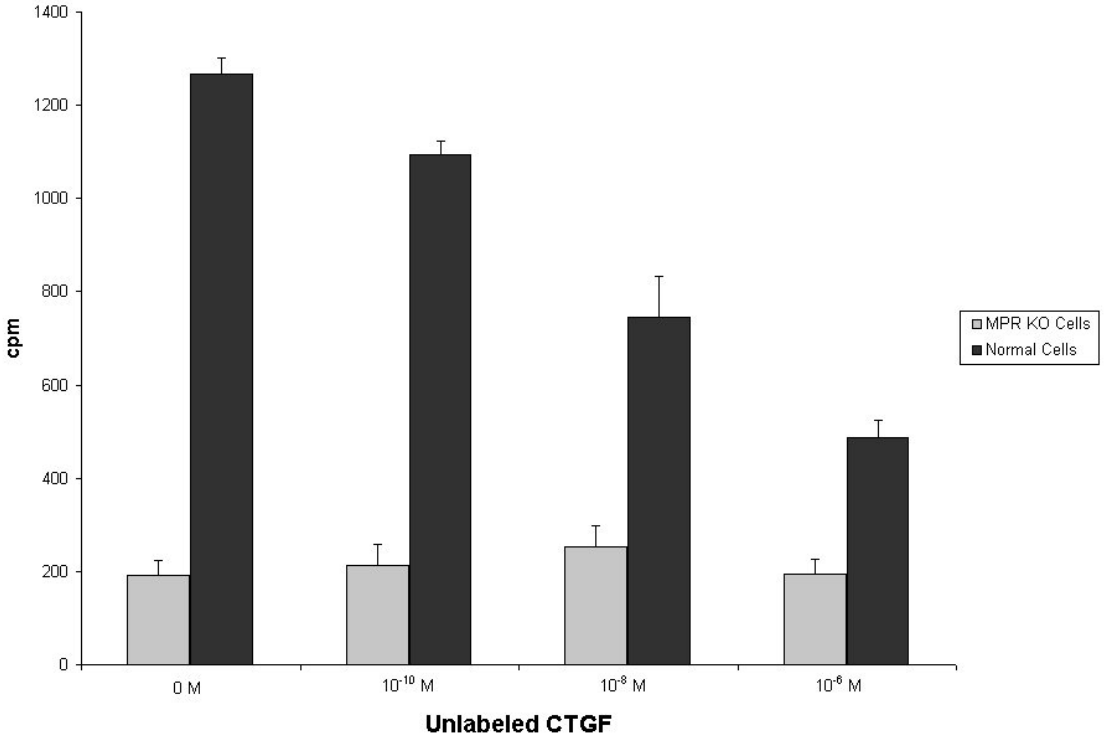

Figure 4-12. CTGF binding in Type II IGF receptor knockout cells. Type II IGF receptor knockout cells and wild type mouse lung fibroblasts were incubated with ^{125}I-CTGF in the presence of absence of excess unlabeled CTGF at 4°C (n = 6).

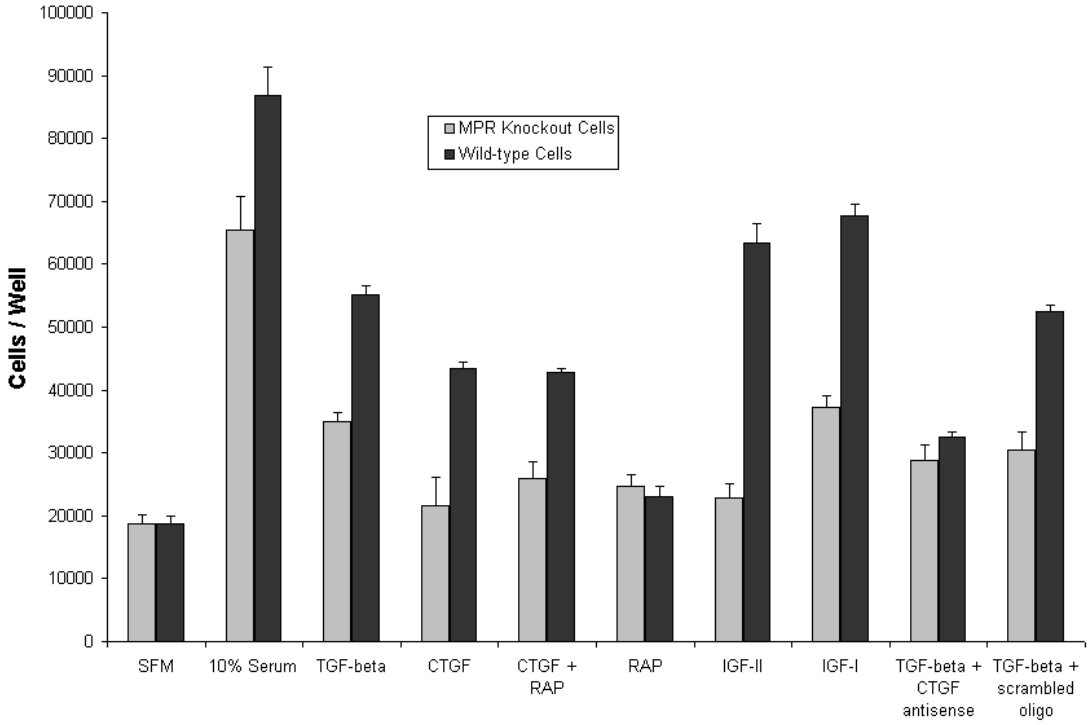

Figure 4-13. Cell proliferation in Type II IGF receptor knockout cells**.** The effect of exogenous agents on cell proliferation in type II IGF receptor knockout cells and wild type mouse lung fibroblasts cultures was measured. Cell proliferation was measured using an MTT assay. Cells were held in serum-free medium (SFM) for 48 hours followed by addition of the stimulants for 24 hours before the assay was performed.

CHAPTER 5
ABLATION OF CONNECTIVE TISSUE GROWTH FACTOR EXPRESSION AND ACTION USING HAMMERHEAD RIBOZYMES

Introduction

Ribozymes are catalytic RNA molecules first discovered twenty years ago that target and cleave specific sequences through base-pairing interactions (Kruger et al., 1982;Guerrier-Takada et al., 1983). After the ribozyme cleaves the bound target RNA, the products are released and recycled so that the process can be repeated many times. Since ribozymes could be repeatedly targeted to cleave almost any target transcript *in vitro* its effectiveness as a therapeutic agent in vivo was investigated (Cech, 1988a;Usman and Blatt, 2000). Extensive study of *trans*-cleaving ribozymes, such as hairpin and hammerhead ribozymes, have shown their abilities in reducing the target RNA of interest (Symons, 1992). Extensive investigations have defined the nucleotide sequences in naturally occurring ribozymes that retain the core catalytic nuclease activity (Scott et al., 1996). This knowledge has enabled investigators to design synthetic ribozymes that act as "gene specific endonucleases" by combining the catalytic core nucleotide sequence with flanking nucleotide sequences that are complementary to a target gene's mRNA sequence (Cech, 1988b;Sullivan, 1994). The consensus structure of the naturally occurring hammerhead ribozyme consists of three helical regions radiating from a central unpaired core, comprising the catalytic domain and the substrate portion. The 'hammerhead' catalytic domain (so named because of its secondary RNA structure) has been mapped to a small core sequence of less than 40 nucleotides. Mutational

analysis showed that base substitutions were responsible for reducing activity in the unpaired regions of the molecule, whereas mutations in the helical regions showed no effect as long as base pairing was maintained. Experimental data has shown that the nucleotide sequence represented by G-U-N, flanked by properly based paired segments, are the best candidates for cleavage (Haseloff and Gerlach, 1988). This suggests the possibilty of engineering a synthetic hammerhead ribozyme that selectively binds and cleaves a complementary mRNA molecule, then releases the fragments to repeat the process with the efficiency of a protein enzyme. Several studies have shown the effectiveness of hammerhead ribozymes in modifying gene expression *in vitro* and *in vivo*. For example, a preformed hammerhead ribozyme directed against tumor necrosis factor alpha (TNF-α) mRNA significantly reduced the expression of both mRNA and protein in human promyelocyte leukemia cells (Sioud et al., 1992). Additionally, a hammerhead ribozyme delivered by an adenovirus vector system led to a significant reduction in human growth hormone mRNA in a transgenic mouse system (Lieber and Kay, 1996). Also, ribozymes targeting oncogenes caused tumor cells to lose their metastatic potential in nude mice (Abounader et al., 1999).

Several clinical trials have focused on the possibility of developing ribozyme-based therapies for reducing human immunodeficiency virus (HIV) infection using retroviral vectors (Bauer et al., 1997;Wong-Staal et al., 1998). A separate study showed that a synthetic hammerhead ribozyme selectively cuts the mRNA for a dominant negative form of rhodopsin that causes an inherited form of retinitis pigmentosa but does not destroy the mRNA for the normal allele of rhodopsin using adeno-associated virus (AAV) vectors (Drenser et al., 1998b). In these experiments, a point mutation in the mutant allele created a hammerhead ribozyme cleavage site. It was further shown that

ribozyme rescue was maintained in rats up to eight months after treatment, and that ribozymes were effective even when injected later in the degeneration after significant photoreceptor cell loss (LaVail et al., 2000). These results show that ribozyme rescue appears to be a potentially effective, long-term therapy for autosomal dominant retinal degeneration and is highly effective even when the gene transfer is performed after significant photoreceptor cell loss.

Since the upregulation of connective tissue growth factor (CTGF) seems to be correlated with increased incidence of fibrosis and collagen deposition in many tissues, especially the cornea, one avenue for antifibrotic therapy is to reduce expression of CTGF. The use of antisense oligonucleotides and neutralizing antibodies to CTGF has been investigated previously (Blalock et al., 2003;Duncan et al., 1999d). To assess the hypothesis that a reduction of CTGF expression can positively affect the rate of wound healing, the influence of gene-specific ribozymes on cleavage of synthetic targets *in vitro* was investigated, the effect of CTGF ribozymes on expression of CTGF mRNA and protein in cell culture was measured, and the effect of CTGF ribozymes on TGF-β-mediated cell proliferation was surveyed.

Materials and Methods

Ribozyme Design and Synthesis

Potential ribozyme target sites within the human CTGF cDNA sequence were initially selected based on identification of the single-stranded regions and elimination of sites based on secondary structure (Wilson et al., 1996) reduced the number to four putative targeting sites within the human CTGF mRNA. Among these four sites, two containing the highest A and U content were selected for subsequent analysis (CHR 745

and CHR 859). Corresponding 33mer RNAs containing a hammerhead ribozyme and 12mer RNA targets were chemically synthesized as 2'-ACE protected oligonucleotides (Dharmacon Research Inc.; Lafayette, CO). The sequences of the synthetic target oligonucleotides were CHR 745: 5'- CCUGGUCCAGAC-3' and CHR 859: 5'-CAUGGUCAGGCC-3' (Figure 5-1). The sequences of the synthetic ribozymes to target these two substrate RNAs were CHR 745: 5'-GUCUGCUGAUGAGUCCUUCGGGACGAAACCAGG-3' and CHR 859: 5'-GGCCUCUGAUGAGUCCUUCGGGACGAAACCAUG-3' (Figure 5-1).

Ribozyme Time-course and Multi-turnover Kinetics

Target oligonucleotides were de-protected according to the manufacturer's directions and labeled with γ-[^{32}P]-dATP using the following reaction: 2 µl oligo-RNA (10pmol/ µl), 1µl RNasin (Promega; Madison, WI), 1µl 0.1M DTT, 3 µl ddH_2O, 1µl [γ^{32}P]-dATP, 1µl 10x PNK buffer, and 1µl T4 polynucleotide kinase (Roche Molecular Biochemicals; Indianapolis, IN). The reaction was incubated at 37°C for 30 minutes, and then diluted to 100 µl with ddH_2O, followed by extraction with phenol/chloroform/isoamyl alcohol (25:24:1). Free nucleotides were removed by passing the aqueous layer on a Sephadex G25 fine spin column. RNA was ethanol precipitated and resuspended in 100 µl ddH_2O to a final concentration of 0.2pmol/µl. Ribozyme cleavage reactions were performed in the presence or absence of various concentrations of ribozyme and target RNA in a reaction mix (20 µl) containing 40 mM Tris/HCl, pH=7.5 and 20 mM $MgCl_2$. Samples were incubated at 37 °C and the reaction was initiated by addition of ribozyme to target RNA. At the increasing times, the reactions were arrested with the addition of a 6 µL of 90% formamide, 50 mM EDTA (pH=8.0), 0.05% xylene cyanol, and 0.05% bromophenol blue. Reaction products were separated on

a 19% polyacrylamide gel containing 8 M urea, and were quantitated by radioanalytic scanning (PhosphorImager; Molecular Dynamics, Durham, NC).

In the time course study, reaction mixtures included 10 pmol ribozyme and 100 pmol target RNA (containing 0.2 pmol γ-[^{32}P]-target). Reactions were stopped at 0.5min, 1min, 2min, 3min, 4min, 5min, 10min, 30min, 1hr, 2hr, 3hr and 15hr. In the multi-turnover study, reactions were stopped at 1min. Reactions included 0.015 pmol/μL of ribozyme and increasing concentrations of target RNA (0.15-15 pmol/μL) shown in Table 5-1. Plots of substrate concentration over velocity versus substrate concentration were used to determine values for maximum velocity (Vmax), Michaelis-Menten constant (Km), and reaction rate at saturating substrate concentration (Kcat).

Table 5-1. Multi-turnover kinetics analysis. For cleavage reactions, increasing amounts of target oligo ranged from 0.15 to 15 micromolar.

	1	2	3	4	5	6	7	8	9	10	11	12
Ribozyme	0	0.015	0.015	0.015	0.015	0.015	0.015	0.015	0.015	0.015	0.015	0.015
Target	0.15	0.15	0.3	0.6	0.9	1.2	1.5	3.0	6.0	9.0	12	15

Plasmid Construction

Because of its better kinetic properties, CHR 745 was chosen as the candidate to test CTGF hammerhead ribozyme efficiency in cells. Single-stranded synthetic DNA oligonucleotides encoding ribozymes were chemically synthesized. The sequences were, CHR745 sense: 5'-AGCTGGCCTCTGATGAGTCCTTCGGGACGAAACCATGTGCA-3', CHR 745 antisense: 5'-CATGGTTTCGTCCCGAAGGACTCATCAGAGGCC. A second pair of oligonucleotides was constructed, replacing underlined nucleotides (C→G, G→C) to create a control inactive ribozyme. The complementary oligonucleotides were

annealed, producing *NsiI* and *HindIII* restriction sites (Promega; Madison, WI). The fragments were inserted into the pTR-UF-21HP vector, which had been linearized with *HindIII* and *NsiI* restriction enzymes. Synthesis of the ribozyme is driven by the chicken β-actin promoter and CMV enhancer in this vector. The presence and correct orientation of the insert was verified by DNA sequencing. Since the pTR-UF21HP vector contains a hairpin ribozyme following the insert site, it can self-cleave the mRNA when transcribed in the cell, yielding a relatively short 3' arm of hammerhead ribozyme, improving cleavage efficiency (Figure 5-2).

Cell Culture and Transfection

Cultures of human newborn foreskin fibroblasts (ATCC; Manassas, VA) were cultured in equal parts Dulbecco's Modified Eagle Medium (DMEM), Medium 199 (Gibco BRL), Ham's F_{12} nutrient mixture (Gibco BRL) containing 1 mM $NaHCO_3$, and buffered with 25 mM HEPES at pH 7.4. The medium was supplemented with 10% heat-inactivated normal calf serum and 1x antibiotic-antimycotic (Gibco BRL). Exponentially growing cells were transfected with vector (pTR-UF21), inactive ribozyme plasmid (pTR-UF21-In) or active CTGF ribozyme plasmid (pTR-UF21-CHR745) using Lipofecatime reagent (Invitrogen Life Technologies; Carlsbad, CA). Since pTR-UF-21 confers neomycin resistance, cells that were transfected stably were selected with Geneticin (G418 Sulfate, Invitrogen Life Technologies Carlsbad, CA). 48 hours after transfection, G418 was added to the culture medium at a concentration of 200 μg/ml. After 7 days, selected cells were transferred to 48-well plates.

Quantitative Reverse-transcription Polymerase Chain Reaction (Q-RT-PCR)

Cells in 48-well plates were held in serum-free medium for 48 hours before RNA extraction (Qiagen; Valencia, CA). CTGF mRNA transcripts were detected using the TaqMan real-time quantitative RT-PCR procedure (Livek et al. 1995). A standard curve was generated using CTGF mRNA transcripts that were transcribed *in vitro* using T7 RNA polymerase from a plasmid containing CTGF cDNA. CTGF transcript was precipitated with ethanol and dissolved in DEPC-treated water. Reactions were assembled in a 96-well optical reaction plate. Each reaction contained 1x TaqMan One-step RT-PCR Master Mix, 900 nM forward primer (5'-AGCCGCCTCTGCATGGT-3'), 900 nM reverse primer (5'-CACTTCTTGCCCTTCTTAATGGTTCT-3'), 2 μM fluorescent TaqMan probe (5'-6FAM-TTCCAGGTCAGCTTCGCAAGGCCT-TAMRA-3'), and RNA sample (CTGF mRNA standard or 500 ng of sample RNA) to a final volume of 25 μL per reaction. The plate was analyzed on the ABI Prism 5700 Sequence Detection System (Applied Biosystem, Foster City, CA), which simultaneously performs the RT-PCR and detects fluorescence signal. A standard curve was generated using the transcribed CTGF mRNA samples (2.3×10^{-2} to 2.3×10^{-6} pmol). The level of glyceraldehyde phosphate dehydrogenase (GAPDH) mRNA was also measured in each sample using the TaqMan GAPDH Control Kit (Applied Biosytems, Foster City CA), and the number of CTGF mRNA molecules in samples was expressed as pmol CTGF mRNA per pmol of GAPDH mRNA. Levels of mRNA were expressed as mean ± standard error of six replicate samples for each condition, and ANOVA and Tukey's HSD post-hoc test were used to assess statistical significance between times and groups.

CTGF Enzyme-linked Immunosorbent Assay (ELISA)

CTGF was measured in conditioned medium and in cytoplasmic extracts of serum-starved, cultured cells using a capture sandwich ELISA with biotinylated and non-biotinylated affinity purified goat polyclonal antibodies to human CTGF. Briefly, a flat-bottom ELISA plate (Costar 96-well) was coated with 50 μL of goat anti-human CTGF antibody at a concentration of 10 μg/mL in PBS/0.02% sodium azide for 1 hour at 37° C. Wells were washed four times and incubated with 300 μL of blocking buffer (PBS/0.02% sodium azide/1% bovine serum albumin) for 1 hour at room temperature. The wells were washed four times and 50 μL of increasing concentrations of recombinant human CTGF protein or sample were added and incubated at room temperature for 1 hour. After washing, 50 μL of biotinylated goat anti-human CTGF (2 μg/mL) was added and incubated at room temperature in the dark for 1 hour, then washed, and 50 μL of alkaline phosphatase-conjugated streptavidin (1.5 μg/ml, Zymed, South San Francisco, CA) was added and incubated at room temperature for 1 hour. The wells were washed again and incubated with 100 μL of alkaline phosphatase substrate solution (1 mg/mL p-nitrophenyl phosphate, Sigma Chemicals, St. Louis, MO) in sodium carbonate/bicarbonate buffer/0.02% sodium azide, pH = 9.6. Absorbance at 405 nm was measured using a microplate reader (Molecular Devices, Sunnyvale, CA). CTGF levels were normalized for total protein content of samples using bicinchoninic acid (BCA) protein assay reagent (Pierce Chemical, Rockford, IL) and were expressed as ng/mg protein for six replicate samples for each condition. Levels of protein were expressed as mean ± standard error of six replicate samples for each condition, and ANOVA and Tukey's HSD post-hoc test were used to assess statistical significance between times and groups.

Cell Proliferation Assay

Control cells (non-transfected), and cells transfected with vector, inactive CTGF ribozyme plasmid, or active CTGF ribozyme plasmid were seeded in a 48-well plate (5000 cells per well) and cultured for 48 hours in serum-supplemented medium. The cultures were stimulated with 5 ng/mL recombinant human TGF-β1 (R&D Systems; Minneapolis, MN) following 48 hours of serum-starvation. Cell proliferation was measured using a non-radioactive MTS cell proliferation assay (Promega; Madison, WI). Absorbance reading corresponding to cell proliferation were expressed as mean ± standard error of six replicate samples for each condition, and ANOVA and Tukey's HSD post-hoc test were used to assess statistical significance between times and groups.

Results

Kinetics of CTGF Hammerhead Ribozymes

Time course and multi-turnover studies were performed to test the kinetic properties of the ribozymes. Chemical synthesized RNA was labeled by γ-[^{32}P]-ATP using polynucleotide kinase (PNK). Polynucleotide kinase catalyzes the transfer of the terminal phosphate of ATP to the 5'-hydroxyl terminus of ribo- and deoxyribonucleotides. Two products were produced following cleavage of the labeled synthetic products by the ribozyme: a 7-nucleotide 5' product and a 5-nucleotide 3' product. The intact oligo-RNA and 5' product, labeled by γ-[^{32}P]-ATP, were detectable by radioanalytic scanning.

In time course studies, CHR 859 was significantly more active than the CHR 745, cleaving 92% compared with 22% at 30 minutes and 94% compared with 46% at the end of incubation (Figure 5-3). Data shown are the result of two experiments. To estimate the catalytic efficiency of these ribozymes, steady-state cleavage velocities were measured

with constant amounts (15 pM) of ribozyme and increasing concentrations (150-15,000pM) of the substrate. The enzymatic reactions demonstrate Michaelis-Menten kinetics and were analyzed using Haynes-Wolff plots (Figure 5-4). CHR 859 showed a K_m of 1.56 μM and a K_{cat} of 2.97/min while CHR 745 had a K_m of 7.80 μM and a K_{cat} of 5.7/min. The turnover numbers (an estimate of the second order rate constant) of CHR 859 and CHR 745 were 1.9 $x10^{-6}$M/min and 7.4 $x10^{-5}$ M/min, respectively, thus CHR 859 is 2.6 times more efficient.

Effect of Ribozymes on CTGF Expression in Cell Culture

Because of its better kinetic parameters, CHR 859 was chosen to test the efficiency of cleavage of CTGF mRNA in cell culture. Expression of CTGF mRNA was measured by quantitative RT-PCR and CTGF protein was measured by enzyme-linked immunosorbent assay (ELISA). Results showed that CTGF mRNA expression in CHR 859-transfected cells was decreased by 55% ($p < 0.01$, $n = 6$) compared with control groups (Figure 5-5). CTGF protein expression was measured in conditioned medium and in cytoplasmic extracts. In cells transfected with the active CTGF ribozyme, CTGF protein was significantly reduced (by 72% in conditioned medium and 71% in the cytoplasm, $p < 0.01$, $n = 6$) compared with control groups (Figure 5-6).

Effect of Ribozymes on TGF-β-mediated Cell Proliferation

Since CTGF is a putative mediator of TGF-β-induced cell proliferation in cells in culture, the effect of ribozymes on hindering this process was performed. As seen in Figure 5-7, cells transfected with the active ribozyme to CTGF showed a marked decrease (90%, $p < 0.01$, $n = 6$) in cell proliferation when compared to control cell

groups. This implies that the use of CTGF ribozymes have a physiological effect on cells as well as decreasing CTGF mRNA and protein expression.

Discussion

The roles of growth factors in wound healing such as epidermal growth factor (EGF), transforming growth factor alpha (TGF-α, basic fibroblast growth factor (bFGF), and interleukin-1 alpha (IL-1α), platelet derived growth factor (PDGF), and TGF-β, are well-established. For example, levels of TGF-β mRNA increase in many fibrotic disorders such as lung fibrosis and liver cirrhosis (Nall et al., 1996;Kurt et al., 1992). These levels are correlated with increased expression of extracellular matrix genes, such as type I and type III collagen, integrins, and fibronectin (Chen et al., 2000b;Irving and Lala, 1995). Treatment of glioblastoma cell lines with antisense oligonucleotides to TGF-β1 decreased expression of collagen types I and IV, laminin, and fibronectin (Paulus et al., 1995). Furthermore, treatment of full-thickness incision wounds with neutralizing antibodies to TGF-β decreased severity of fibrosis (Brahmatewari et al., 2000).

Changes in CTGF expression during wound healing and the interactions between the TGF-β and CTGF system have been established in several systems. All three isoforms of TGF-β increase CTGF mRNA and protein expression in human dermal and corneal fibroblasts (Tamatani et al., 1998;Blalock et al., 2003). CTGF also mediates the effects of TGF-β on collagen synthesis and cell proliferation in fibroblast cultures (Duncan et al., 1999c;Blalock et al., 2003;Hashimoto et al., 1998b;Shimo et al., 1999). Antisense oligonucleotides and neutralizing antibodies to CTGF decrease TGF-β-

mediated collagen synthesis (Duncan et al., 1999b;Blalock et al., 2003). This suggests that CTGF may be an important target in reducing scarring, however antisense oligonucleotides and neutralizing antibodies may prove to be more effective if used in conjuction with ribozymes.

Since ribozyme technology has been used successfully in reducing mRNAs in various experimental systems, it is likely to be effective in reducing the rate of fibrosis *in vivo* by blocking CTGF expression. The CTGF ribozymes used in these experiments show kinetics similar to other hammerhead ribozymes used in similar assays as seen in Figures 5-3 and 5-4 (Lewin et al., 1998;Drenser et al., 1998a). Some differences exist between the kinetics of CHR 745 and CHR 859, which may be due to some unexpected secondary structure which can inhibit the efficiency of the ribozyme to cleave the target RNA. There are limitations to data obtained from *in vitro* cleavage experiments because of the complex secondary structure of full length mRNA, which is why it will be necessary to test the effectiveness of ribozymes in cell culture before developing a suitable animal model.

Expression of ribozymes in fibroblast cell cultures have been shown to effectively reduce the expression of mRNAs of interest (Propsting et al., 2000;Dawson and Marini, 2000). Similarly, ribozymes targeted to CTGF mRNA significantly reduced the expression of CTGF mRNA and protein in human dermal fibroblasts (Figures 5-5 and 5-6). TGF-β-induced cell proliferation was measured to prove that the ribozyme-mediated reduction in CTGF expression has a physiological effect on cells. As seen in Figure 5-7, reduction of CTGF expression was sufficient enough to significantly reduce the capacity of TGF-β to induce cell proliferation in the fibroblast cultures.

These experiments prove that synthetic ribozymes cleave CTGF target mRNA *in vitro* and that dermal fibroblasts expressing an active CTGF ribozyme show decreased expression of CTGF mRNA and protein compared to control cells or cells expressing an inactive CTGF ribozyme. In addition, cells expressing an active CTGF ribozyme exhibit a reduced response to TGF-β on stimulating fibroblast proliferation in cultures. These results further prove that CTGF mediates some of the effects of TGF-β in wound healing and that CTGF may be a key target for therapies by selectively reducing expression. CTGF ribozyme used in conjunction with antisense oligonucleotides or neutralizing antibodies may have a maximal effect in reducing the expression of CTGF and potentially reducing scarring and fibrosis. Ribozymes were developed that effectively cleave target sequences of mRNAs for CTGF, and the significantly reduced the levels of CTGF mRNA and protein in cultured cells. The next phase of the development is to begin testing the ribozymes in vivo using rat and rabbit models of excimer-induced corneal haze. It may be necessary to suppress the actions of CTGF for weeks or months after corneal injury to reduce corneal scarring, in which case delivery of the ribozymes by an adenovirus or adeno-associated virus (AAV) vector may be very effective.

One of the goals of this project is to develop agents that will reduce corneal scarring with minimal side effects. To test this possibility, initial experiments using ribozymes to target CTGF mRNA were performed. Development of ribozyme therapy is important because there are no agents to block corneal scarring other than steroids, which have not shown to be of much benefit after PRK. Some non-specific anti-cancer drugs have been used to treat corneal scarring such as 5-fluorouracil and mitomycin C but they cause serious side effects in some instances such as epithelial defects and endothelial cell

damage. Because of these problems ribozyme-mediated gene therapy may be a good candidate for treatment. In these studies, a gene-specific hammerhead ribozyme targeting CTGF was developed and was shown to reduce the expression of CTGF in cell culture as well as reduce the biological effects of CTGF. Further animal studies will be performed in the future to confirm that the ribozyme has a similar effect *in vivo* in a wound healing model. It is likely that the use of ribozymes in conjunction with treatment with antisense oligonucleotides or neutralizing antibodies will reduce the fibrosis in the cornea after injury that leads to haze. These treatments have many advantages over current treatment options because they will selectively inhibit scarring without resulting in serious side effects. These modes of treatment can also be modified to act not only on corneal fibrosis, but also on fibrotic conditions throughout the body.

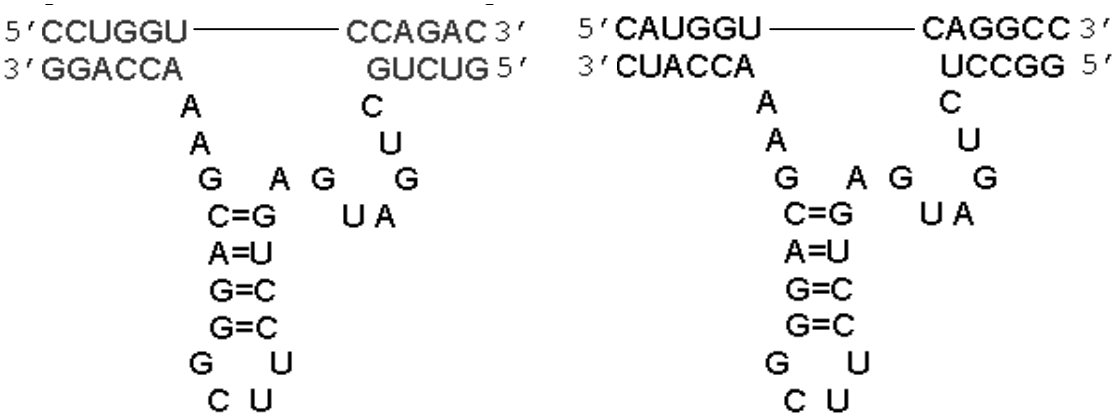

Figure 5-1. Structure of synthetic RNA oligonucleotides. CTGF hammerhead ribozyme (CHR 745, left and CHR 859, right) 33mer RNAs were synthesized along with corresponding 12mer target RNA to the sequence of CTGF. The target RNA is shown on the top and the ribozyme RNA is directly below the complimentary base pairs

Figure 5-2. Structure of self-cleaving hairpin ribozyme. The self-cleaving hairpin ribozyme follows the hammerhead ribozyme cloning site in pTR-UF-21. When transcribed the hairpin ribozyme cleaves the sequence following the right arm of hammerhead ribozyme.

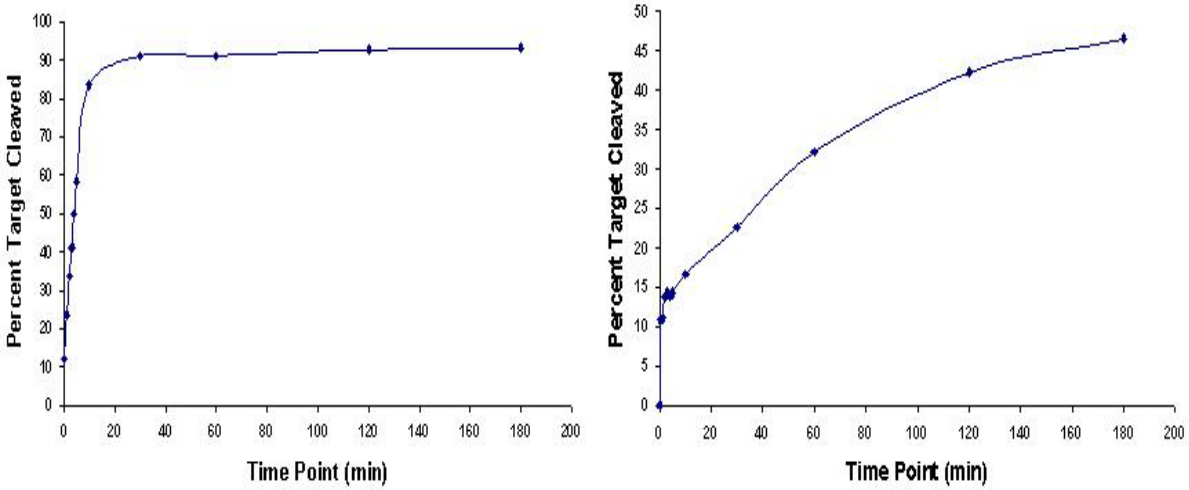

Figure 5-3. Ribozyme cleavage time-course analysis. Time course of CTGF target RNA cleavage by CHR 859 (left) and 745 (right). Cleavage reaction durations ranged from 0 minutes to 15 hours (15 hour data point not shown).

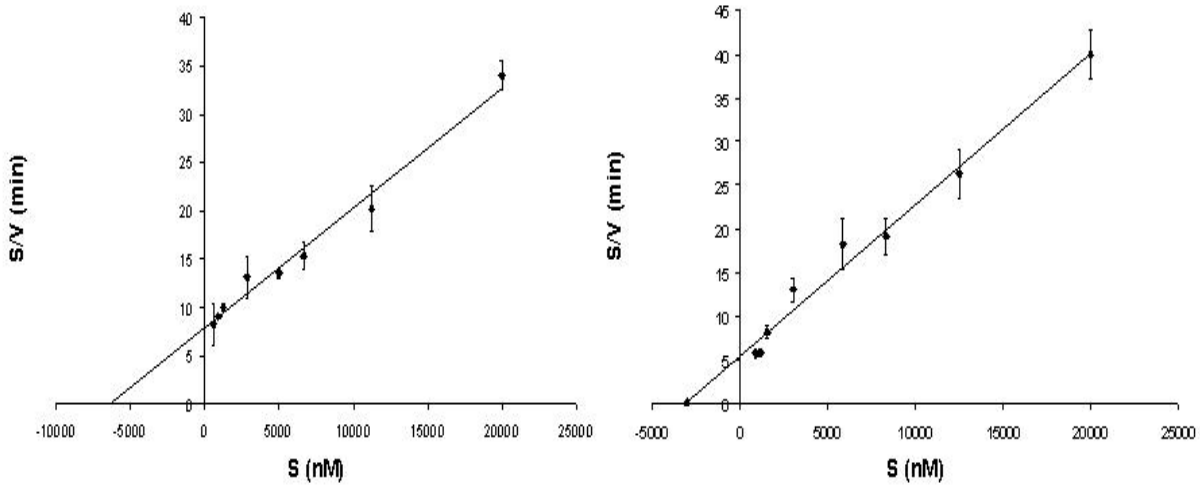

Figure 5-4. Multi-turnover kinetic analysis. Haynes-Wolff plots are shown indicating Michaelis-Menton kinetics for CHR 859 (left) and 745 (right). The duration of the cleavage reactions was one minute.

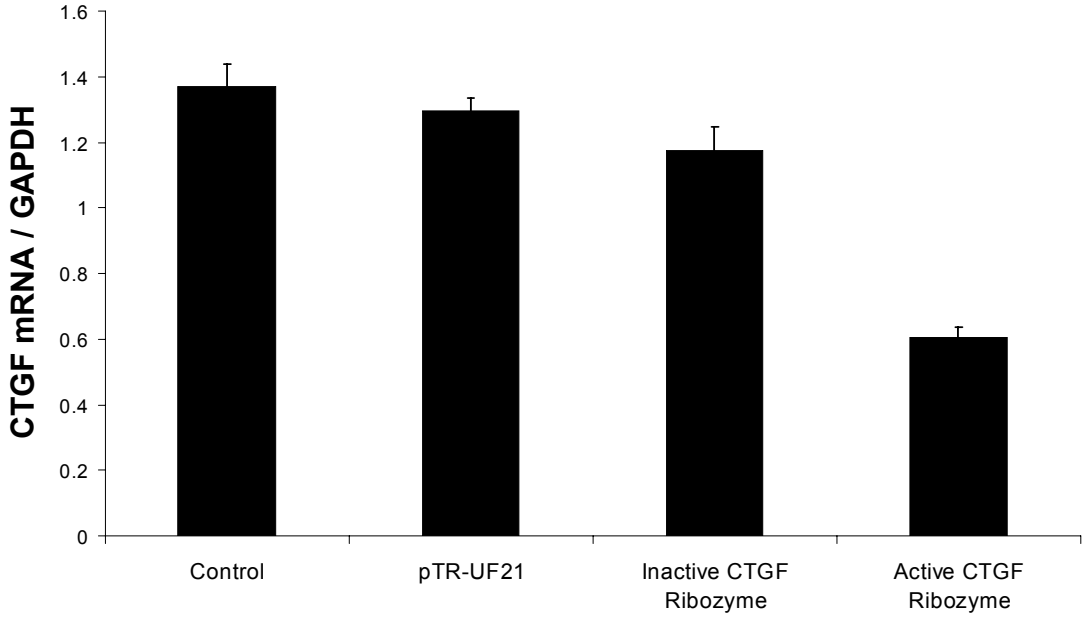

Figure 5-5. Effect of CHR 745 on mRNA expression. The effect of CHR 745 on CTGF mRNA expression in human dermal fibroblast cultures was examined. CTGF mRNA was measured using TaqMan quantitative RT-PCR and results were normalized to GAPDH mRNA. Cells were transfected with vector, inactive ribozyme plasmid, or active ribozyme plasmid and selected with G418.

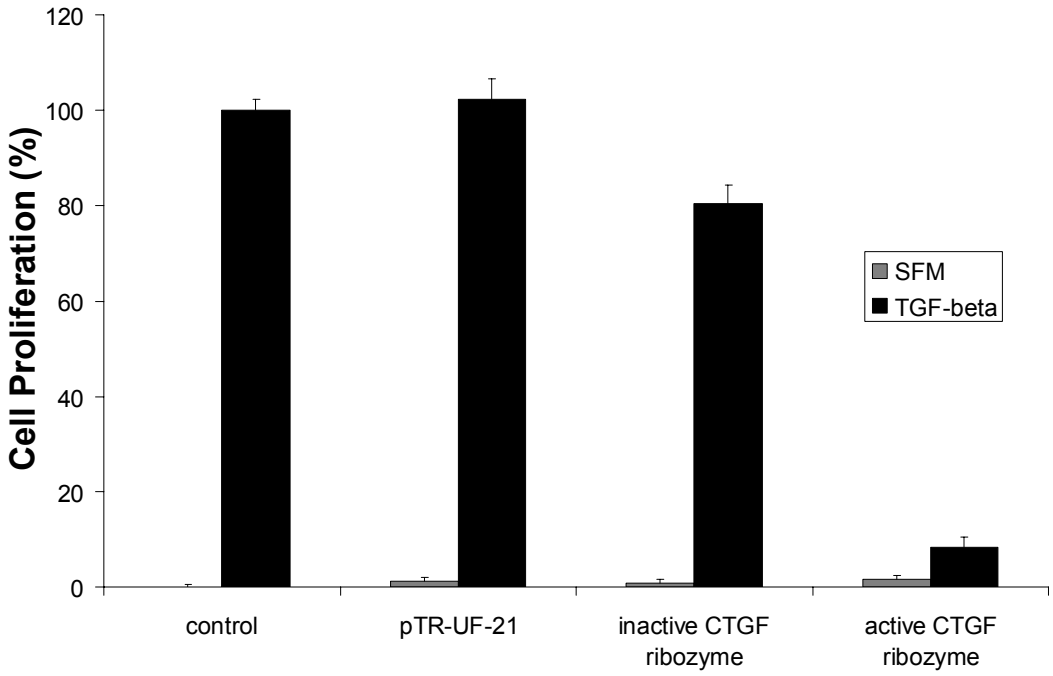

Figure 5-6. Effect of CHR 745 on protein expression. CTGF protein was measured in cytoplasmic extracts and conditioned medium samples of human dermal fibroblast cultures using a CTGF 'sandwich' ELISA and results were normalized for total protein concentration.

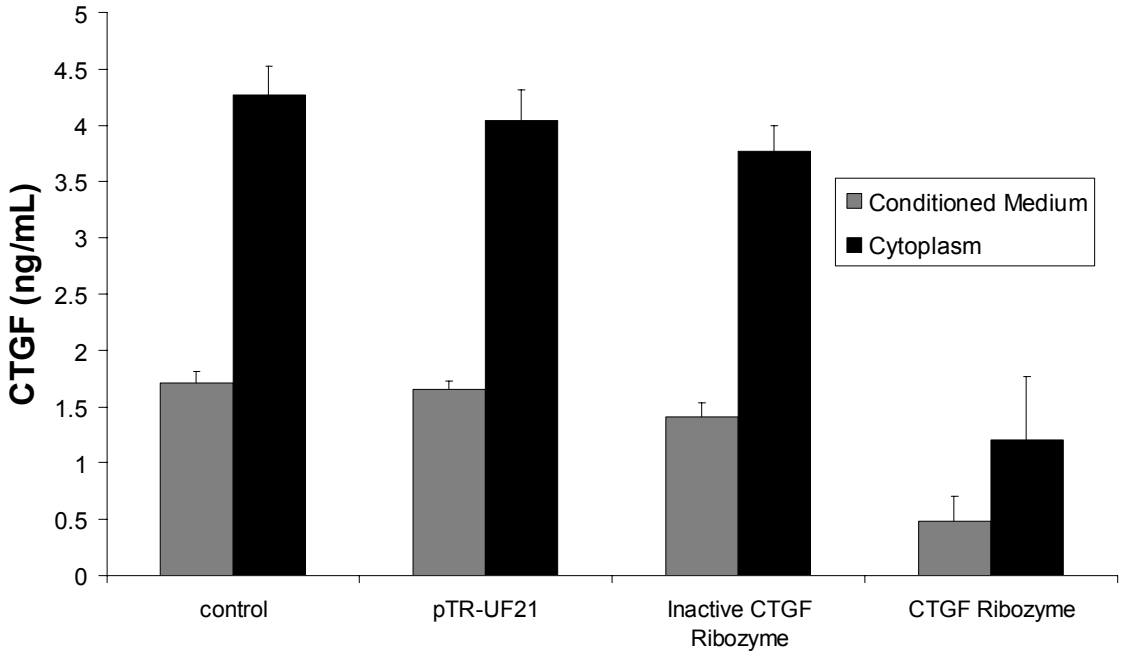

Figure 5-7. Effect of CHR 745 on TGF-β-induced cell proliferation. The effect of CHR 745 on TGF-β-induced cell proliferation in human dermal fibroblast cultures was examined. Cell proliferation was measured using an MTT assay. Cells were transfected with vector, inactive ribozyme plasmid, or active ribozyme plasmid and selected in G418. Cells were held in either serum-free medium (SFM) or medium containing 10 ng/mL TGF-β1 24 hours before assaying. Data are normalized based on control cells in serum-free medium (0% proliferation) and control cells treated with TGF-β (100% proliferation).

CHAPTER 6
GENE EXPRESSION ANALYSIS OF CONNECTIVE TISSUE GROWTH FACTOR STIMULATED HUMAN CORNEAL FIBROBLASTS

Introduction

The field of microarray technology utilizes the hybridization properties of nucleic acids to measure the expression of DNA or RNA on a very large scale. Genomics research has been revolutionized by advances in microarray procedures and data analysis because of the possibility of examining the expression of thousands of genes simultaneously. It is important to understand the roles that genes and their products play in the context of biological processes and functions. This can be accomplished by correlating sequences of genes to specific biological functions through the study of gene expression patterns. This advantage of simultaneously studying thousands of genes under different conditions of stimulation or disease states offers great potential to the study of human disease and prevention. Several methods are currently available for the large-scale analysis of gene expression patterns such as gene membrane arrays and GeneChip microarrays. Gene chip microarrays have many advantages, especially the ability to measure the expression of thousands of genes in one sample with very rigorous analysis procedures.

Affymetrix expression probe array chips utilize immobilized 25-base pair oligonucleotide probes. For each gene, 11-16 probes or tiles are present on the chip and the sequences are taken from different locations along the transcript. Perfect match and mismatch probes are present on the chip microarrays. The perfect match probes are

designed to be complementary to a reference sequence and the mismatch probes are also designed to be complementary to the reference sequence except for a homomeric base mismatch at the central position. Mismatch probes serve as control for cross-hybridization. The probes are organized into probe cells, which contain millions of probe molecules. A probe pair consists of two probe cells, a perfect match and its corresponding mismatch. A probe set consists of 11-16 probe pairs and provides the information necessary for the expression analysis of each gene. In the first step of the analysis, the scanned image is imported into the GeneChip software and a grid is automatically placed and aligned over the scanned image of the array. The average intensity of each probe cell is then calculated along with the background and noise values. The noise is a measure of the degree of pixel-to-pixel variation within the same probe cell. To obtain the net intensity, the software subtracts the background and noise from the average intensity of each probe cell. Next, the average difference for each probe set is calculated. Statistical algorithms are used to determine significance in detected probe sets. The average difference is an average of the differences in net intensity between every perfect match probe cell and its control mismatch probe cell within each probe set and is directly related to the level of expression of the transcript. The average difference value for each gene at each experimental time point undergoes variance normalization and the most variable genes and ESTs are clustered through hierarchical algorithms using Cluster and Treeview (Eisen et al. 1998). The clustering procedure groups together genes on the basis of their common expression patterns across the time points. Each cluster is then identified and an analysis is performed on any gene that encodes for proteins of interest.

The classes of genes regulated by CTGF need to be examined to better understand how CTGF affects wound healing. Currently, only a few genes are known to be regulated by CTGF. For example, CTGF increased mRNA levels for type I collagen, type IV collagen, fibronectin, α5 integrin, laminin, and caspase 3 while decreasing mRNA levels for several anti-apoptosis genes including BCL-2, apoptosis inhibitors 1 and 2, and survivin (Hishikawa et al. 2001). Microarray technology is the best way to efficiently and accurately attempt to broadly define the action of CTGF on gene expression in human corneal fibroblasts. This approach allows for simultaneous measurement of thousands of known genes and expressed sequence tags (EST) in the same samples. These experiments will help assess our hypothesis that CTGF is integral in the regulation of corneal wound healing and will elucidate the classes of genes that are involved in this process.

Materials and Methods

Cell Culture and RNA Isolation

Cultures of corneal fibroblasts were established by outgrowth from human corneal explants as described previously (Woost et al. 1992). Briefly, epithelial and endothelial cells were removed from corneas that were unsuitable for corneal transplantation, the stroma was cut into cubes approximately 1 mm^3, placed in culture medium consisting of equal parts Dulbecco's Modified Eagle Medium (DMEM), Medium 199 (Gibco BRL), Ham's F_{12} nutrient mixture (Gibco BRL) containing 1 mM $NaHCO_3$, and buffered with 25 mM HEPES at pH 7.4. The medium was supplemented with 10% heat-inactivated normal calf serum and 1x antibiotic-antimycotic (Gibco BRL). Cell cultures were used at passage 2 for all experiments. Cells were seeded in twelve 75-cm^2 tissue culture flasks.

Prior to treatment, cells were rinsed with serum-free medium and incubated with serum-free medium for an additional 48 hours. After exposure to 25 ng/mL recombinant human CTGF for 0, 0.5 or 24 hours, total RNA was isolated using RNeasy kits (Qiagen; Valencia, CA). Total RNA was isolated from four independent replicates of each time point of CTGF exposure and processed in parallel.

cRNA Preparation and Array Hybridization

Total RNA was converted into double-stranded cDNA using a custom double-stranded cDNA synthesis kit (SuperScript II; Invitrogen, Gaithersburg, MD). cDNA was extracted and in vitro transcription reactions were performed (BioArray HighYield RNA Transcript Labeling Kit; Enzo Biochemicals, Inc.; Farmingdale, NY) according to the manufacturer's protocol. Following purification, the labeled cRNA was quantified by spectrophotometric analysis, and fragmented to 30 to 60 base fragments with Tris-acetate (pH 8.1; 40 mM), KOAc (100 mM), and MgOAc (30 mM) in a 40-μL volume heated for 35 minutes at 94°C. Protocols for instrumentation, cRNA sample preparation and labeling, hybridization to U95A v2 human microarrays, washing, staining, and scanning were followed as recommended in the Affymetrix Expression Analysis technical manual (Affymetrix, Santa Clara, CA).

Data Analysis

Microarray data analysis: Scanned images (*.dat files) were analyzed with Affymetrix® Microarray Suite V 5. Raw Qs ranged from 1.6 to 2.9. Average Background ranged from 42 to 95. Chips were normalized using global normalization with an average target gene intensity of 500. Scaling factors ranged from 2.5 to 10.

Expression filter: Probe Sets that were flagged as absent on all arrays analyzed in this study by the Affymetrix® Microarray Suite v 5 software using default settings were removed from the datasets subjected to k-means, hierarchical cluster analysis, and supervised learning analysis. After this expression filter was applied the dataset was reduced from 12,625 probe sets to 7,834 probe sets.

Variation Filter: The gene expression observations (signal intensities) of the probe sets remaining after applying the expression filter obtained from the 12 U95Av2 GeneChips™ were subjected to a variation filter. The coefficient of variation was calculated for each probe set across the 12 chips and the probe sets were ranked by the coefficient of variation of the observed single intensities.

V*ariance Normalization:* After removing Affymetrix control probe sets, the top-half of the dataset (observation of 3,894 probe sets) as determined by ranking of the coefficient of variation was normalized to a mean of 0 and a standard deviation of 1.

Cluster Analyses: K-means and hierarchical cluster analyses were preformed using the variance normalized dataset and viewed with the algorithms in the software packages Cluster and TreeView (Eisen et al. 1998). Hierarchical clustering arranges genes into tree structures to view gene linkages while K-means clustering partitions genes into a pre-determined amount of clusters. "Spaghetti" graphs were generated using Genesis 1.13 developed by Sturn to examine the gene expression profiles in each group of the K-means clustering analysis (Wenger et al., 1999a).

Supervised Learning, Discrimination Analysis, and Cross Validation: The hybridization signal intensities of the 7,834 probe sets that passed the expression filter were analyzed to identify probe sets, that displayed differential hybridization signal

intensities, $p < 0.001$, between the three treatment classes, unstimulated (0 hr CTGF stimulation), 0.5 hr CTGF stimulation, and 24 hr CTGF stimulation using BRB Array Tools (Ye et al. 2003). The validity of probe sets identified at the p 0.001 significance level in predicting treatment class was established using "leave-one-out" cross validation where the data from one array was left out of the training set and probe sets with differential hybridization signal intensities (p 0.001) were identified from the remaining 8 arrays. The probe sets so identified were then used to predict the class label (unstimulated, 0.5 hr CTGF stimulation, or 24 hr CTGF stimulation) of the array that was left out of the training set. Three methods of class prediction were used: nearest neighbor, three nearest neighbor, and nearest centroid analysis.

Results

Unsupersived Analysis

Four flasks of human corneal fibroblasts were evaluated in each of three groups: control (cells held in serum-free medium) and two experimental groups. The experimental groups were treated with recombinant human CTGF for either 30 minutes of 24 hours. The RNA was isolated from the fibroblast cultures and processed for microarray analysis in the manner described above. The resulting data set was filtered to remove data from probe sets that were not detected above background on any of the arrays. A variation filter was applied to remove signals from probe sets that did not vary much in the experiment. The signals of the remaining probe sets were then subjected to unsupervised hierarchical cluster analysis as shown in Figure 6-1. The primary node of separation was between control and 30 minute samples, indicating that cells treated with CTGF have significant expression changes compared to cells grown in serum-free

medium with no treatment. The results also suggest that after 24 hours of CTGF stimulation, gene expression patterns had not returned to those seen in control (unstimulated cells).

Table 6-1. Leave-one-out cross-validation analysis

Chip number	Array ID	1 nearest neighbor correct?	3 nearest neighbors correct?	Nearest centroid correct?
1	0 hr – r1	YES	YES	YES
2	0 hr – r2	YES	YES	YES
3	0 hr – r3	YES	YES	YES
4	0 hr – r4	YES	YES	YES
5	0.5 hr – r1	YES	YES	YES
6	0.5 hr – r2	YES	YES	YES
7	0.5 hr – r3	YES	YES	YES
8	0.5 hr – r4	YES	YES	YES
9	24 hr – r1	YES	YES	YES
10	24 hr – r2	YES	YES	YES
11	24 hr – r3	YES	YES	YES
12	24 hr – r4	YES	YES	YES
Percent correctly classified		100	100	100

The image presented in Figure 6-1 shows the hierarchical cluster pattern of the top half of hybridization intensities ranked based on coefficient of variation (representing 3,894 probe sets) whose expression varied the most upon stimulation of the cells with CTGF. This figure shows the TreeView representation of the data set after clustering. The color scale shows whether the expression of the gene is higher (red) or lower (green) than its mean expression value across the time course of CTGF stimulation. Genes with similar expression patterns cluster together in this view. The dendrogram at the top of the figure shows the similarity of the expression patterns observed throughout the time course. The dendrogram shows that replicate arrays cluster together, and that there are

discrete groups of genes that are positively and/or negatively affected in response to CTGF at 0.5 and 24 hours when compared to non-treated cells.

Supervised Analysis

To identify genes whose expression levels varied between treatment classes, a supervised learning method was used to identify probe sets representing genes with significant differences in expression. The dataset was divided among three classes (0 hr, 0.5 hr and 24 hr exposure to CTGF) and significant differences in hybridization signal intensity at the $p < 0.001$ level of significance were identified using an F-test. In all 2,761 probe sets were identified as significant at $p < 0.001$. The ability of these probe sets to act as a classifier of time of exposure to CTGF was assesed using leave-one-out cross validation and permutation analysis. Results of this analysis show that the classifiers were able to correctly identify all the correct treatment group (Table 6-1).

The changes in gene expression in the corneal fibroblasts throughout the time course of CTGF stimulation are most easily visualized using k-means clustering (Figure 6-2). Ten groups were chosen for the K-means clustering analysis to examine the expression profiles after CTGF stimulation. Clusters 1-5 represent classes of genes that were down-regulated in the corneal fibroblasts upon exposure to CTGF and clusters 6-10 represent classes of genes that were up-regulated. The pie charts in Figure 6-3 show the gene functional groups present in each of the clusters which comprise 5% or more of the total cluster. The 'other' category represents genes of unknown function, ESTs, unclassified genes, and functional groups comprising less than 5% of the cluster. Certain functional groups fall into logical clusters based on the limited number of genes that are known to be affected by CTGF. For example, about 8% of the genes in cluster 9 fall into

the ‘extracellular matrix proteins’ family. Several members of this group, such as collagen I, fibronectin, and laminin have been previously shown to be upregulated at 24 hours after stimulation by CTGF (Hishikawa et al. 2001). The functional group ‘intracellular kinase network members’ (containing such genes as mitogen-activated protein kinases and other protein kinases) is present in clusters 2 through 5, all of which show a down-regulation by CTGF. Also of interest, a substantial number of ribosomal protein genes grouped into clusters that were up-regulated by CTGF at 0.5 and 24 hours (clusters 8 and 9). In contrast, some of the RNA processing, turnover, and transport genes grouped into clusters that were down-regulated at 0.5 and 24 hours, while others showed patterns similar to the ribosome protein genes. Other genes of interest had more complex patterns of regulation. Genes in clusters 5 and 6 (including groups such as oncogenes/tumor suppressors and cytoskeleton/motility proteins) were down regulated at 0.5 hours but were up-regulated at 24 hours, while genes in clusters 1 and 10 (including groups such as general trafficking genes and nucleotide metabolism genes) were the inverse pattern, and were up-regulated at 0.5 hours but down-regulated at 24 hours.

Selected Genes of Interest

Examination of the groups in Figure 6-2 shows the distinct gene expression responses to corneal fibroblasts when treated with CTGF. Ten groups were examined using k-means clustering of the 2,761 genes with an F-test $p < 0.001$ for variance normalized data presented in Figures 6-2 and 6-3 show the overall patterns of changes in gene expression at the two time points. In addition, 141 genes from the 2,761 genes were selected that fall into functional groups of particular interest to CTGF physiology. For example, previous reports have theorized that CTGF mediates TGF-β-induced apoptosis

in aortic smooth muscle cells and hepatoma cells (Hishikawa et al. 1999a; Hishikawa et al. 2000; Coyle et al. 2002). Certain apoptosis-associated genes, such as the caspases, have been previously shown to be up-regulated by CTGF (Frazier et al. 1996). As shown in Table 6-2, caspases 4, 7, and 8 fall into clusters 8 and 10, which contain genes that were up-regulated at 0.5 hours by CTGF. In addition, the anti-apoptosis gene, BCL2, was rapidly down-regulated by CTGF (2.3-fold decrease at 0.5 hours, cluster 5), then returned to near 0 hour levels at 24 hours in accordance with previously published reports (Frazier et al. 1996; Hishikawa et al. 1999b). Thus, the array data support the hypothesis that CTGF has a transient influence on expression of apoptosis-related genes.

Since CTGF is implicated in regulating scar formation, it is also of particular importance to note the influence of CTGF on expression of extracellular matrix genes. Collagens I, III, IV, fibronectin, laminin, and integrins are all important extracellular matrix genes and all are present in clusters that show increased expression after 24 hours of CTGF stimulation. Additionally, CTGF upregulated levels of mRNAs for chondroitin sulfate proteoglycan (versican) and heparan sulfate proteoglycan (perlecan), which play key roles in hydration of the corneal matrix and act as ligands for integrin receptors (Hirose et al. 2001; Saika et al. 2000), indicating that it may play a role in regulating adhesion between the cell and substratum (Yamagata et al, 1993; Malmstrom et al, 2002). CTGF is a member of the insulin-like growth factor binding protein (IGFBP) family and seems to have an effect on numerous members of this family (Bork 1993). This observation is important because alteration of IGFBP family member expression has been associated with various tumors (Astifoli et al. 2001; Vorwerk et al. 2002). CTGF also upregulates matrix metalloproteinase-1 (MMP-1, interstitial collagenase), suggesting a

role in adhesive signaling (Chen et al, 2001). Another interesting trend to note is that expression of alpha smooth muscle actin increases 2.4-fold in response to CTGF. This may imply that CTGF plays a role in the transformation of corneal keratocytes to myofibroblasts and cellular contraction (Jester et al. 1999). These findings are consistent with unpublished data on the stimulation of human corneal fibroblast contraction of relaxed collagen gels by CTGF and different from the lack of an effect on rabbit corneal fibroblasts (Folger et al. 2001).

CTGF has also been suggested to play a role in regulating angiogenesis. CTGF decreased thrombospondin type 1 mRNA (cluster 3) and increased expression of vascular endothelial growth factor (cluster 8). Thrombospondin-1 (TSP-1) is a bifunctional regulator of angiogenesis that depends on its concentration and the state of its proteolytic fragmentation. At low concentrations, the whole TSP-1 molecule and the amino-terminus stimulated angiogenesis in a rabbit cornea model, perhaps by up regulating expression of MMPs that are necessary for degrading basement membranes of capillaries and CTGF in the inactive CTGF/VEGF complex which releases active VEGF (Hashimoto et al, 2002; Ferrara 2002). This is consistent with report of CTGF stimulating migration of vascular endothelial cells and angiogenesis in the chick chorioallantoic membrane assay (Shimo et al. 1999). At higher concentrations, thrombospondin inhibits angiogensis, perhaps by binding and inactivating VEGF (Ferrara 2002).

Table 6-2. Selected genes of interest. Genes of interest from the data in Figure 6-2 were chosen. Genes likely to be most affected by CTGF stimulation are involved in wound healing, cell signaling, and extracellular matrix production. Fold changes (FC) are shown along with the clusters identified in Figure 6-2.

Gene	F-test P value	Cluster	FC (0.5 vs. 0)	FC (24 vs. 0)	FC (24 vs. 0.5)
Caspases					
caspase 4, apoptosis-related cysteine protease	5.68E-06	8	1.46	1.69	1.16
caspase 7, apoptosis-related cysteine protease	0.000638	10	1.33	-1.00	-1.33
caspase 8, apoptosis-related cysteine protease	2.97E-05	10	1.52	1.10	-1.38
Cell adhesion receptors/proteins					
chondroitin sulfate proteoglycan 2 (versican)	9.83E-08	8	1.46	1.97	1.84
chondroitin sulfate proteoglycan 2 (versican)	2.75E-05	8	1.89	2.68	1.95
fibronectin leucine rich transmembrane protein 2	4.58E-05	1	1.21	-1.12	-1.35
Cell surface antigens					
integrin, alpha 3 (antigen CD49C)	0.000127	5	-2.14	-1.67	1.28
integrin, alpha V (vitronectin receptor)	9.08E-06	9	1.02	1.74	1.71
Cell-cell adhesion receptors					
cadherin 11, type 2, OB-cadherin	9.28E-07	2	-1.11	-1.42	-1.28
cadherin 11, type 2, OB-cadherin	1.75E-05	2	-1.23	-2.31	-1.89
cadherin 13, H-cadherin	6.02E-06	3	-1.69	-1.98	1.65
cadherin 2, type 1, N-cadherin	7.64E-05	8	1.19	1.31	1.11
catenin (cadherin-associated protein), alpha-like 1	4.99E-06	8	1.53	1.94	1.27
desmocollin 2	0.000189	10	1.34	1.12	-1.20
integrin, alpha 1	1.73E-05	6	-1.03	1.43	1.47
integrin, alpha 1	0.000287	7	1.03	1.63	1.58
integrin, alpha 4 (antigen CD49D)	0.000957	7	1.02	1.74	1.71
integrin, alpha 4 (antigen CD49D)	0.000977	7	1.10	1.77	1.61
integrin, alpha 5 (fibronectin receptor)	7.72E-05	5	-1.42	-1.21	1.17
integrin, alpha 6	9.36E-05	3	-1.93	-2.21	-1.15
integrin, beta 5	5.63E-05	4	-1.35	-1.38	-1.03
integrin, beta 6	1.64E-05	6	-1.31	1.38	1.80
Cyclins					
cyclin B1	3.85E-05	1	1.25	-1.07	-1.34
cyclin B1	0.000667	1	1.17	-1.11	-1.31
cyclin D1 (PRAD1)	4.36E-08	3	-1.36	-1.30	1.04
cyclin D1 (PRAD1)	7.46E-07	4	-3.46	-3.39	1.02
cyclin D3	1.47E-05	4	-2.59	-2.27	1.14
cyclin F	1.73E-05	3	-1.87	-1.67	1.12
cyclin I	3.16E-07	8	1.37	1.69	1.24
Cytoskeleton/motility proteins					
actin, alpha 1, skeletal muscle	0.000604	7	1.13	1.66	1.48
actin, alpha 2, smooth muscle, aorta	1.70E-09	8	1.62	2.47	1.52
actinin, alpha 4	1.54E-07	5	1.44	1.99	1.38
mutant beta-actin	1.74E-07	7	1.07	1.91	1.79
actin, gamma 1	2.26E-09	7	1.21	2.13	1.75
actinin, alpha 1	4.34E-09	7	1.44	1.99	1.38
Exocytosis					
annexin A1	2.15E-06	8	1.49	1.91	1.28
annexin A2	3.35E-09	8	1.73	2.89	1.67
annexin II	1.09E-06	3	-1.08	-1.19	1.10
Extracellular matrix proteins					
collagen alpha-2 type I	2.94E-08	7	3.00	3.93	1.18
collagen alpha-2 type I	3.95E-07	7	1.99	2.77	1.12
collagen, type I, alpha 1	8.82E-08	6	-1.79	1.59	-1.75
collagen, type I, alpha 2	2.28E-07	7	1.20	1.38	1.15
collagen, type III, alpha 1	1.34E-05	7	1.59	1.82	1.14
collagen, type IV, alpha 1	1.63E-07	8	2.51	1.33	-1.89
collagen, type IV, alpha 4	0.000699	6	-1.00	2.93	2.18
collagen, type VI, alpha 1	1.20E-09	6	-1.34	2.64	2.26
collagen, type VI, alpha 2	4.37E-10	8	1.63	2.53	1.55
collagen, type VI, alpha 2	2.19E-09	9	1.99	2.77	1.12
collagen, type VI, alpha 3	0.000591	8	1.20	1.62	1.93
collagen, type VII, alpha 1	1.29E-06	9	1.24	1.85	1.29
collagen, type X, alpha 1	0.000433	7	1.38	1.58	1.15
collagen, type XV, alpha 1	8.18E-05	7	2.53	1.88	-1.34
collagen, type XVI, alpha 1	1.88E-07	8	1.45	2.05	1.64
collagen, type XVI, alpha 1	4.96E-07	5	-1.04	1.01	2.01
fibronectin 1	6.99E-08	7	1.61	2.88	1.78

Table 6-2. Selected genes of interest – continued

fibronectin 1	4.49E-05	7	1.48	2.73	1.85
fibronectin, alt. splice 1	1.27E-08	7	1.29	2.34	1.82
heparan sulfate proteoglycan 2 (perlecan)	1.22E-07	10	2.52	1.86	-1.36
laminin B2 chain gene, exon 28	0.00017	7	1.11	1.29	1.17
laminin, alpha 4	1.20E-06	9	1.56	1.46	-1.07
laminin, beta 2 (laminin S)	0.00068	3	-1.36	-1.55	-1.14
thrombospondin 1	3.48E-06	3	-1.94	-2.20	-1.14
thrombospondin 3	5.62E-05	3	-1.53	-1.98	-1.30
thrombospondin-1	9.60E-09	3	-3.14	-5.34	-1.70
Extracellular transport/carrier proteins					
insulin-like growth factor binding protein 2	2.10E-06	5	-2.24	-1.65	1.35
insulin-like growth factor binding protein 3	5.45E-10	7	1.32	2.07	1.57
insulin-like growth factor binding protein 3	1.23E-07	7	1.54	2.44	1.59
insulin-like growth factor binding protein 6	4.61E-08	4	-1.90	-1.95	-1.03
insulin-like growth factor binding protein 7	1.11E-06	7	1.21	2.03	1.68
insulin-like growth factor-binding protein 4	2.56E-09	7	-2.24	-1.65	1.35
insulin-like growth factor-binding protein 4	2.57E-09	5	-2.14	-1.15	1.86
G-proteins					
G protein-coupled receptor	1.67E-05	8	-1.34	-1.23	1.09
G protein-coupled receptor 1	0.000507	2	-1.29	-1.87	-1.45
G protein-coupled receptor 35	0.000605	5	-1.68	-1.34	1.25
G protein-coupled receptor, family C, group 5	0.000834	10	1.33	1.00	-1.33
Growth factor and chemokine receptors					
activin A receptor, type I	0.00032	1	1.40	-1.31	-1.83
fibroblast growth factor receptor 1	5.40E-08	10	1.49	-1.78	2.19
fibroblast growth factor receptor 1	5.60E-06	10	1.98	-1.40	-1.41
hepatocyte growth factor receptor	0.000108	3	-1.48	-1.80	-1.22
platelet-derived growth factor alpha receptor	0.000217	7	1.67	-2.86	-1.71
platelet-derived growth factor receptor, beta	5.62E-10	9	3.18	3.49	-1.10
Growth factors and chemokines					
basic fibroblast growth factor	1.53E-05	8	1.65	1.74	1.06
brain-derived neurotrophic factor	1.74E-05	7	1.23	1.68	1.37
brain-derived neurotrophic factor	0.00012	7	1.08	1.59	1.47
macrophage colony stimulating factor 1	0.000503	5	-1.33	-1.02	1.30
keratinocyte growth factor	0.000687	3	-1.10	-1.71	-1.71
insulin-like growth factor 2	3.73E-08	4	-1.93	-1.95	-1.01
insulin-like growth factor 2	3.02E-05	5	-2.10	-1.58	1.33
serine proteinase inhibitor, clade F	3.64E-05	2	-1.07	-1.54	-1.44
vascular endothelial growth factor A	4.60E-08	8	1.67	1.75	1.05
vascular endothelial growth factor A	6.77E-06	8	1.40	1.58	1.13
vascular endothelial growth factor B	0.000445	3	-4.03	-2.76	1.46
vascular endothelial growth factor B	4.17E-06	4	-2.72	-2.17	1.26
Inhibitors of proteases					
cystatin B (stefin B)	2.46E-06	7	1.17	1.30	1.12
secretory leukocyte protease inhibitor	6.88E-06	7	1.27	1.42	1.11
tissue inhibitor of metalloproteinase 1	9.75E-07	4	-1.03	1.55	1.60
tissue inhibitor of metalloproteinase 2	1.63E-05	5	-4.84	-2.16	2.24
tissue inhibitor of metalloproteinase-2	6.14E-05	5	-4.84	-2.16	2.24
Interleukins and interferons					
interleukin 10 receptor, beta	0.000296	2	1.14	2.52	2.21
interleukin 11 receptor, alpha	7.78E-06	3	-1.09	-1.83	-1.68
interleukin 13 receptor, alpha 1	1.70E-05	5	-1.38	-1.94	-1.41
interleukin 2 receptor, beta	1.42E-05	4	1.11	1.05	-1.05
interleukin 1, beta	1.89E-05	7	1.65	1.65	1.00
interleukin 6 (interferon, beta 2)	2.25E-11	8	2.09	3.19	1.53
oncostatin M receptor	3.25E-11	4	-2.66	-2.25	1.19
oncostatin M receptor	3.65E-05	5	-1.90	-1.56	1.22
Intermediate filament proteins					
keratin 10	1.68E-05	8	1.25	1.27	1.02
keratin 15	1.32E-05	7	1.23	2.26	1.84
keratin 18	8.50E-05	7	1.03	2.03	1.97
keratin 19	0.000363	6	-1.16	1.52	1.76
keratin 5	0.000166	8	1.27	1.42	1.12
vimentin	9.89E-08	7	1.56	2.92	1.88
Matrix adhesion receptors					
integrin beta 1 subunit	3.30E-08	7	1.51	2.53	1.68

Table 6-2. Selected genes of interest – continued

integrin, alpha 2 (CD49B, alpha 2 subunit)	0.000724	6	-3.02	2.77	1.89
integrin, beta 4	0.00038	5	-2.29	-1.54	1.48
laminin receptor 1	3.20E-05	7	1.10	1.49	1.35
thrombospondin 2	2.30E-07	7	1.92	2.40	1.25
thrombospondin 2	8.21E-05	8	1.29	1.66	1.28
Metalloproteinases					
bone morphogenetic protein 1	3.72E-06	3	-2.39	-2.67	-1.12
bone morphogenetic protein 1	0.000626	5	-2.01	-1.29	1.63
matrilysin	0.000119	6	-1.12	1.48	1.65
matrix metalloproteinase 1	1.46E-06	8	1.47	2.08	1.41
matrix metalloproteinase 9 (gelatinase B)	6.44E-05	8	1.78	2.06	1.68
Oncogenes and tumor suppressors					
B cell/lymphoma 2 (BCL2)	0.000417	5	-2.31	-1.20	1.27
epidermal growth factor receptor	8.52E-10	5	-4.07	-2.90	1.40
serine proteinase inhibitor, clade B	0.000273	6	-1.15	1.39	1.60
serine proteinase inhibitor, clade B	0.000419	7	1.07	1.13	1.06
tissue inhibitor of metalloproteinase 3	4.88E-12	4	-2.72	-2.47	1.10
tissue inhibitor of metalloproteinase 3	2.64E-08	4	-1.66	-1.68	-1.01
Proteases					
cathepsin D	2.54E-08	3	-3.07	-4.40	-1.43
bleomycin hydrolase	0.000492	3	-1.95	-2.26	-1.16
calpain 1, (mu/I) large subunit	4.27E-06	4	-2.03	-1.96	1.04
cathepsin K (pycnodysostosis)	1.53E-10	1	-1.58	-3.20	-2.02
cathepsin K (pycnodysostosis)	1.11E-06	2	-1.27	-2.43	-1.92
cathepsin K (pycnodysostosis)	4.79E-06	2	1.46	-1.27	-1.84
cathepsin O	0.000369	4	-1.47	-1.47	-1.01
chymotrypsin-like	2.42E-07	3	-4.87	-6.65	-1.37
plasminogen activator, tissue	0.000407	7	1.38	2.05	1.48
plasminogen activator, urokinase	0.000126	5	-1.31	-1.17	1.11
serine protease 11 (IGF binding)	8.18E-09	6	-1.03	1.24	1.27
serine protease 11 (IGF binding)	1.24E-05	8	1.60	2.08	1.30
serine protease 12 (neurotrypsin)	4.30E-08	8	1.59	1.50	-1.06
serine protease 15	0.000397	9	1.10	2.88	2.62

Discussion

Gene expression in human corneal fibroblasts were examined at two time points during culturing with CTGF. The patterns of expression of genes in four of the ten clusters (1, 5, 6, and 10) showed striking changes in the levels at 0.5 hours compared to the levels at 0 and 24 hours. We interpret the changes observed at the 0.5 hour time point to represent the most immediate, direct effect of CTGF on the regulation of expression of each gene. The level of expression for each gene at 24 hours probably represents the integration of both the direct effects of CTGF combined with possible indirect effects of genes regulated by CTGF. Thus, measuring expression levels at only 24 hours would indicate the opposite trend measured at 0.5 hours for genes in clusters 1 and 6, and would have missed important information about the temporal response of genes to CTGF. This

would be important for some irreversible physiological processes such as apoptosis that are triggered by transient changes in gene expression.

In these experiments, the predominate interest is in the roles that CTGF plays in corneal wound healing. There are several important events in this process that may utilize CTGF as a regulatory mediator. Apoptosis of fibroblasts occurs very rapidly after an injury to the corneal epithelium. Also, formation and remodeling of scar tissue occurs involving extracellular matrix turnover, changes in growth factor levels, corneal scar contraction, loss of corneal clarity, and scar turnover. A third important event that CTGF may regulate is corneal angiogenesis, which is a critical component of the wound healing process.

A previous report showed that apoptosis occurs in quiescent keratocytes within the first 24 hours following corneal injury. This process may be a physiological response to reduce the development or establishment of viral infections after an injury to corneal epithelial cells (Wilson et al. 1997). This phenomenon is partially attributed to the Fas/Fas ligand system proven by the fact that Fas knockout mice show decreased incidence of keratocyte apoptosis in response to epithelial scrape injury (Wilson et al. 1997). CTGF may prove to be another rapid inducer of apoptosis because caspases 4, 7, and 8 are turned on and off rapidly whereas BCL2 is turned off and on rapidly. Later actions of CTGF may be to promote migration, cell proliferation, and extracellular matrix production. In previous reports, CTGF increased collagen synthesis in human corneal fibroblasts and cell proliferation in normal rat kidney cells (Duncan et al. 1999; Blalock et al. 2003). It is interesting to note that apoptosis was not observed in these experiments. This could be due to the fact that CTGF was present continuously over 24 hours, where

the initial pulse of CTGF may be responsible for the upregulation of caspases and downregulation of BCL2 seen at 0.5 hours. Continuous CTGF exposure has been reported to stimulate mitosis in other systems such as in smooth muscle cells and cultured hepatocytes, which may account for the lack of apoptosis in this experiment (Fan et al. 2000; Paradis et al. 2002).

CTGF has also been implicated in regulating production of the extracellular matrix. The general trend in this study was that CTGF upregulated ECM components, up-regulated proteases that degrade the ECM at 24 hours (MMP1, 9, 3), and regulated the inhibitors of MMPs (TIMPs). This suggests that CTGF plays an important role in regulating the turnover of the extracellular matrix during corneal wound healing. CTGF also regulated the expression of a number of growth factors associated with wound healing. CTGF downregulates macrophage colony stimulating factor and insulin-like growth factor 2 (IGF-2), two factors that are extremely important in regulating the metastatic state of cells (Pederson et al. 1999). Also, CTGF was not found to be autoregulatory as has been shown with TGF-β (Kelley et al. 1993). At the same time, CTGF upregulated basic fibroblast growth factor (bFGF) and vascular endothelial growth factor (VEGF), which are heavily involved in the regulation of angiogenesis. Previous reports have shown that CTGF appears to have a direct effect on angiogenic actions in the chick chorioallantoic membrane assay (Eguchi et al. 2001). Here, we report the downregulation of thrombospondin-1, which is an inhibitor of angiogenesis (Lawler 2002). Taken together, these results suggest a role for CTGF in the regulation of angiogenesis.

There are no other published reports of microarray analysis of gene expression in cells exposed to CTGF, especially corneal fibroblasts. However, there is a report of changes in gene expression of human corneal fibroblast cultures exposed to interleukin-1 alpha (IL-1α) (Mahajan et al. 2002). This report showed changes in expression of approximately 165 genes after culturing cells for 24 hours in IL-1α, using a low stringency probability cut off of $p = 0.05$. These experiments showed that CTGF expression was decreased 3.2-fold in response to IL-1α, but CTGF did not significantly alter expression of IL-1α in this study. However, with 12,000 genes and ESTs on the chip microarray, it is possible that as many as 600 genes could randomly be misidentified as having changes in expression. Another report showed microarray analysis of stimulation of human corneal epithelial cells by TGF-β (Hayashida-Hibino et al. 2001). TGF-β downregulated caspases in these experiments while upregulating genes such as α3 integrin and cyclin D1. In a closely related experiment, microarray analysis of rat corneas following photorefractive keratectomy was performed to better understand the cellular response to injury and the dynamic changes that occur in gene expression patterns as the wound heals.(Varela et al. 2002) The proposed role of CTGF in corneal fibroblasts is presented in Figure 6-4. These experiments suggest that CTGF is one such gene that is heavily involved in regulating the response to injury in the cornea.

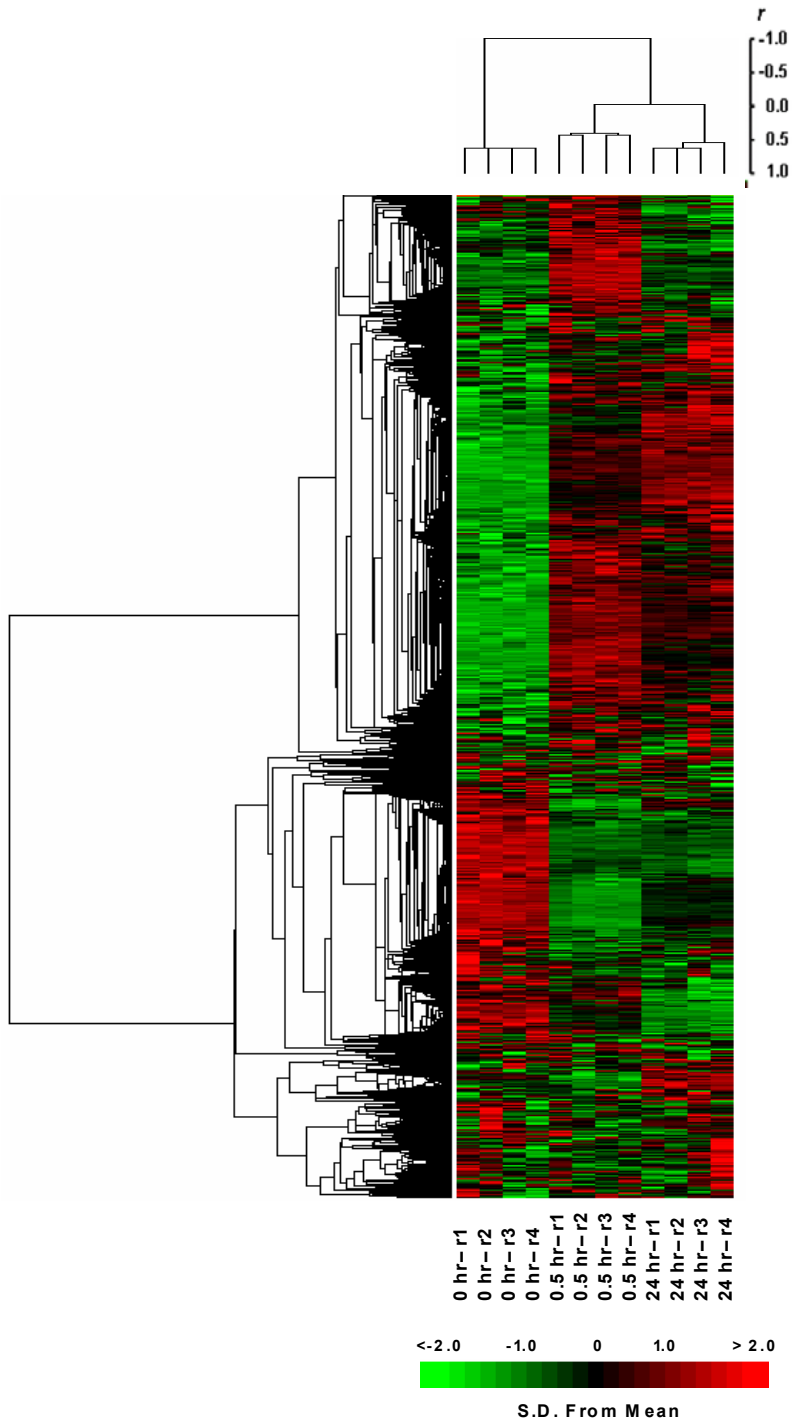

Figure 6-1. Hierarchical clustering patterns. The top half of hybridization intensities (3,894 probe sets) of genes responding to CTGF stimulation was clustered (using Cluster software) and organized with TreeView (shown here). The dendrogram at the top of the figure shows similarities between chips. The color scale at the bottom represents standard deviation from the mean. Genes which are green are down-regulated and genes which are red are up-regulated in human corneal fibroblasts upon exposure to CTGF. r= replicate number; *r* = Pearson's correlation coefficient.

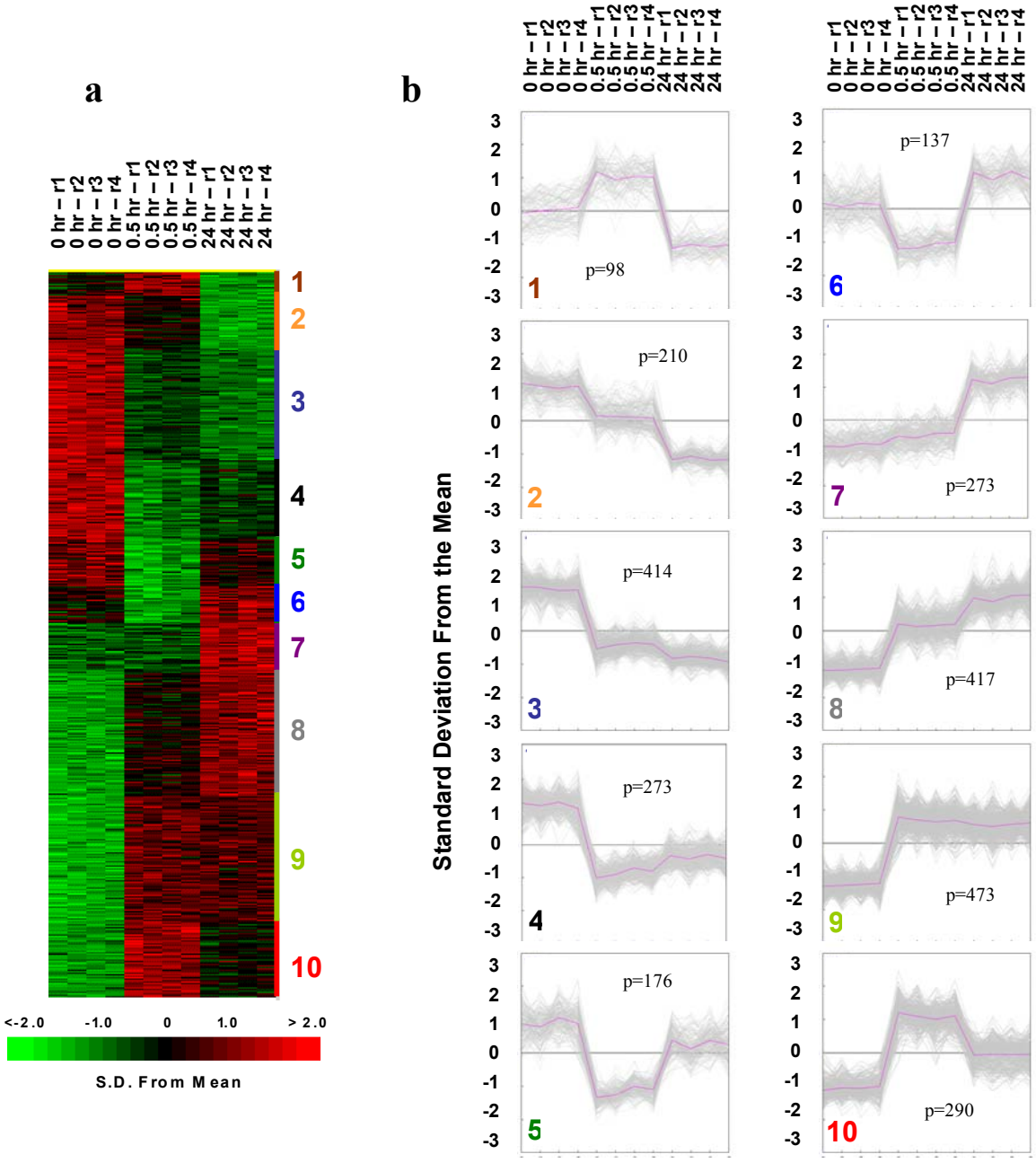

Figure 6-2. K-means clustering analysis. K-means clustering analysis was performed on 2,761 genes (F test $P < 0.001$) to ten binds using Cluster software and organized with TreeView (a). The ten bins (b) illustrate the classes of genes that are differentially expressed in human corneal fibroblasts upon stimulation by CTGF. The 'spaghetti' graphs shown on the right illustrate the expression profiles of the individual genes contained within each of the same ten clusters present in the TreeView image on the left. p = number of probe sets in each bin.

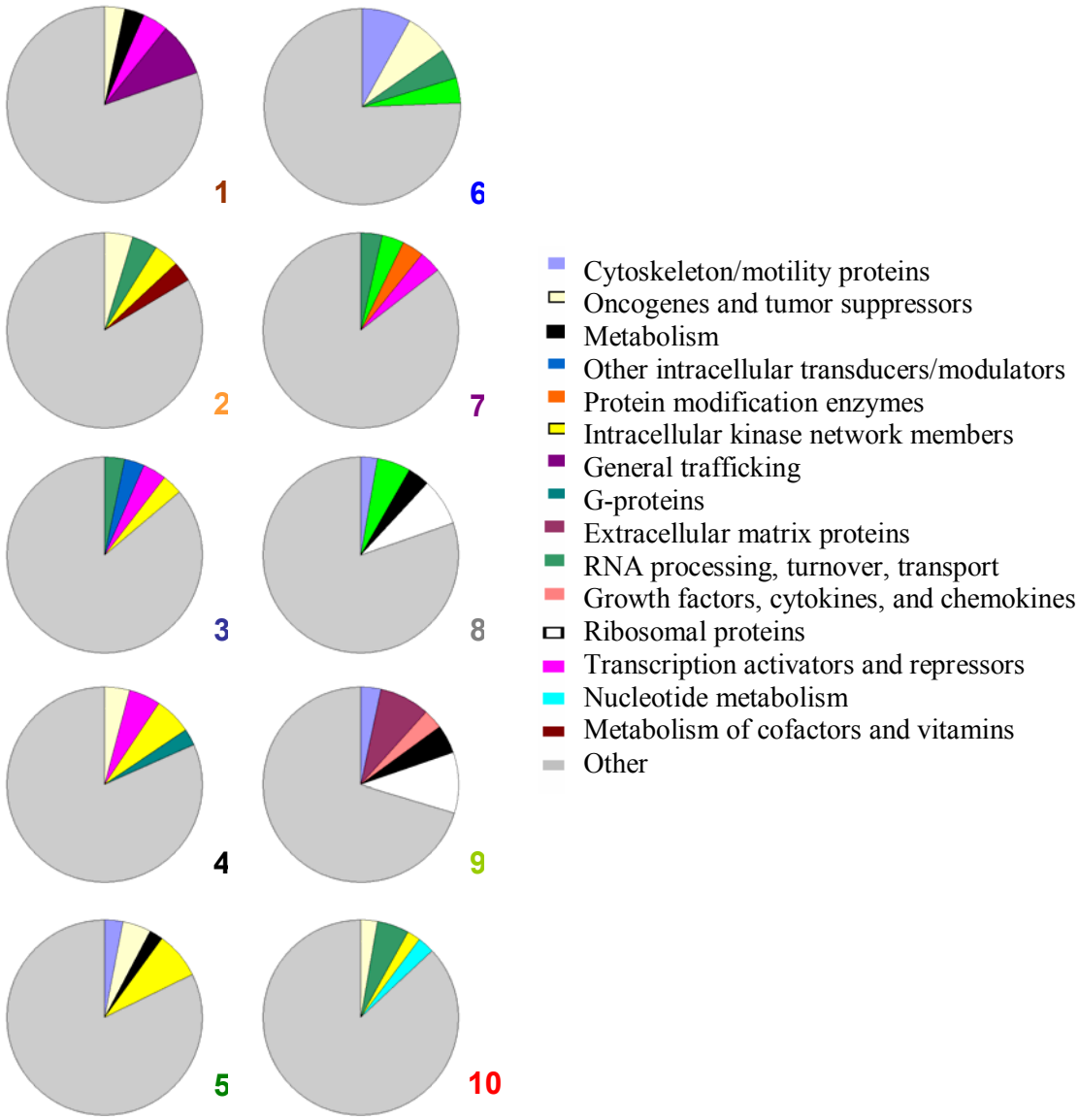

Figure 6-3. Functional groups of genes regulated by CTGF. K-means clustering analysis was performed on 2,761 genes (F test $P < 0.001$). Ten clusters were chosen to illustrate the classes of genes that are differentially expressed in human corneal fibroblasts upon stimulation by CTGF. The functional groups of genes which comprised the greatest percentage of each cluster are shown in the pie charts. Expressed sequence tags, unknown proteins, and genes comprising less than 5% of the total number of genes are grouped together in the 'other' category.

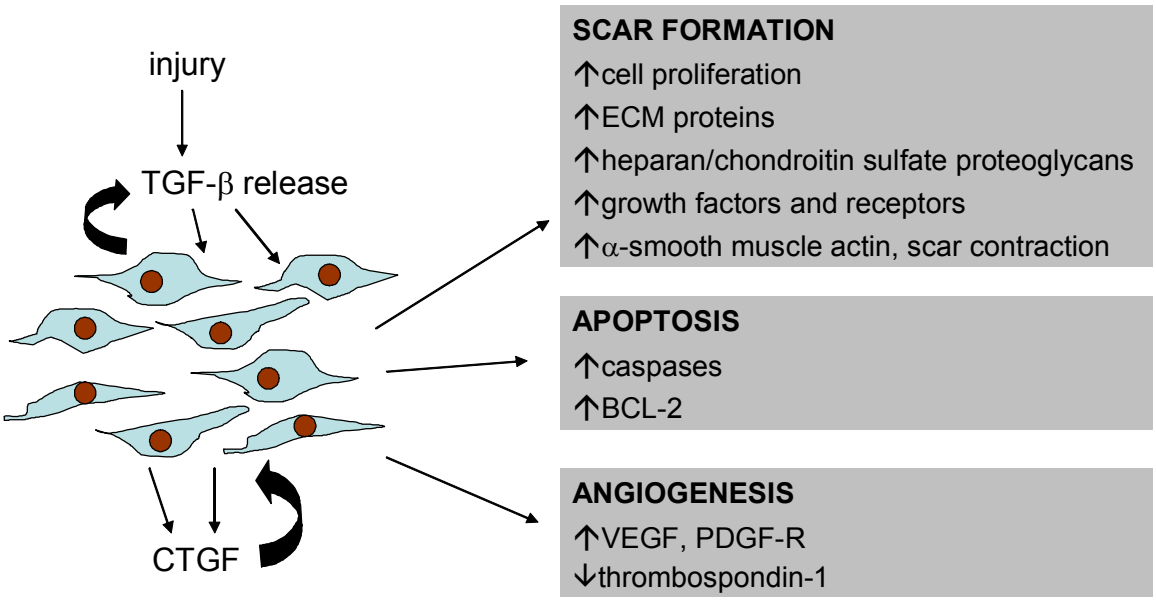

Figure 6-4. The proposed role of the effect of CTGF on corneal fibroblasts.

CHAPTER 7
CONCLUSIONS

One of the major complications of corneal trauma, infection and refractive surgery is the phenomenon of corneal scarring. A vast amount of research on the field of stromal wound healing and corneal haze formation exists yet there are still many events that are not well understood. The major objective of this research is to understand the regulatory events of stromal wound healing at the molecular level and to apply this knowledge towards the design of treatments that will selectively inhibit certain molecular pathways that may promote scarring. It is currently known that the transforming growth factor beta (TGF-β) family plays a dominant role in the regulation of stromal scarring. More specifically, it is known to play a crucial role in the formation of corneal haze in rats following a refractive surgery model (Chen et al., 2000a). The results of these experiments specifically provided support for the hypothesis of the involvement of CTGF in the process because of its established regulation by TGF-β.

The hypothesis for these experiments is that CTGF is a major factor that induces scar formation by mediating many of the effects of TGF-β on extracellular matrix production and the development of corneal haze after injury. Prior to this research, very little was known about the involvement of CTGF in the cornea. Only two reports showed the detection of CTGF mRNA in retrocorneal membranes and the upregulation of CTGF by TGF-β in cultured rabbit corneal fibroblasts (Wunderlich et al., 2000a;Folger et al., 2001d). These preliminary findings support the hypothesis of the involvement of CTGF

in corneal wound healing. The examination of human clinical specimens can provide some important information about the levels of CTGF at one particular stage of a disease process, but what would be of more value is a chronological analysis of CTGF in a controlled reproducible corneal wound model. Based on the information that is known about TGF-β, it is likely that it will also upregulate expression of CTGF mRNA and protein in corneal fibroblasts as well as the CTGF receptor. The increased amounts of CTGF message would then likely regulate many genes that are involved in the formation of scar tissue. It is also likely that CTGF expression increases in healing corneal wounds. In addition, stimulation of corneal fibroblasts by CTGF is likely to stimulate classes of genes at many time points, especially groups that are known to be involved in wound healing and regulation of the extracellular matrix. Therefore, agents that reduce CTGF and/or the CTGF receptor would be good candidates for reducing corneal scarring whether using ribozymes or antisense oligonucleotides.

One of the goals of these experiments was to prove the hypothesis that CTGF is a major inducer of corneal scarring and that it is a mediator of the effects of TGF-β on cellular responses in fibrosis. Perhaps the strongest evidence is given in Figure 3-2, showing that blocking CTGF with antisense oligonucleotides or a neutralizing antibody blocks the induction of collagen synthesis by TGF-β. Increased expression of CTGF protein and mRNA were also found (Figure 3-4) which correlates with several experiments showing the same result in other fibrotic animal models. This is the first example of an analysis of CTGF expression in human corneal tissue as well as patterns of expression in a healing corneal wound. This experiment was important to answer the question of the time course of CTGF expression in the cornea. It was not known if

corneal injury caused an early 'spike' of CTGF expression or whether there is a more prolonged and gradual elevation. Also, this information is necessary with regards to the development of anti-scarring treatments so that the optimal time of delivery can be determined.

It was also important to identify which cells in the cornea synthesize CTGF during corneal wound healing, as well as which isoforms of TGF-β induce this response. This is important so that the target cells can be identified for treatment with antisense oligonucleotides and ribozymes to achieve the maximal effect in the reduction of corneal scarring. Figure 3-1 showed that all three isoforms of TGF-β induce CTGF mRNA and protein expression. Current data would suggest that CTGF is synthesized by corneal fibroblasts and acts through a paracrine mechanism to stimulate the surrounding fibroblasts. However, Figure 3-5 shows that CTGF immunostaining in rat corneas localizes to the corneal epithelium (which was confirmed by RT-PCR and ELISA) as well as to the fibroblasts in the corneal stroma. This may suggest a constant constitutive expression of CTGF in the epithelium, while expression in the corneal fibroblasts may increase in response to corneal injury.

As with all growth factor systems, it is very important to characterize both the growth factor and its specific receptor because the response of cells is determined by the interaction between the ligand and its receptor. Furthermore, reducing the expression of the CTGF receptor in corneal fibroblasts may reduce the response of corneal cells to CTGF more effectively than attempting to reduce synthesis of CTGF, especially if it has multiple sources. For example, it is now known that CTGF is synthesized and secreted into tears by lacrimal gland cells (van Setten et al., 2002c). Also, if activated

macrophages synthesize CTGF, the cells that enter the cornea several days after the initial injury might not be effected by topical eye drops of antisense oligonucleotides or ribozymes given when the injury is first created. Therefore, the optimal strategy to reduce CTGF signaling in corneal fibroblasts or epithelial cells may be to reduce synthesis or availability of the putative CTGF receptor.

These experiments also showed specific binding of ^{125}I-CTGF to cultured human corneal fibroblasts consisting of two classes of binding, a lower-abundance, high affinity binding component with a K_d of 5 nM and a higher-abundance lower affinity class of sites with a K_d of 166 nM. Chemical cross-linking of ^{125}I-CTGF to a single high molecular weight protein of 250 kDa was also achieved whose binding is competed for by unlabeled CTGF. CTGF affinity column chromatography was also used to purify a protein fraction from Triton X-100 solubilized human corneal fibroblasts. When the fraction that purified with the CTGF-affinity column was incubated with a goat antibody to the type II-IGF receptor, 80% of the ^{125}I-CTGF binding was immunoprecipitated. This indicates that the vast majority of the ^{125}I-CTGF specific binding in human corneal fibroblasts is due to the type II IGF receptor protein. Also, fibroblasts lacking the type II IGR receptor do not show CTGF binding and do not respond to induction of cell proliferation by TGF-β. This is similar to other unpublished findings showing that incubation of NRK fibroblasts with an antibody to the type II IGF receptor blocked approximately 60% of the TGF-β-induced increase in collagen synthesis. Additionally, the levels of ^{125}I-CTGF binding at various time points in rat corneas following PRK were measured to calculate the number of available receptors following corneal injury. Figure 4-6 shows a coordinated increase in both CTGF binding and CTGF protein and mRNA

(Figure 3-4) in corneas in the early period after corneal injury. In summary, these biochemical and cell culture data strongly indicate that the type II IGF receptor is the CTGF signaling receptor. The type II IGF receptor is a well-characterized integral membrane protein that is also known as the cation independent mannose 6-phosphate receptor. Two distinct, non-interacting binding sites have been identified, one for IGF-II and one for mannose 6-phosphate. In addition to binding IGF-II and proteins that contain mannose 6-phosphate groups in N-linked glycosylation side chains, the type II IGF receptor is also involved in activation of latent TGF-β. The activation occurs through binding the mannose 6-phosphate groups on the latency-associated peptide of latent TGF-β and binding of cell membrane associated transglutaminase. These experiments have confirmed the hypothesis that the type II IGF receptor is the CTGF signaling receptor. Therefore, it is most likely that antisense oligonucleotides and ribozymes that target the type II IGF receptor will block the mitogenic effects of CTGF on fibroblasts in the cornea.

Since the long-term goal of this project is to develop agents that will reduce corneal scarring with minimal side effects, initial experiments using ribozymes to target CTGF mRNA were performed. Development of ribozyme therapy is important because there are no agents to block corneal scarring other than steroids, which have not shown to be of much benefit after PRK. Some non-specific anti-cancer drugs have been used to treat corneal scarring such as 5-fluorouracil and mitomycin C but they cause serious side effects in some instances such as epithelial defects and endothelial cell damage. Because of these problems ribozyme-mediated gene therapy may be a good candidate for treatment. In these studies, a gene-specific hammerhead ribozyme targeting CTGF was

developed and was shown to reduce the expression of CTGF in cell culture as well as reduce the biological effects of CTGF. Further animal studies will be performed in the future to confirm that the ribozyme has a similar effect *in vivo* in a wound healing model. It is likely that the use of ribozymes in conjunction with treatment with antisense oligonucleotides or neutralizing antibodies will reduce the fibrosis in the cornea after injury that leads to haze. These treatments have many advantages over current treatment options because they will selectively inhibit scarring without resulting in serious side effects. These modes of treatment can also be modified to act not only on corneal fibrosis, but also on fibrotic conditions throughout the body.

Figure 3-2 established the hypothesis that CTGF is a potent inducer of type I collagen synthesis in cultures of human corneal fibroblasts. Also, it was shown that CTGF mediates TGF-β induction of collagen and that all three isoforms of TGF-β induce CTGF mRNA and protein as seen in normal rat kidney fibroblasts (Duncan et al., 1999a). These findings alone justify defining the role of CTGF in corneal wound healing. However, to understand how CTGF affects the process of corneal wound healing, it is necessary to examine the genes that are regulated by CTGF as broadly as possible. Presently, only a few genes are known that are regulated by CTGF as mentioned in Chapter 6. The most efficient and accurate approach to broadly define the action of CTGF on gene expression in the cornea is to utilize microarray technology with cultured human corneal fibroblasts. This allows for the simultaneous measurement of thousands of known genes and expressed sequence tags in one sample. Analysis of microarray data by variance normalization, hierarchical and K-means clustering reveals important relationships between groups of genes that will permit the testing of previous concepts

and the generation of new hypotheses in corneal wound healing. Data obtained from these microarray experiments show that CTGF regulates many components of the extracellular matrix in corneal fibroblasts, such as collagen, integrin, fibronectin, and laminin. This suggests that CTGF is a potent inducer of scar formation in the cornea. Also, CTGF seems to regulate events in apoptosis and angiogenesis as discussed in Chapter 6. These experiments demonstrate that CTGF has an impact on the expression of groups of genes in the cornea and that expression of genes involved in corneal scar formation could be lowered by blocking CTGF, leading to a reduction in corneal scarring.

In summary, the experiments represented here support the proposed hypothesis that CTGF is a key player in regulating corneal scarring. The data show that levels of CTGF mRNA and protein increase in rat corneas during healing of excimer ablation wounds, that all three TGF-β isoforms induce CTGF mRNA and protein in cultured human fibroblasts, that CTGF induces collagen synthesis, and most importantly that inhibiting CTGF blocks the TGF-β-induced collagen synthesis in cultured human fibroblasts. The CTGF binding protein in cultured human fibroblasts was also identified using a combination of biochemical techniques that include chemical cross-linking of ^{125}I-CTGF to cultured fibroblasts, CTGF affinity column chromatography and immunoprecipitation. Results of these binding studies as well as experiments performed on knockout cell lines have led to the identification of the type II IGF receptor, also known as the cation-independent mannose 6-phosphate receptor, as a candidate CTGF receptor. Although CTGF is a mitogen for fibroblasts and a strong inducer of collagen synthesis, very little is known about the regulation of other genes by CTGF. The most

effective method to understand the broad actions of CTGF on corneal gene expression and wound healing is to use microarray gene chip technology to initially identify genes that are changing. The microarray analysis of CTGF-regulated gene expression in cultured human corneal fibroblasts has identified a number of genes that are up-regulated by CTGF including multiple collagens, actin, and fibronectin. More importantly, the microarray data indicates that CTGF also down-regulates many gene classes, showing that it does not have purely stimulatory effects on corneal cells. The microarray data was used to test previous hypotheses about corneal wound healing and to generate new hypotheses about how CTGF influences scar formation. The results suggest that CTGF regulates key genes involved in corneal wound healing events such as scar formation, angiogenesis, and apoptosis.

These experiments have made tremendous progress in developing and evaluating the role of CTGF and its receptor in the process of corneal scarring. Based on the reported effects of CTGF in other fibrotic conditions and in these experiments, evidence suggests that CTGF is a major regulator of corneal scar formation and mediates many of the fibrotic effects of TGF-β in corneal scarring.

LIST OF REFERENCES

1. Abounader R, Ranganathan S, Lal B, Fielding K, Book A, Dietz H, Burger P, and Laterra J. 1999. Reversion of human glioblastoma malignancy by U1 small nuclear RNA/ribozyme targeting of scatter factor/hepatocyte growth factor and c-met expression. *J. Natl. Cancer Inst.* 91:1548-1556.

2. Albrecht C, von Der Kammer H, Mayhaus M, Klaudiny J, Schweizer M, and Nitsch RM. 2000. Muscarinic acetylcholine receptors induce the expression of the immediate early growth regulatory gene CYR61. *J. Biol. Chem.* 275:28929-28936.

3. Andersen A, Kjeldsen T, Wiberg F, Christensen P, Rasmussen J, Norris K, and Moller K. 1990. Changing the insulin receptor to possess insulin-like growth factor I ligand specificity. *Biochemistry.* 29, 7363-7366.

4. Andreo RH, and Farrell RA. 1982. Corneal small-angle light-scattering theory: wavy fibril models. *J. Opt. Soc. Am.* 72:1479-1492.

5. Applegate RA and Howland HC. 1997. Refractive surgery, optical aberrations, and visual performance. *J. Refract. Surg.* 13:295-299.

6. Astifoli A, Giovanni C, Lanuzza L, Nicoletti G, Ricci C, Croci S, and Scopece L. 2001. Identification of new genes related to the myogenic differentiation arrest of human rhabdosarcoma cells. *Gene.* 274(1):139-49.

7. Barishak YR. 1992. Embryology of the eye and its adnexae. *Dev. Ophthalmol.* 24:1-142.

8. Bauer G, Valdez P, Kearns K, Bahner I, Wen SF, Zaia JA, and Kohn DB. 1997. Inhibition of human immunodeficiency virus-1 (HIV-1) replication after transduction of granulocyte colony-stimulating factor-mobilized CD34+ cells from HIV-1-infected donors using retroviral vectors containing anti-HIV-1 genes. *Blood.* 89:2259-2267.

9. Beck LS, Chen TL, Hirabayashi SE, Deguzman L, Lee WP, McFatridge LL, Xu Y, Bates RL, and Ammann AJ. 1990. Accelerated healing of ulcer wounds in the rabbit ear by recombinant human transforming growth factor-beta 1. *Growth Factors.* 2:273-282.

10. Bennett NT and Schultz GS. 1993. Growth factors and wound healing: biochemical properties of growth factors and their receptors. *Am. J. Surg.* 165:728-737.

11. Bilgihan K, Ozdek S, Ozogul C, Gurelik G, Bilgihan A, and Hasanreisoglu B. 2000. Topical vitamin E and hydrocortisone acetate treatment after photorefractive keratectomy. *Eye.* 14 (Pt 2):231-237.

12. Birk DE and Lande MA. 1981. Corneal and scleral collagen fiber formation in vitro. *Biochim. Biophys. Acta.* 670:362-369.

13. Blalock TD, Duncan MR, Varela JC, Goldstein MH, Grotendorst GR, and Schultz GS. 2003. Connective Tissue Growth Factor Expression and Action in Human Corneal Fibroblast Cultures and in Rat Corneas following Phototherapeutic Keratectomy. *Invest. Ophtahlmol. Vis. Sci.* 44(5):1879-1887.

14. Border WA and Noble NA. 1994. Transforming growth factor beta in tissue fibrosis. *N. Engl. J. Med.* 331:1286-1292.

15. Border WA, Noble NA, Yamamoto T, Harper JR, Yamaguchi Y, Pierschbacher MD, and Ruoslahti E. 1992. Natural inhibitor of transforming growth factor-beta protects against scarring in experimental kidney disease. *Nature.* 360:361-364.

16. Border WA, Okuda S, Languino LR, Sporn MB, and Ruoslahti E. 1990. Suppression of experimental glomerulonephritis by antiserum against transforming growth factor beta 1. *Nature.* 346:371-374.

17. Bork P. 1993. The modular architecture of a new family of growth regulators related to connective tissue growth factor. *FEBS Lett.* 327:125-130.

18. Bradham DM, Igarashi A, Potter RL, and Grotendorst GR. 1991. Connective tissue growth factor: a cysteine-rich mitogen secreted by human vascular endothelial cells is related to the SRC-induced immediate early gene product CEF-10. *J. Cell Biol.* 114:1285-1294.

19. Brahmatewari J, Serafini A, Serralta V, Mertz PM, and Eaglstein WH. 2000. The effects of topical transforming growth factor-beta2 and anti- transforming growth factor-beta2,3 on scarring in pigs. *J. Cutan. Med. Surg.* 4:126-131.

20. Brigstock DR. 1999. The connective tissue growth factor/cysteine-rich 61/nephroblastoma overexpressed (CCN) family. *Endocr. Rev.* 20:189-206.

21. Castilla A, Prieto J, and Fausto N. 1991. Transforming growth factors beta 1 and alpha in chronic liver disease. Effects of interferon alpha therapy. *N. Engl. J. Med.* 324:933-940.

22. Cech TR. 1988. Ribozymes and their medical implications. *JAMA*. 260:3030-3034.

23. Chaudhuri A, Hallett PE, and Parker JA. 1983. Aspheric curvatures, refractive indices and chromatic aberration for the rat eye. *Vision Res.* 23:1351-1363.

24. Chen CC, Chen N, and Lau LF. 2001. The angiogenic factors Cyr61 and connective tissue growth factor induce adhesive signalling in primary human skin fibroblasts. *J. Biol. Chem.* 276(13):10443-10452.

25. Chen C, Michelini-Norris B, Stevens S, Rowsey J, Ren X, Goldstein MH, and Schultz GS. 2000a. Measurement of mRNAs for TGFbeta and extracellular matrix proteins in corneas of rats after PRK. *Invest. Ophthalmol. Vis. Sci.* 41:4108-4116.

26. Chen MM, Lam A, Abraham JA, Schreiner GF, and Joly AH. 2000b. CTGF expression is induced by TGF- beta in cardiac fibroblasts and cardiac myocytes: a potential role in heart fibrosis. *J. Mol. Cell Cardiol.* 32:1805-1819.

27. Choi DM, Thompson RW Jr, and Price FW Jr. 2002. Incisional refractive surgery. *Curr. Opin. Ophthalmol.* 13:237-241.

28. Clark RAF and Henson PM. 1996. Wound repair: Overview and general considerations. *In* The molecular and cellular biology of wound repair. Plenum press, New York, NY. 3-50.

29. Cohen S. 1976. Cell mediated immunity and the inflammatory system. *Hum. Pathol.* 7:249-264.

30. Cordeiro MF, Gay JA, and Khaw PT. 1999a. Human anti-transforming growth factor-beta2 antibody: a new glaucoma anti-scarring agent. *Invest. Ophthalmol. Vis. Sci.* 40:2225-2234.

31. Cordeiro MF, Reichel MB, Gay JA, D'Esposita F, Alexander RA, and Khaw PT. 1999b. Transforming growth factor-beta1, -beta2, and -beta3 in vivo: effects on normal and mitomycin C-modulated conjunctival scarring. *Invest. Ophthalmol. Vis. Sci.* 40:1975-1982.

32. Coyle B, Freathy C, Gant TW, Roberts RA, and Cain K. 2003. Characterization of the transforming growth factor beta-1-induced apoptotic transcriptome in FaO hepatoma cells. *J. Biol. Chem.* 278(8):5920-8.

33. Cromack DT, Pierce GF, and Mustoe TA. 1991. TGF-beta and PDGF mediated tissue repair: identifying mechanisms of action using impaired and normal models of wound healing. *Prog. Clin. Biol. Res.* 365:359-373.

34. Dammeier J, Brauchle M, Falk W, Grotendorst GR, and Werner S. 1998. Connective tissue growth factor: a novel regulator of mucosal repair and fibrosis in inflammatory bowel disease? *Int. J. Biochem. Cell Biol.* 30:909-922.

35. Daoud AS, Fritz KE, Jarmolych J, and Frank AS. 1985. Role of macrophages in regression of atherosclerosis. *Ann. N. Y. Acad. Sci.* 454:101-114.

36. Dawson PA and Marini JC. 2000. Hammerhead ribozymes selectively suppress mutant type I collagen mRNA in osteogenesis imperfecta fibroblasts. *Nucleic Acids Res.* 28:4013-4020.

37. Daxer A, Misof K, Grabner B, Ettl A, and Fratzl P. 1998. Collagen fibrils in the human corneal stroma: structure and aging. *Invest. Ophthalmol. Vis. Sci.* 39:644-648.

38. Dean NM and Griffey RH. 1997. Identification and characterization of second-generation antisense oligonucleotides. *Antisense Nucleic Acid Drug Dev.* 7:229-233.

39. Doane MG, Jensen AD, and Dohlman CH. 1978. Penetration routes of topically applied eye medications. *Am. J. Ophthalmol.* 85:383-386.

40. Dou Q, Williams RS, and Chegini N. 1997. Inhibition of transforming growth factor-beta 1 alters the growth, anchor-dependent cell aggregation and integrin mRNA expression in human promonocytes: implications for endometriosis and peritoneal adhesion formation. *Mol. Hum. Reprod.* 3:383-391.

41. Drenser KA, Timmers AM, Hauswirth WW, and Lewin AS. 1998. Ribozyme-targeted destruction of RNA associated with autosomal-dominant retinitis pigmentosa. *Invest. Ophthalmol. Vis. Sci.* 39:681-689.

42. Duffey RJ. 1995. Post-operative complications of radial keratectomy. *In* Cornea. Krachmer JH, Mannis MJ, and Holland EJ, editors. Mosby, Chicago.

43. Duffey RJ and Leaming D. 2002. U.S. trends in refractive surgery: 2001 International Society of Refractive Surgery Survey. *J. Refract. Surg.* 18:185-188.

44. Duncan MR, Frazier KS, Abramson S, Williams S, Klapper H, Huang X, and Grotendorst GR. 1999. Connective tissue growth factor mediates transforming growth factor beta-induced collagen synthesis: down-regulation by cAMP. *FASEB J.* 13:1774-1786.

45. Eiferman RA. 1992. Corneal wound healing and its pharmacologica modification after radial keratotomy. *In* Refractive keratectomy for myopia and astigmatism. Waring GO, editor. Mosby, Chicago.

46. Eisen MB, Spellman PT, Brown PO, and Botstein D. 1998. Cluster analysis and display of genome-wide expression patterns. *Proc Natl Acad Sci U S A*. 95:14863-8.

47. Eguchi T, Kubota S, Koudo S, Shimo T, Hittori T, Nikanishi T, and Kuboki T. 2001. Regulatory mechanism of human connective tissue growth factor gene expression in a human chondrocytic cell line, HCS-2/8. *J. Biochem. (Tokyo)* 130(1): 79-87.

48. Fan WH, Pech M, Karnovsky MJ. 2000. Connective tissue growth factor stimulates vascular smooth muscle cell growth and migration in vitro. *Eur. J. Cell Biol.* 79(12):915-923.

49. Ferrara N. 2002. Vascular endothelial growth vactor and the quest for tumor angiogenic factors. *Nat. Rev. Cancer.* 2(10):795-803.

50. Folger PA, Zekaria D, Grotendorst GR, and Masur SK. 2001. Transforming growth factor-beta-stimulated connective tissue growth factor expression during corneal myofibroblast differentiation. *Invest. Ophthalmol. Vis. Sci.* 42:2534-2541.

51. Frank S, Madlener M, and Werner S. 1996. Transforming growth factors beta1, beta2, and beta3 and their receptors are differentially regulated during normal and impaired wound healing. *J. Biol. Chem.* 271:10188-10193.

52. Frazier K, Williams S, Kothapalli D, Klapper H, and Grotendorst GR. 1996. Stimulation of fibroblast cell growth, matrix production, and granulation tissue formation by connective tissue growth factor. *J. Invest. Dermatol.* 107:404-411.

53. Furie MB and McHugh DD. 1989. Migration of neutrophils across endothelial monolayers is stimulated by treatment of the monolayers with interleukin-1 or tumor necrosis factor-alpha. *J. Immunol.* 143:3309-3317.

54. Gharaee-Kermani M and Phan SH. 2001. Role of cytokines and cytokine therapy in wound healing and fibrotic diseases. *Curr. Pharm. Des.* 7:1083-1103.

55. Gillitzer R and Goebeler M. 2001. Chemokines in cutaneous wound healing. *J. Leukoc. Biol.* 69:513-521.

56. Gimbel H, Sun R, and Kaye GB. 2000. Refractive error in cataract surgery after previous refractive surgery. *J. Cataract Refract. Surg.* 26:142-144.

57. Ginsberg MH, Du X, and Plow EF. 1992. Inside-out integrin signalling. *Curr. Opin. Cell Biol.* 4:766-771.

58. Gliemann J. 1998. Receptors of the low density lipoprotein (LDL) receptor family in man. Multiple functions of the large family members via interaction with complex ligands. *Biol. Chem.* 379, 951-64.

59. Goldschmeding R, Aten J, Ito Y, Blom I, Rabelink T, and Weening JJ. 2000. Connective tissue growth factor: just another factor in renal fibrosis? *Nephrol. Dial. Transplant.* 15:296-299.

60. Golub TR, Slonim DK, Tamayo P, Huard C, Gaasenbeek M, and Mesirov JP. 1999. Molecular classification of cancer: class discovery and class prediction by gene expression monitoring. *Science*. 286(5439):531-537.

61. Grant MB, Khaw PT, Schultz GS, Adams JL, and Shimizu RW. 1992. Effects of epidermal growth factor, fibroblast growth factor, and transforming growth factor-beta on corneal cell chemotaxis. *Invest. Ophthalmol. Vis. Sci.* 33:3292-3301.

62. Greenhalgh DG. 1996. The role of growth factors in wound healing. *J. Trauma* 41:159-167.

63. Grotendorst GR. 1997. Connective tissue growth factor: a mediator of TGF-beta action on fibroblasts. *Cytokine Growth Factor Rev.* 8:171-179.

64. Grotendorst GR, Okochi H, and Hayashi N. 1996. A novel transforming growth factor beta response element controls the expression of the connective tissue growth factor gene. *Cell Growth Differ.* 7:469-480.

65. Guerrier-Takada C, Gardiner K, Marsh T, Pace N, and Altman S. 1983. The RNA moiety of ribonuclease P is the catalytic subunit of the enzyme. *Cell.* 35:849-857.

66. Gullino PM. 1986. Considerations on the mechanism of the angiogenic response. *Anticancer Res.* 6:153-158.

67. Guo N, Krutzsch HC, Inman JK, and Roberts DD. 1997. Thrombospondin 1 and type I repeat peptides of thrombospondin 1 specifically induce apoptosis of endothelial cells. *Cancer Res.* 57:1735-1742.

68. Gupta A, Monroy D, Ji Z, Yoshino K, Huang A, and Pflugfelder SC. 1996. Transforming growth factor beta-1 and beta-2 in human tear fluid. *Curr. Eye Res.* 15:605-614.

69. Gustafson T and Ritter WR. 1990. The cysteine rich-domains of the insulin and the insulin-like growth factor I receptors are primary determinants of hormone binding specificity. *J. Biol. Chem.* 265, 18663-18667.

70. Gutierrez GE, Mundy GR, Derynck R, Hewlett EL, and Katz MS. 1987. Inhibition of parathyroid hormone-responsive adenylate cyclase in clonal osteoblast-like cells by transforming growth factor alpha and epidermal growth factor. *J. Biol. Chem.* 262:15845-15850.

71. Haseloff J and Gerlach WL. 1988. Simple RNA enzymes with new and highly specific endoribonuclease activities. *Nature.* 334:585-591.

72. Hashimoto G, Inoki I, Fuiji Y, Aoki T, Ikeda E, and Okada Y. 2002. Matrix metalloproteinases cleave connective tissue growth factor and reactivate angiogenic activiy of VEGF 165. *J. Biol. Chem.* 277(39):36288-36296.

73. Hashimoto Y, Shindo-Okada N, Tani M, Nagamachi Y, Takeuchi K, Shiroishi T, Toma H, and Yokota J. 1998. Expression of the Elm1 gene, a novel gene of the CCN (connective tissue growth factor, Cyr61/Cef10, and neuroblastoma overexpressed gene) family, suppresses In vivo tumor growth and metastasis of K-1735 murine melanoma cells. *J. Exp. Med.* 187:289-296.

74. Hay ED. 1981. Extracellular matrix. *J. Cell Biol.* 91:205s-223s.

75. Hayashida-Hibino S, Watanabe H, Nishiba K, Tsujikawa M, Tanaka T, and Hori Y 2001. The effect of transforming growth factor beta-1 on differential gene expression profiling in human corneal epithelium studied by cDNA expression array. *Invest. Ophthalmol. Vis. Sci.* 42(8):1691-1697.

76. Heid CA, Stevens J, Livak KJ, and Williams DM. 1996. Real time quantitative PCR. *Genome Research.* 10:986-984.

77. Heitzmann J, Binder PS, Kassar BS, and Nordan LT. 1993. The correction of high myopia using the excimer laser. *Arch. Ophthalmol.* 111:1627-1634.

78. Heldin CH, Miyazono K, and ten Dijke P. 1997. TGF-beta signalling from cell membrane to nucleus through SMAD proteins. *Nature.* 390:465-471.

79. Herz J and Strickland D. 2001. LRP: a multifunctional scavenger and signaling receptor. *J. Clin. Invest.* 108, 779-784.

80. Hirose J, Kawashima H, Yoshie O, Tashiro K, and Miyasaka M. 2001. Versican interacts with chemokines and modulates cellular responses. *J. Biol. Chem.* 276(7):5228-5234.

81. Hishikawa K, Nakaki T, and Fuiji T. 2000. Connective tissue growth factor induces apoptosis via caspase 3 in cultures human aortic smooth muscle cells. *Eur. J. Pharmacol.* 392(1):19-22.

82. Hishikawa K, Oemar BS, Tanner FC, Nakaki T, Fujii T, and Luscher TF. 1999a. Overexpression of connective tissue growth factor gene induces apoptosis in human aortic smooth muscle cells. *Circulation.* 100:2108-2112.

83. Hishikawa K, Oemar BS, Tanner FC, Nakaki T, Luscher TF, and Fujii T. 1999b. Connective tissue growth factor induces apoptosis in human breast cancer cell line MCF-7. *J. Biol. Chem.* 274:37461-37466.

84. Hishikawa K, Nakaki T, and Fuiji T. 1999c. Transforming growth factor beta-1 induces apoptosis via connective tissue growth factor in human aortic smooth muscle cells. *Eur. J. Pharmacol.* 385(2):287-90.

85. Hishikawa K, Oemar BS, and Nakaki T. 2001. Static pressure regulates connective tissue growth factor expression in human mesangial cells. *J. Biol. Chem.* 276(20):16797-803.

86. Holland PM, Abramson RD, Watson R, and Gelfand DH. 1991. Detection of specific polymerase chain reaction product by utilizing the 5'----3' exonuclease activity of Thermus aquaticus DNA polymerase. *Proc. Natl. Acad. Sci. USA.* 88:7276-7280.

87. Hoppenreijs VPT, Pels E, Vrensen GFJM, Felten PC, and Treffers WF. 1993. Platelet-Derived Growth Factor: Receptor Expression in Corneas and Effects on Corneal Cells. *Invest. Optholmol. Vis. Sci.* 34:637-649.

88. Hoppenreijs VPT, Pels E, Vrensen GFJM, Oosting J, and Treffers FW. 1992. Effects of human epidermal growth factor on endothelial wound healing of human corneas. *Invest. Ophthalmol. Vis. Sci.* 33(6):1946-1957.

89. Hunt TK, Knighton DR, Thakral KK, Goodson WH III, and Andrews WS. 1984. Studies on inflammation and wound healing: angiogenesis and collagen synthesis stimulated in vivo by resident and activated wound macrophages. *Surgery.* 96:48-54.

90. Hurvitz JR, Suwairi WM, VanHul W, El-Shanti H, Superti-Furga A et al. 1999. Mutations in the CCN gene family member WISP3 cause progressive pseudorheumatoid dysplasia. *Nat. Genet.* 23:94-98.

91. Igarashi A, Hayashi N, Nashiro K, and Takehara K. 1998. Differential expression of connective tissue growth factor gene in cutaneous fibrohistiocytic and vascular tumors. *J. Cutan. Pathol.* 25:143-148.

92. Igarashi A, Nashiro K, Kikuchi K, Sato S, Ihn H, Grotendorst GR, and Takehara K. 1995. Significant correlation between connective tissue growth factor gene expression and skin sclerosis in tissue sections from patients with systemic sclerosis. *J. Invest Dermatol.* 105:280-284.

93. Igarashi A, Okochi H, Bradham DM, and Grotendorst GR. 1993. Regulation of connective tissue growth factor gene expression in human skin fibroblasts and during wound repair. *Mol. Biol. Cell.* 4:637-645.

94. Inagaki Y, Truter S, and Ramirez F. 1994. Transforming growth factor-beta stimulates alpha 2(I) collagen gene expression through a cis-acting element that contains an Sp1-binding site. *J. Biol. Chem.* 269:14828-14834.

95. Incardona F, Lawler J, Cataldo D, Panet A, Legrand Y, Foidart JM, and Legrand C. 1996. Heparin-binding domain, type 1 and type 2 repeats of thrombospondin mediate its interaction with human breast cancer cells. *J. Cell Biochem.* 62:431-442.

96. Irving JA and Lala PK. 1995. Functional role of cell surface integrins on human trophoblast cell migration: regulation by TGF-beta, IGF-II, and IGFBP-1. *Exp. Cell Res.* 217:419-427.

97. Ito Y, Aten J, Bende RJ, Oemar BS, Rabelink TJ, Weening JJ, and Goldschmeding R. 1998. Expression of connective tissue growth factor in human renal fibrosis. *Kidney Int.* 53:853-861.

98. Jampel HD, Roche N, Stark WJ, and Roberts AB. 1990. Transforming growth factor-beta in human aqueous humor. *Curr. Eye Res.* 9:963-969.

99. Jester JV, Barry-Lane PA, Petroll WM, Olsen DR, and Cavanagh HD. 1997. Inhibition of corneal fibrosis by topical application of blocking antibodies to TGF beta in the rabbit. *Cornea.* 16:177-187.

100. Jester JV, Moller-Pedersen T, Huang J, Sax CM, Kays WT, and Cavanagh HD. 1999. The cellular basis of corneal transparency: evidence for 'corneal crystallins'. *J. Cell Sci.* 112(Pt 5):613-22.

101. Jones J and Clemmons D. 1995. Insulin-like growth factors and their binding proteins: biological actions. *Endocr. Rev.* 16:3-34.

102. Kaleko M, Rutter W, and Miller A. 1990. Overexpression of the human insulin-like growth factor I receptor promotes ligand dependent neoplastic transformation. *Mol. Cell. Biol.* 10:464-473.

103. Kelley J, Shull S, Walsh JJ, Cutroneo KR, and Absher M. 1993. Auto-induction of human transforming growth factor beta in human lung fibroblasts. *Am. J. Respir. Cell Molec. Biol.* 8(4):417-424.

104. Kenney MC, Shih LM, Labermeir U, and Satterfield D. 1986. Modulation of rabbit keratocyte production of collagen, sulfated glycosaminoglycans and fibronectin by retinol and retinoic acid. *Biochim. Biophys. Acta.* 889:156-162.

105. Khalil N, O'Connor RN, Unruh HW, Warren PW, Flanders KC, Kemp A, Bereznay OH, and Greenberg AH. 1991. Increased production and immunohistochemical localization of transforming growth factor-beta in idiopathic pulmonary fibrosis. *Am. J. Respir. Cell Mol. Biol.* 5:155-162.

106. Khaw PT, Doyle JW, Sherwood MB, Grierson I, Schultz GS, and McGorray S. 1993. Prolonged localized tissue effects from 5-minute exposures to fluorouracil and mitomycin C. *Arch. Ophthalmol.* 111:263-267.

107. Kikuchi K, Kadono T, Ihn H, Sato S, Igarashi A, Nakagawa H, Tamaki K, and Takehara K. 1995. Growth regulation in scleroderma fibroblasts: increased response to transforming growth factor-beta 1. *J. Invest Dermatol.* 105:128-132.

108. Kim HS, Nagalla SR, Oh Y, Wilson E, Roberts CT Jr, and Rosenfeld RG. 1997. Identification of a family of low-affinity insulin-like growth factor binding proteins (IGFBPs): characterization of connective tissue growth factor as a member of the IGFBP superfamily. *Proc. Natl. Acad. Sci. USA.* 94:12981-12986.

109. Komai Y and Ushiki T. 1991. The three-dimensional organization of collagen fibrils in the human cornea and sclera. *Invest. Ophthalmol. Vis. Sci.* 32:2244-2258.

110. Kornfeld S. 1992. Structure and function of the mannose-6-phosphate/ insulinlike growth factor-II receptors. *Annu. Rev. Biochem.* 61:307-330.

111. Kothapalli D, Frazier KS, Welply A, Segarini PR, and Grotendorst GR. 1997. Transforming growth factor beta induces anchorage-independent growth of NRK fibroblasts via a connective tissue growth factor-dependent signaling pathway. *Cell Growth Differ.* 8:61-68.

112. Kruger K, Grabowski PJ, Zaug AJ, Sands J, Gottschling DE, and Cech TR. 1982. Self-splicing RNA: autoexcision and autocyclization of the ribosomal RNA intervening sequence of Tetrahymena. *Cell.* 31:147-157.

113. Ksander GA, Chu GH, McMullin H, Ogawa Y, Pratt BM, Rosenblatt JS, and McPherson JM. 1990. Transforming growth factors-beta 1 and beta 2 enhance connective tissue formation in animal models of dermal wound healing by secondary intent. *Ann. N. Y. Acad. Sci.* 593:135-147.

114. Kurt S, Theodore JCIV, Alfred WG, Carolyn LJ, and Gibbes RJ. 1992. Transforming growth factor-α acts as an autocrine growth factor in ovarian carcinoma cell lines. *Cancer Res.* 52:341-347.

115. Lankat-Buttgereit B, Kulozik MK, Hunzelmann N, and Krieg T. 1991. Cytokines alter mRNA steady state levels for basement membrane proteins in human skin fibroblasts. *J. Dermatol. Sci.* 2:300-307.

116. LaVail MM, Yasumura D, Matthes MT, Drenser KA, Flannery JG, Lewin AS, and Hauswirth WW. 2000. Ribozyme rescue of photoreceptor cells in P23H transgenic rats: long-term survival and late-stage therapy. *Proc. Natl. Acad. Sci. USA.* 97:11488-11493.

117. Lawler J. 2002. Thrombospondin-1 as an endogenous inhibotory of angiogenic and tumor growth. *J. Cell Mol. Med.* 6(1):1-12.

118. Lee DA. 1994. Antifibrosis agents and glaucoma surgery. *Invest. Ophthalmol. Vis. Sci.* 35:3789-3791.

119. Lee YC, Wang IJ, Hu FR, and Kao WW. 2001. Immunohistochemical study of subepithelial haze after phototherapeutic keratectomy. *J. Refract. Surg.* 17:334-341.

120. Leibovich SJ and Ross R. 1976. A macrophage-dependent factor that stimulates the proliferation of fibroblasts in vitro. *Am. J. Pathol.* 84:501-514.

121. Lewin AS, Drenser KA, Hauswirth WW, Nishikawa S, Yasumura D, Flannery JG, and LaVail MM. 1998. Ribozyme rescue of photoreceptor cells in a transgenic rat model of autosomal dominant retinitis pigmentosa. *Nat. Med.* 4:967-971.

122. Li DQ and Tseng SC. 1995. Three patterns of cytokine expression potentially involved in epithelial-fibroblast interactions of human ocular surface. *J. Cell Physiol.* 163:61-79.

123. Lieber A. and Kay MA. 1996. Adenovirus-mediated expression of ribozymes in mice. *J. Virol.* 70:3153-3158.

124. Lindblad WJ. 1998. Perspective article: collagen expression by novel cell populations in the dermal wound environment. *Wound. Repair Regen.* 6:186-193.

125. Liu C, Liu XJ, Crowe PD, Kelner GS, Fan J, Barry G, Manu F, Ling N, De Souza EB, and Maki RA. 1999. Nephroblastoma overexpressed gene (NOV) codes for a growth factor that induces protein tyrosine phosphorylation. *Gene.* 238:471-478.

126. Livak KJ, Flood SAJ, Marmaro J, Giusti W, and Deetz K. 1995. Oligonucleotides with fluorescent dyes at opposite ends provide a quenched probe system useful for detecting PCR product and nucleic acid hybridization. *PCR Meth. Appl.* 4:357-362.

127. Ljubimov AV, Alba SA, Burgeson RE, Ninomiya Y, Sado Y, Sun TT, Nesburn AB, Kenney MC, and Maguen E. 1998. Extracellular matrix changes in human corneas after radial keratotomy. *Exp. Eye Res.* 67:265-272.

128. Lyon M, Deakin J, Mizuno K, Nakamura T, and Gallagher J. 1994. Interaction of hepatocyte growth factor with heparan sulfate. Elucidation of the major heparan sulfate structural determinants. *J. Biol. Chem.* 269, 11216-11213.

129. Madtes DK, Raines EW, Sakariassen KS, Assoian RK, Sporn MB, Bell GI, and Ross R. 1988. Induction of transforming growth factor-alpha in activated human alveolar macrophages. *Cell.* 53:285-293.

130. Mahajan VB, Wei C, and McDonnell PJ. 2002. Microarray analysis of corneal fibroblast gene expression after interleukin-1 treatment. *Invest. Ophthalmol. Vis. Sci.* 43(7):2143-2151.

131. Malley DS, Steinert RF, Puliafito CA, and Dobi ET. 1990. Immunofluorescence study of corneal wound healing after excimer laser anterior keratectomy in the monkey eye. *Arch. Ophthalmol.* 108:1316-1322.

132. Malmstrom J, Larsen K, Hansson L, Lofdahl CG, Norregard-Jensen O, Marko-Varga G, and Westergren-Thorsson G. 2002. Proteoclycan and proteome profiling of central human pulmonary fibrotic tissue utilizing miniature sample preparations. *Proteomics*. 2(4):394-404.

133. Marron-Teraga P, Brzycki-Wessell M, and Dahms N. 1998. The two mannose 6-phosphate binding sites of the insulin-like growth factor-II/mannose 6-phosphate receptor display different ligand binding properties. *J. Biol. Chem.* 273:22358-22366.

134. Martinerie C, Viegas-Pequignot E, Guenard I, Dutrillaux B, Nguyen VC, Bernheim A, and Perbal B. 1992. Physical mapping of human loci homologous to the chicken nov proto-oncogene. *Oncogene.* 7:2529-2534.

135. Mason ED, Konrad KD, Webb CD, and Marsh JL. 1994. Dorsal midline fate in Drosophila embryos requires twisted gastrulation, a gene encoding a secreted protein related to human connective tissue growth factor. *Genes Dev.* 8:1489-1501.

136. Mast BA and Schultz GS. 1996. Interaction of cytokines, growth factors and proteases in acute and chronic wounds. *Wounds.* 4, 411-420.

137. Maurice DM. 1984. The cornea and sclera. *In* The eye. Davison H, editor. Academic Press, Orlando.

138. McDermott ML. 1993. Stromal wound healing. *In* Corneal surgery. Brightbill FS, editor. Mosby, Chicago.

139. Melles GR, SundarRaj N, Binder PS, van der Weiden MM, Wijdh RH, Beekhuis WH, and Anderson JA. 1995. Immunohistochemical analysis of unsutured and sutured corneal wound healing. *Curr. Eye Res.* 14:809-817.

140. Meyer P, Wunderlich K, Kain HL, Prunte C, and Flammer J. 2002. Human connective tissue growth factor mRNA expression of epiretinal and subretinal fibrovascular membranes: a report of three cases. *Ophthalmologica.* 216:284-291.

141. Mints M, Blomgren B, Falconer C, and Palmblad J. 2002. Expression of the vascular endothelial growth factor (VEGF) family in human endometrial blood vessels. *Scand. J. Clin. Lab Invest.* 62:167-175.

142. Moore JE, McMullen CB, Mahon G, and Adamis AP. 2002. The corneal epithelial stem cell. *DNA Cell Biol.* 21:443-451.

143. Moussad EE and Brigstock DR. 2000. Connective tissue growth factor: What's in a name? *Mol. Genet. Metab.* 71:276-292.

144. Murphy G, Cockett MI, Ward RV, and Docherty AJ. 1991. Matrix metalloproteinase degradation of elastin, type IV collagen and proteoglycan. A quantitative comparison of the activities of 95 kDa and 72 kDa gelatinases, stromelysins-1 and -2 and punctuated metalloproteinase (PUMP). *Biochem. J.* 277(Pt 1):277-279.

145. Murray-Rust J, McDonald NQ, Blundell TL, Hosang M, Oefner C, Winkler F, and Bradshaw RA. 1993. Topological similarities in TGF-beta 2, PDGF-BB and NGF define a superfamily of polypeptide growth factors. *Structure.* 1:153-159.

146. Mutsaers SE, Bishop JE, McGrouther G, and Laurent GJ. 1997. Mechanisms of tissue repair: from wound healing to fibrosis. *Int. J. Biochem. Cell Biol.* 29:5-17.

147. Nakae J, Kido Y, and Accili D. 2001. Distinct and overlapping functions of insulin and IGF-I receptors. *Endocr. Rev.* 22, 818-835.

148. Nakao A, Imamura T, Souchelnytskyi S, Kawabata M, Ishisaki A, Oeda E, Tamaki K, Hanai J, Heldin CH, Miyazono K, and ten Dijke P. 1997. TGF-beta receptor-mediated signalling through Smad2, Smad3 and Smad4. *EMBO J.* 16:5353-5362.

149. Nall AV, Brownlee RE, Colvin CP, Schultz G, Fein D, Cassisi NJ, Nguyen T, and Kalara A. 1996. Transforming growth factor β_1 improves wound healing and random flap survival in normal and irradiated rats. *Arch. Otolaryngol. Head Neck Surg.* 122(2):171-177.

150. Nishida T, Nakanishi T, Shimo T, Asano M, Hattori T, Tamatani T, Tezuka K, and Takigawa M. 1998. Demonstration of receptors specific for connective tissue growth factor on a human chondrocytic cell line (HCS-2/8). *Biochem. Biophys. Res. Commun.* 247:905-909.

151. Nishida T, Yasumoto K, Otori T, and Desaki J. 1988. The network structure of corneal fibroblasts in the rat as revealed by scanning electron microscopy. *Invest. Ophthalmol. Vis. Sci.* 29:1887-1890.

152. Noble PW, Henson PM, Lucas C, Mora-Worms M, Carre PC, and Riches DW. 1993. Transforming growth factor-beta primes macrophages to express inflammatory gene products in response to particulate stimuli by an autocrine/paracrine mechanism. *J. Immunol.* 151:979-989.

153. O'Brien TP and Lau LF. 1992. Expression of the growth factor-inducible immediate early gene cyr61 correlates with chondrogenesis during mouse embryonic development. *Cell Growth Differ.* 3:645-654.

154. Ohtsuki M and Massague J. 1992. Evidence for the involvement of protein kinase activity in transforming growth factor-beta signal transduction. *Mol. Cell Biol.* 12:261-265.

155. Otori T. 1967. Electrolyte content of the rabbit corneal stroma. *Exp. Eye Res.* 6:356-367.

156. Paradis V, Dargere D, Bonvoust F, Vidaud M, Segarini P, and Bedossa P. 2002. Effects and regulation of connective tissue growth factor on hepatic stellate cells. *Lab. Invest.* 82(6):767-774.

157. Parrish R and Minckler D. 1996. "Late endophthalmitis"--filtering surgery time bomb? *Ophthalmology.* 103:1167-1168.

158. Paulus W, Baur I, Huettner C, Schmausser B, Roggendorf W, Schlingensiepen KH, and Brysch W. 1995. Effects of transforming growth factor-beta 1 on collagen synthesis, integrin expression, adhesion and invasion of glioma cells. *J. Neuropathol. Exp. Neurol.* 54:236-244.

159. Pederson L, Winding B, Foged NT, Spelsberg TC, and Ourster MJ. 1999. Identification of breast cancer cell line-derived paracrine factors that stimulate osteoclast activity. *Cancer Res.* 59(22):5849-5855.

160. Pelton RW, Hogan BL, Miller DA, and Moses HL. 1990. Differential expression of genes encoding TGFs beta 1, beta 2, and beta 3 during murine palate formation. *Dev. Biol.* 141:456-460.

161. Perkett EA. 1995. Role of growth factors in lung repair and diseases. *Curr. Opin. Pediatr.* 7:242-249.

162. Pierce GF, Brown D, and Mustoe TA. 1991. Quantitative analysis of inflammatory cell influx, procollagen type I synthesis, and collagen cross-linking in incisional wounds: influence of PDGF-BB and TGF-beta 1 therapy. *J. Lab Clin. Med.* 117:373-382.

163. Piscatelli SJ, Michaels BM, Gregory P, Jennings RW, Longaker MT, Harrison MR, and Siebert JW. 1994. Fetal fibroblast contraction of collagen matrices in vitro: the effects of epidermal growth factor and transforming growth factor-beta. *Ann. Plast. Surg.* 33:38-45.

164. Pollack SV. 1984. The wound healing process. *Clin. Dermatol.* 2:8-16.

165. Porges Y, Ben Haim O, Hirsh A, and Levinger S. 2003. Phototherapeutic keratectomy with mitomycin C for corneal haze following photorefractive keratectomy for myopia. *J. Refract. Surg.* 19:40-43.

166. Price FW Jr, Willes L, Price M, Lyng A, and Ries J. 2001. A prospective, randomized comparison of the use versus non-use of topical corticosteroids after laser in situ keratomileusis. *Ophthalmology.* 108:1236-1244.

167. Propsting MJ, Kubicka S, Genschel J, Manns MP, Lochs H, and Schmidt HH. 2000. Inhibition of transthyretin-met30 expression using Inosine(15.1)- Hammerhead ribozymes in cell culture. *Biochem. Biophys. Res. Commun.* 279:970-973.

168. Ramaswamy, S., K.N.Ross, E.S.Lander, and T.R.Golub. 2003. A molecular signature of metastasis in primary solid tumors. *Nat. Genet.* 33(1):49-54.

169. Ramaswamy S, Tamayo P, Rifkin R, Mukharjee S, Yeang CH, and Angelo M. 2001. Multiclass cancer diagnosis using tumor gene expression signatures. *Proc. Nat. Acad. Sci. USA*. 98(26):15149-15154.

170. Rendell MS, Johnson ML, Smith D, Finney D, Capp C, Lammers R, and Lancaster S. 2002. Skin blood flow response in the rat model of wound healing: expression of vasoactive factors. *J. Surg. Res.* 107:18-26.

171. Riser BL, Denichilo M, Cortes P, Baker C, Grondin JM, Yee J, and Narins RG. 2000. Regulation of connective tissue growth factor activity in cultured rat mesangial cells and its expression in experimental diabetic glomerulosclerosis. *J. Am. Soc. Nephrol.* 11:25-38.

172. Roberts AB. 1995. Tranforming growth factor-beta: activity and efficacy in animal models of wound healing. *Wound. Repair Regen.* 3, 408-418.

173. Roberts AB and Sporn MB. 1990. The transforming growth factors beta. *In* Handbook of experimental pharmacology. Peptide growth factors and their receptors. Roberts AB and Sporn MB, editors. Springer-Verlag, New York. 419-472.

174. Roberts AB, Sporn MB, Assoian RK, Smith JM, Roche NS, Wakefield LM, Heine UI, Liotta LA, Falanga V, Kehrl JH, and . 1986. Transforming growth factor type beta: rapid induction of fibrosis and angiogenesis in vivo and stimulation of collagen formation in vitro. *Proc. Natl. Acad. Sci. USA*. 83:4167-4171.

175. Ross R, Masuda J, Raines EW, Gown AM, Katsuda S, Sasahara M, Malden LT, Masuko H, and Sato H. 1990. Localization of PDGF-B protein in macrophages in all phases of atherogenesis. *Science*. 248:1009-1012.

176. Rossi P, Karsenty G, Roberts AB, Roche NS, Sporn MB, and de Crombrugghe B. 1988. A nuclear factor 1 binding site mediates the transcriptional activation of a type I collagen promoter by transforming growth factor-beta. *Cell*. 52:405-414.

177. Ryseck RP, Macdonald-Bravo H, Mattei MG, and Bravo R. 1991. Structure, mapping, and expression of fisp-12, a growth factor- inducible gene encoding a secreted cysteine-rich protein. *Cell Growth Differ.* 2:225-233.

178. Saika S, Shiraishi A, Liu CY, Funderburgh JL, Kao CW, Converse RL, and Kao WW. 2000. Role of lumican in the corneal epithelium during wound healing. *J. Biol. Chem.* 275(4):2607-2612.

179. Sara V and Hall K. 1990. Insulin-like growth factors and their binding proteins. *Physiol. Rev.* 70:591-614.

180. Sato S, Nagaoka T, Hasegawa M, Tamatani T, Nakanishi T, Takigawa M, and Takehara K. 2000. Serum levels of connective tissue growth factor are elevated in patients with systemic sclerosis: association with extent of skin sclerosis and severity of pulmonary fibrosis. *J. Rheumatol.* 27:149-154.

181. Scatchard G. 1949. The attraction of proteins for small molecules and ions. *Ann. N. Y. Acad. Sci*. 51, 660-673.

182. Schlessinger J, Lax I, and Lemmon M. 1995. Regulation of growth factor activation by proteoglycans: what is the role of the low affinity receptors? *Cell.* 83:357-360.

183. Schmid P, Kunz S, Cerletti N, McMaster G, and Cox D. 1993. Injury induced expression of TGF-beta 1 mRNA is enhanced by exogenously applied TGF-beta S. *Biochem. Biophys. Res. Commun.* 194:399-406.

184. Schultz GS, Chegini N, Grant MB, Khaw PT, and MacKay SA. 1992. Effects of growth factors on corneal wound healing. *Acta Ophthalmol. Suppl.* 60-66.

185. Schultz GS. 1995. Modulation of corneal wound healing. *In* Cornea. Krachmer JH, Mannis MJ, and Holland EJ, editors. Mosby, Chicago.

186. Schumacher R, Mosthaf L, Schlessinger J, Brandenburg D, and Ullrich A. 1991. Insulin and insulin-like growth factor 1 binding specificity is determined by distinct regions of their cognate receptors. *J. Biol. Chem.* 266:19288-19295.

187. Scott WG, Murray JB, Arnold JRP, Stoddard BL, and Klug A. 1996. Capturing the Structure of a Catalytic RNA Intermediate: The Hammerhead Ribozyme. *Science.* 274:2065-2069.

188. Segarini PR, Nesbitt JE, Li D, Hays LG, Yates JR III, and Carmichael DF. 2001. The low density lipoprotein receptor-related protein/alpha2-macroglobulin receptor is a receptor for connective tissue growth factor. *J. Biol. Chem.* 276:40659-40667.

189. Shah M, Foreman DM, and Ferguson MW. 1994. Neutralising antibody to TGF-beta 1,2 reduces cutaneous scarring in adult rodents. *J. Cell Sci.* 107(Pt 5):1137-1157.

190. Shimo T, Nakanishi T, Nishida T, Asano M, Kanyama M, Kuboki T, Tamatani T, Tezuka K, Takemura M, Matsumura T, and Takigawa M. 1999. Connective tissue growth factor induces the proliferation, migration, and tube formation of vascular endothelial cells in vitro, and angiogenesis in vivo. *J. Biochem. (Tokyo)* 126:137-145.

191. Siganos DS, Katsanevaki VJ, and Pallikaris IG. 1999. Correlation of subepithelial haze and refractive regression 1 month after photorefractive keratectomy for myopia. *J. Refract. Surg.* 15:338-342.

192. Simpson DM and Ross R. 1972. The neutrophilic leukocyte in wound repair a study with antineutrophil serum. *J. Clin. Invest.* 51:2009-2023.

193. Singer AJ and Clark RA. 1999. Cutaneous wound healing. *N. Engl. J. Med.* 341:738-746.

194. Sioud M, Natvig JB, and Forre O. 1992. Preformed ribozyme destroys tumour necrosis factor mRNA in human cells. *J. Mol. Biol.* 223:831-835.

195. Siriwardena D, Khaw PT, King AJ, Donaldson ML, Overton BM, Migdal C, and Cordeiro MF. 2002. Human antitransforming growth factor beta(2) monoclonal antibody--a new modulator of wound healing in trabeculectomy: a randomized placebo controlled clinical study. *Ophthalmology.* 109:427-431.

196. Snaith MR, Natarajan D, Taylor LB, Choi CP, Martinerie C, Perbal B, Schofield PN, and Boulter CA. 1996. Genomic structure and chromosomal mapping of the mouse nov gene. *Genomics.* 38:425-428.

197. Snyder MC, Bergmanson JP, and Doughty MJ. 1998. Keratocytes: no more the quiet cells. *J. Am. Optom. Assoc.* 69:180-187.

198. Sotozono C, Inatomi T, Nakamura M, and Kinoshita S. 1995. Keratinocyte growth factor accelerates corneal epithelial wound healing in vivo. *Invest. Ophthalmol. Vis. Sci.* 36:1524-1529.

199. Sporn MB and Roberts AB. 1992. Transforming growth factor-beta: recent progress and new challenges. *J. Cell Biol.* 119:1017-1021.

200. Stark WJ, Chamon W, Kamp MT, Enger CL, Rencs EV, and Gottsh JD. 1992. Clinical follow-up of 193-nm ArF excimer laser photokeratectomy. *Ophthalmology.* 99:805-812.

201. Steenfos HH. 1994. Growth factors and wound healing. *Scand. J. Plast. Reconstr. Surg. Hand Surg.* 28:95-105.

202. Stewart C, James P, Fant ME, and Rotwein P. 1996. Overexpression of insulin-like growth factor-II induces accelerated myoblast differentiation. *J. Cell Physiol.* 169, 23-32.

203. Streuli CH, Schmidhauser C, Kobrin M, Bissell MJ, and Derynck R. 1993. Extracellular matrix regulates expression of the TGF-beta 1 gene. *J. Cell Biol.* 120:253-260.

204. Sullivan SM. 1994. Dvevelopment of Ribozymes For Gene Therapy. *J. Invest. Dermatol.* 103:85S-89S.

205. Sunderkotter C, Beil W, Roth J, and Sorg C. 1991. Cellular events associated with inflammatory angiogenesis in the mouse cornea. *Am. J. Pathol.* 138:931-939.

206. Sutton G, Kalski RS, Lawless MA, and Rogers C. 1995. Excimer retreatment for scarring and regression after photorefractive keratectomy for myopia. *Br. J. Ophthalmol.* 79:756-759.

207. Symons RH. 1992. Small catalytic RNAs. *Annu. Rev. Biochem.* 61:641-671.

208. Tamatani T, Kobayashi H, Tezuka K, Sakamoto S, Suzuki K, Nakanishi T, Takigawa M, and Miyano T. 1998. Establishment of the enzyme-linked immunosorbent assay for connective tissue growth factor (CTGF) and its detection in the sera of biliary atresia. *Biochem. Biophys. Res. Commun.* 251:748-752.

209. Tanaka S, Sugimachi K, Saeki H, Kinoshita J, Ohga T, Shimada M, Maehara Y, and Sugimachi K. 2001. A novel variant of WISP1 lacking a Von Willebrand type C module overexpressed in scirrhous gastric carcinoma. *Oncogene.* 20:5525-5532.

210. Ticho U and Ophir A. 1993. Late complications after glaucoma filtering surgery with adjunctive 5-fluorouracil. *Am. J. Ophthalmol.* 115:506-510.

211. Tuft SJ, Zabel RW, and Marshall J. 1989. Corneal repair following keratectomy. A comparison between conventional surgery and laser photoablation. *Invest. Ophthalmol. Vis. Sci.* 30:1769-1777.

212. Ullrich A and Schlessinger J. 1990. Signal transduction by receptors with tyrosine kinase activity. *Cell.* 61:203-212.

213. Usman N and Blatt LM. 2000. Nuclease-resistant synthetic ribozymes: developing a new class of therapeutics. *J. Clin. Invest.* 106:1197-1202.

214. van Setten GB, Aspiotis M, Blalock TD, Grotendorst GR, and Schultz GS. 2003a. Connective tissue growth factor in pterygium: simultaneous presence with vascular endothelial growth factor - possible contributing factor to conjunctival scarring. *Graefes Arch. Clin. Exp. Ophthalmol.* 241:135-139.

215. van Setten GB, Blalock TD, Grotendorst GR, and Schultz GS. 2003b. Detection of connective tissue growth factor (CTGF) in human tear fluid: preliminary results. *Acta Ophthalmol. Scand.* 81:51-53.

216. van Setten GB, Blalock TD, Grotendorst GR, and Schultz GS. 2002. Detection of connective tissue growth factor in human aqueous humor. *Ophthalmic Res.* 34:306-308.

217. van Setten GB, Schultz GS, and Macauley S. 1994. Growth factors in human tear fluid and in lacrimal glands. *Adv. Exp. Med. Biol.* 350:315-319.

218. Varela JC, Goldstein MH, Baker HV, and Schultz GS. 2002. Microarray analysis of gene expression patterns during healing of rat corneas after excimer laser photorefractive keratectomy. *Invest. Ophthalmol. Vis. Sci.* 43(6):1772-1782.

219. Vogelmann R, Ruf D, Wagner M, Adler G, and Menke A. 2001. Effects of fibrogenic mediators on the development of pancreatic fibrosis in a TGF-beta1 transgenic mouse model. *Am. J. Physiol Gastrointest. Liver Physiol* 280:G164-G172.

220. Vorwerk P, Wex H, Hohmann B, Mohnike K, Schmidt U, and Mittler U. 2002. Expression of components of the IGF signaling system in childhood acute lymphoblastic leukemia. *Mol. Pathol.* 55(1)40-5.

221. Wachtlin J, Langenbeck K, Schrunder S, Zhang EP, and Hoffmann F. 1999. Immunohistology of corneal wound healing after photorefractive keratectomy and laser in situ keratomileusis. *J. Refract. Surg.* 15:451-458.

222. Webster DF and Harvey W. 1979. A quantitative assay for collagen synthesis in microwell fibroblast cultures. *Anal. Biochem.* 96:220-224.

223. Weibrich G, Kleis WK, Hafner G, and Hitzler WE. 2002. Growth factor levels in platelet-rich plasma and correlations with donor age, sex, and platelet count. *J. Craniomaxillofac. Surg.* 30:97-102.

224. Weksler BB. 2000. Antiplatelet agents in stroke prevention. combination therapy: present and future. *Cerebrovasc. Dis.* 10(5):41-48.

225. Wenger C, Ellenrieder V, Alber B, Lacher U, Menke A, Hameister H, Wilda M, Iwamura T, Beger HG, Adler G, and Gress TM. 1999. Expression and differential regulation of connective tissue growth factor in pancreatic cancer cells. *Oncogene.* 18:1073-1080.

226. Westergren-Thorsson G, Hernnas J, Sarnstrand B, Oldberg A, Heinegard D, and Malmstrom A. 1993. Altered expression of small proteoglycans, collagen, and transforming growth factor-beta 1 in developing bleomycin-induced pulmonary fibrosis in rats. *J. Clin. Invest.* 92:632-637.

227. Wikner NE, Persichitte KA, Baskin JB, Nielsen LD, and Clark RA. 1988. Transforming growth factor-beta stimulates the expression of fibronectin by human keratinocytes. *J. Invest Dermatol.* 91:207-212.

228. Wilson SE, Pedroza L, Beuerman R, and Hill JM. 1997. Herpes simplex virus-type 1 infection of corneal epithelial cells induces apoptosis of the underlying keratocytes. *Exp. Eye Res.* 64(5):775-779.

229. Wilson SE, Li Q, Weng J, Barry-Lane PA, Jester JV, Liang Q, and Wardinger RJ. 1996a. The Fas-Fas ligand system and other moderators of apoptosis in the cornea. *Invest. Ophthalmol. Vis. Sci.* 37(8):1582-1592.

230. Wilson, S.E., Y.G.He, J.Weng, Q.Li, A.W.McDowall, M.Vital, and E.L.Chwang. 1996b. Epithelial injury induces keratocyte apoptosis: hypothesized role for the interleukin-1 system in the modulation of corneal tissue organization and wound healing. *Exp. Eye Res.* 62:325-327.

231. Wilson SE, Lloyd SA, and He YG. 1992. EGF, basic FGF, and TGF beta-1 messenger RNA production in rabbit corneal epithelial cells. *Invest. Ophthalmol. Vis. Sci.* 33:1987-1995.

232. Wilson SE, Schultz GS, Chegini N, Weng J, and He YG. 1994. Epidermal growth factor, transforming growth factor alpha, transforming growth factor beta, acidic fibroblast growth factor, basic fibroblast growth factor, and interleukin-1 proteins in the cornea. *Exp. Eye Res.* 59:63-71.

233. Wiseman DM, Polverini PJ, Kamp DW, and S.J.Leibovich. 1988. Transforming growth factor-beta (TGF-beta) is chemotactic for human monocytes and induces their expression of angiogenic activity. *Biochem. Biophys. Res. Commun.* 157:793-800.

234. Wong-Staal F, Poeschla EM, and Looney DJ. 1998. A controlled, Phase 1 clinical trial to evaluate the safety and effects in HIV-1 infected humans of autologous lymphocytes transduced with a ribozyme that cleaves HIV-1 RNA. *Hum. Gene Ther.* 9:2407-2425.

235. Woost PG, Jumblatt MM, Eiferman RA, and Schultz GS. 1992. Growth factors and corneal endothelial cells: I. Stimulation of bovine corneal endothelial cell DNA synthesis by defined growth factors. *Cornea.* 11:1-10.

236. Wrana JL, Attisano L, Wieser R, Ventura F, and Massague J. 1994. Mechanism of activation of the TGF-beta receptor. *Nature.* 370:341-347.

237. Wu HK. 2002. Astigmatism and LASIK. *Curr. Opin. Ophthalmol.* 13:250-255.

238. Wunderlich K, Senn BC, Reiser P, Pech M, Flammer J, and Meyer P. 2000. Connective tissue growth factor in retrocorneal membranes and corneal scars. *Ophthalmologica.* 214:341-346.

239. Yamagata M, Saga S, Kato M, Bernfield M, and Kimata K. 1993. Selective distribution of proteoglycans and their ligands in pericellular matrix of cultured fibroblasts. *J. Cell Sci.* 106:55-65.

240. Ye QH, Qin LX, Forgues M, He P, Kim JW, Peng AC, Simon R, Li Y, Robles AI, Chen Y, Ma ZC, Wu ZQ, Ye SL, Liu YK, Tang ZY, Wang XW. 2003. Predicting hepatitis B virus-positive metastatic hepatocellular carcinomas using gene expression profiling and supervised machine learning. *Nat Med.* 9(4):416-23.

241. Ying Z and King ML. 1996. Isolation and characterization of xnov, a Xenopus laevis ortholog of the chicken nov gene. *Gene.* 171:243-248.

242. Zhou L, Dosanjh A, Chen H, and Karasek M. 2000. Divergent effects of extracellular oxygen on the growth, morphology, and function of human skin microvascular endothelial cells. *J. Cell Physiol.* 182:134-140.

243. Zieske JD, Takahashi H, Hutcheon AE, and Dalbone AC. 2000. Activation of epidermal growth factor receptor during corneal epithelial migration. *Invest Ophthalmol. Vis. Sci.* 41:1346-1355.

BIOGRAPHICAL SKETCH

Timothy Daniel Blalock, the third child of James and Ida Blalock, was born on July 7, 1977 in Tullahoma, Tennessee. He grew up in Manchester, Tennessee until his family moved to South Carolina in 1989. Timothy attended Charleston Southern University in Charleston, South Carolina on a Board of Trustees academic scholarship. He graduated *magna cum laude* in 1999 with majors in chemistry and biology. He also received the award for Most Outstanding Student in Biology upon graduation. He is a member of Beta Beta Beta biological honor society and Alpha Chi academic honor society. While attending college, Timothy gained scientific experience working as a laboratory assistant in student teaching labs and in summer internships in local biotechnology laboratories.

In 1999, Timothy was accepted to the Interdisciplinary Program in Biomedical Sciences (IDP) at the University of Florida College of Medicine. He joined the Biochemistry and Molecular Biology Advanced Concentration under the leadership of Dr. Gregory Schultz. In 2003, he received the Boyce Award for Outstanding Graduate Research awarded by the Department of Biochemistry and Molecular Biology. In August 2003, Timothy will be conferred the degree of Doctor of Philosophy. Upon graduation, he will move with his wife, LeeAnn Blalock who is receiving a Ph.D. in microbiology from the University of Florida, to Boston, MA to pursue a post-doctoral position at Harvard Medical School.